


8-2017

WISP1 IS AN OVEREXPRESSED DRIVER OF GLIOBLASTOMA

Pushan R. Dasgupta

Follow this and additional works at: https://digitalcommons.library.tmc.edu/utgsbs_dissertations

 Part of the [Cancer Biology Commons](#), [Medicine and Health Sciences Commons](#), and the [Molecular Genetics Commons](#)

Recommended Citation

Dasgupta, Pushan R., "WISP1 IS AN OVEREXPRESSED DRIVER OF GLIOBLASTOMA" (2017). *The University of Texas MD Anderson Cancer Center UTHealth Graduate School of Biomedical Sciences Dissertations and Theses (Open Access)*. 780.

https://digitalcommons.library.tmc.edu/utgsbs_dissertations/780

This Dissertation (PhD) is brought to you for free and open access by the The University of Texas MD Anderson Cancer Center UTHealth Graduate School of Biomedical Sciences at DigitalCommons@TMC. It has been accepted for inclusion in The University of Texas MD Anderson Cancer Center UTHealth Graduate School of Biomedical Sciences Dissertations and Theses (Open Access) by an authorized administrator of DigitalCommons@TMC. For more information, please contact digitalcommons@library.tmc.edu.

WISP1 IS AN OVEREXPRESSED DRIVER OF GLIOBLASTOMA

by

Pushan R. Dasgupta, A.B.

APPROVED:

Giulio F. Draetta, M.D. Ph.D.
Advisory Professor

Russell Broadus, M.D. Ph.D.

Sadhan Majumder, Ph.D.

Alfred Yung, M.D.

Ralf Krahe, Ph.D.

APPROVED:

Dean, The University of Texas
MD Anderson Cancer Center UTHHealth Graduate School of Biomedical
Sciences

WISP1 IS AN OVEREXPRESSED DRIVER OF GLIOBLASTOMA

A

DISSERTATION

Presented to the Faculty of

The University of Texas

MD Anderson Cancer Center UTHealth

Graduate School of Biomedical Sciences

in Partial Fulfillment

of the Requirements

for the Degree of

DOCTOR OF PHILOSOPHY

By

Pushan R. Dasgupta, A.B.

Houston, Texas

August 2017

Dedication

This work is dedicated to my Late loving father Partha Sarathi Dasgupta

Acknowledgements

Nothing in life is possible without the blessing of the Divine. I would like to begin by first mentioning my transcendental awareness of the Supreme authority that guides everything in this universe.

I was very fortunate in life to get my parents. My late father, Partha Sarathi Dasgupta, instilled in me a deep passion for knowledge and science. I have never met someone with such a profound understanding of the universe. From him I learned to see the world in a different light. Everytime I would speak to him it would feel like the day to day life we live in barely matters and that the infinite search for greater truth superseded all else. In the relatively short life he lived he did everything he could to support my continued quest for greater knowledge. I learned from him that one of the greatest joys in life is to develop a deeper understanding of the natural universe of which we are only a tiny part. Sometimes I feel like I was the most important thing in his life and I probably was. He always prioritized me first no matter what. Though my time with him was cut short he left an immeasurable mark on me. I guess in certain cases something immeasurable can fit in something very small which makes me remember a quote from Shakespeare that my father would tell me “I could be bounded in a nutshell, and count myself a king of infinite space.”

I have no words to describe the sacrifice that my mother Manisha Dasgupta has been making for my education. If I did not know her I would not think it is even possible for someone to be so supportive of her son. Despite numerous

unfortunate struggles that followed my father's tragic death my mother never lost her focus and determination to help me succeed. Even if it means not sleeping for 10 days straight she will do it and has done so at times to help me. I have never seen someone so multitalented. Though her field was not science when she would see me struggling on an experimental problem, she would try to understand what it is I was trying to do and figure out a solution. To my utter surprise she has given me experimental advice that really helped me in my project. I really have no idea how she is able to think so solidly about something so foreign to her based on her academic training. Most importantly she is my best friend, philosopher, and guide. She is the energy that drives my inspiration.

I would like to convey my deepest gratitude and admiration towards my PhD mentor Dr. Giulio Francesco Draetta. I have been extremely fortunate to have him as my mentor. I have had research experiences in numerous institutions from Harvard, MIT, and NASA to MD Anderson Cancer Center. I have met many great faculty in all of these wonderful places. They were all amazing and I learned a lot from them but I have found Dr. Draetta to be truly exceptional. He really loves science and has an internal drive to conduct research that has the potential to make a difference for patients. He is kindhearted, has a great personality, and is very friendly. As a mentor he is not only very kind but he is also extremely compassionate. No matter how busy he was I never felt that he did not have time. Even when he was traveling for business to the other side of the globe he was more accessible than someone perhaps near me. I was amazed by his level of responsibility and diligence. He is very meticulous and has great attention to detail

with a very practical approach. I was able to learn a lot from him and I feel it has helped me develop my abilities to conduct research. Dr. Draetta gave me abundant freedom and flexibility for my research and enabled me to exercise my own creativity in many ways. He allowed me to develop my own project, learn experimental techniques, think deeply about my project, chase my own hypotheses, and ultimately become a good researcher. I believe this contribution of his will really help me in my life and scientific pursuits. He has done something amazing. I am really grateful to have him.

I would like to thank my “dream team” advisory committee. I was very fortunate to have such a good group of very distinguished faculty.

I would like to thank Dr. Russell Broaddus as has played multiple roles during the course of my training. I met him when I started in the MD-PhD program here. He has done a fantastic job as our MD-PhD program Co-director. He has a deep passion to train physician scientists and he loves his students. I think all of us in the program are fortunate to have him. I am also grateful that he is my MD-PhD program advisor. His advice helped me to get to where I am. He has also been kind enough to be on my Candidacy exam committee and Advisory committee.

Dr. Sadhan Majumder is a real gentleman. When I joined the PhD program he was the Program Director for Genes and Development. That’s how I got to know him. He is a kind hearted person. He helped me quite a bit throughout my PhD years. I was also fortunate to also have him chair my Candidacy exam

committee. His presence in my Advisory committee has also been a blessing for me.

It has been truly wonderful having Dr. Alfred Yung in my advisory committee. When he joined my advisory committee he was the Chair of the Department of Neuro-Oncology but when I asked him to serve on my committee he agreed immediately regardless of his other commitments. That amazed me. He is a man of integrity. I am fortunate for his advice throughout my PhD years.

I had to immediately take a new committee member since a previous one moved suddenly. Dr. Ralf Krahe agreed immediately. What a life-saver! I did not know him very well at that time but sometimes people don't need to know someone that much. Some people have a special personality that makes you feel like you have known them forever. Dr. Krahe is just like that. I am really thankful to him. He is really a nice man.

I also had two other committee members who could not stay during the full course of my PhD. One of them was Dr. Kenneth Tsai who moved. The other is a former MD Anderson faculty member. I would like to thank both of them.

I would like to thank my Candidacy exam committee members. Besides Dr. Majumder and Dr. Broaddus I also had Dr. Heinrich Taegtmeyer, Dr. Michael Galko, and Dr. Dean Lee on my committee. I am really grateful to all of them.

I was fortunate to be in the wonderful Genes and Development program. Currently Dr. Michael Galko has been doing a great job as our program director. I am thankful that Dr. Galko is our program director. I was fortunate to have him as

both a candidacy exam committee member and my Genes and Development program director.

I must thank Elizabeth Lindheim. She is doing an amazing job as our Genes and Development program manager.

It has been a wonderful time with my lab members in the Draetta Lab. I felt like we were all family. Everyone was very friendly and nice. I am thankful to them.

Dr. Bill Mattox has been very helpful throughout my PhD training. I am always impressed by his personality and his kindness. He is truly a gentleman.

I am also grateful for the excellent Deans we have: Dr. Michael Blackburn and Dr. Michelle Barton. As professors and as Deans, they are both praiseworthy.

I am very pleased with our MD-PhD program here. Dr. Dianna Milewicz, our program co-director, is a wonderful person. She is affectionate and loves her students. She is always there when we have problems. From my very first day in the program to today she has always had a tremendous helping attitude. Betsey Kindred is our new program manager but already it feels like she has contributed so much. She is always helpful and understanding towards the students. She is too nice. Whenever I talk to her I feel like she really cares.

Finally, I am thankful towards my wonderful institutions: McGovern Medical School and the MD Anderson Cancer Center. I was offered admission to many nationally recognized medical schools to pursue my MD-PhD training. It was a

tough decision but I decided to come here. When I came for the interview and revisit I liked it and thought it was a good school. My thinking was correct. I am very happy with my decision and am fortunate to have come here. I would like to thank both institutions and their wonderful people.

WISP1 IS AN OVEREXPRESSED DRIVER OF GLIOBLASTOMA

Pushan R. Dasgupta, A.B.

Advisory Professor: Giulio F. Draetta, M.D., Ph.D

Despite current multimodal therapies for glioblastoma (GBM) the prognosis remains very grim. There is a tremendous need to identify new genetic drivers which can serve as potential therapeutic targets. In order to find new drivers we leveraged genomic datasets to conduct a context specific in vivo functional genomic screen of overexpressed and/or amplified genes in GBM. We identified WISP1, a secreted extracellular matrix protein, to be an overexpressed driver in GBM. Overexpression of WISP1 was able to drive tumor growth in various in vivo models. Knockdown of WISP1 with shRNAs resulted in reduced colony formation in vitro and reduced tumor growth in vivo. Rescue experiments validated that the shRNAs were on target. Functional characterization of the protein revealed that the TSP module is necessary for the phenotype. Intriguingly, overexpression of WISP1 lacking the signal peptide module for secretion resulted in a strong phenotype. Co-culture and conditioned medium experiments further supported a secretion independent intracellular role of WISP1 in GBM. Though WISP1 is a secreted protein we have found some localization in the cytosol. Overall, we have revealed WISP1 to be a driver of GBM with possible therapeutic potential as a target. This study has resulted in a paradigm shift in our current understanding of WISP1 as merely a secreted extracellular matrix protein as we have shown here

that it can drive GBM in a non-canonical manner in the cytosol.

Table of Contents

Approvals	i
Title	ii
Dedication	iii
Acknowledgements.....	iv
Abstract.....	x
Table of Contents.....	xii
List of Figures.....	xiii
Chapter 1: Introduction	1
Chapter 2: Material and Methods.....	12
Chapter 3: Results	22
Chapter 4: Discussion	136
Chapter 5: Future Directions	145
Chapter 6: Conclusion	149
Appendix.....	151
Bibliography	156
Vita:.....	168

List of Figures

Figure 1	24
Figure 2	28
Figure 3	30
Figure 4	33
Figure 5	35
Figure 6	37
Figure 7	39
Figure 8.....	42
Figure 9	44
Figure 10	46
Figure 11	48
Figure 12	52
Figure 13	54
Figure 14	56
Figure 15	58
Figure 16	60
Figure 17	63
Figure 18	65
Figure 19	67
Figure 20	69
Figure 21	71
Figure 22	73

Figure 23	77
Figure 24	79
Figure 25	81
Figure 26	84
Figure 27	86
Figure 28	88
Figure 29	91
Figure 30	93
Figure 31	95
Figure 32	97
Figure 33	99
Figure 34	102
Figure 35	104-106
Figure 36	109-111
Figure 37	115
Figure 38	117
Figure 39	119
Figure 40	121
Figure 41	123
Figure 42	125
Figure 43	130

Figure 44	132
Figure 45	134
Figure 46.....	143
Appendix 1.....	152
Appendix 2.....	154

Introduction

Introduction 1.1: Background on GBM

Close examination of some ancient Egyptian mummies serves as a direct reminder that humankind has been haunted by a very awful disease for thousands upon thousands of years. In the 5000 year old Egyptian Edwin Smith Papyrus, possibly the oldest medical literature available, it is written that this is a grave disease with no known cure. This disease happens to be cancer. In particular they were referring to breast cancer in the Edwin Smith Papyrus. One of the most devastating types of cancer happens to be a form of brain cancer. Glioblastoma multiforme (GBM) is the most common and most malignant primary central nervous system tumor (1-5). In fact 16% of all primary and central nervous system neoplasms are due to glioblastoma (6). GBM is a grade IV tumor with a median age of presentation of 64 years but the disease can occur at any age (6, 7). It has an incidence of 3-4 per 100,000/year (1, 4, 5). Roughly 12,000 new patients are diagnosed a year in the United States alone. The median survival of patients with GBM is 12.1-14.6 months, and only 3-5% of patients survive longer than 3 years (8).

Uncontrolled cellular proliferation, widespread invasion throughout the brain, profound angiogenesis, and a proclivity for necrosis are just some of its key characteristics (9). Regions of necrosis, microvascular proliferation, abundant mitoses, and pleiomorphic cells are some of the histological features of GBM (10). Glioblastoma tumors are also characterized by their resemblance to glia, which are non-neuronal cells that provide support and protection for neurons in the central and peripheral nervous systems (7, 11). Intriguingly, though glioblastoma was

originally thought to be derived from glial cells, the current experimental evidence suggests that they may develop from multiple cell types with neural stem cell-like properties (12, 13). It seems that these cells are in different stages of differentiation. Moreover, the phenotypic variations can largely be attributed to molecular alterations in signaling pathways rather than by differences in cell type of origin (12, 13).

Risk factors and environmental causes of GBM are poorly understood. One of the few identified risk factors for GBM is exposure to ionizing radiation (14). There are a few genetic diseases known to increase the risk for glioma such as Turcot syndrome, Li-Fraumeni syndrome, retinoblastoma, and neurofibromatosis 1 and 2 (14). However, these diseases account for less than 1% of glioma patients (14).

The size and location of the tumor dictate the presentation of a patient with GBM (12). Seizures are common presenting symptoms. Symptoms of increased intracranial pressure like headaches and focal or progressive neurologic deficits are also common (12). Computed tomography (CT) and magnetic resonance imaging (MRI) are used for initial diagnostic imaging. It is common for GBMs to enhance with gadolinium contrast on MRI displaying a ring of enhancement with a hypointense center of necrosis (12).

Introduction 1.2: Treatment

Before 2005 the standard treatment consisted of surgical resection of the tumor followed by radiation therapy (RT) alone (15). However, the standard of care

for GBM changed after the results of a phase III trial showed that external beam RT with concomitant temozolamide (TMZ) chemotherapy, an oral alkylating agent, was more effective than RT alone (15). The addition of TMZ resulted in a median survival of 14.6 months whereas the median survival for RT alone was 12.1 months (15).

In 2011 Optune which is a device that delivers tumor-treating fields (TTFields) was approved by the FDA as monotherapy for recurrent GBM, while in 2015 the FDA approved the use of Optune to be used alongside TMZ for adults with newly diagnosed supratentorial GBM (12). TTFields deliver low-intensity, intermediate frequency alternating electric fields that impede the division of cells (16). Interim analysis data from 315 patients comparing the addition of Optune to TMZ versus TMZ alone in the adjuvant setting showed that Optune plus TMZ resulted in superior progression-free survival and overall survival (16).

Unfortunately, despite maximal surgical resection and multimodal therapy around 70% of GBM patients will have disease progression within one year of diagnosis (15). This nearly inevitable recurrence is a major contributor for why only 3-5% of patients survive longer than 3 years (8). In terms of the prognosis and poor response to current treatment, GBM is one of the worst forms of cancer. Thus, there is a tremendous need to find new therapies for GBM.

Introduction 1.3: The Genomic landscape of GBM and its subtypes

Since cancer is a disease largely driven by genomic aberrations, the hope is that a better genomic understanding of the disease will allow for the discovery of

new therapeutic targets. In general, there has been some historical success in a few types of cancer through the inhibition of pathogenetic cancer alterations (17). For instance, imatinib, an inhibitor of the Abelson kinase, has led to an enormous decline in disease mortality for CML (18). Thus, great effort has been placed in gaining a deeper understanding of the genomic aberrations that lead to GBM. Multiplatform studies like The Cancer Genome Atlas (TCGA) Research Network consortium have analyzed the DNA mutations, copy number variations, and mRNA expressions in tumor tissue samples from hundreds of patients with untreated primary GBM (19). Somatic alterations in these samples revealed that GBM consists of deregulation in key components of the p53, RTK (receptor tyrosine kinase), and RB (retinoblastoma) pathways. In the p53 pathway homozygous deletion and mutation in TP53 and CDKN2A (ARF) account for most the aberrations (19). Mutation or amplification in EGFR and mutation or homozygous deletion in NF1 and PTEN represent most of the alterations in the RTK pathway (19). Most of the alterations in the RB pathway are: homozygous deletion/mutation in CDKN2A (p16/INK4A), homozygous deletion in CDKN2B, amplification in CDK4, and homozygous deletion/mutation in RB1 (19). This further confirmed years of experimental evidence implicating these core pathways in GBM and validated the power of these datasets (9).

GBM can also be categorized in various ways. Some of these distinctions were made even before the molecular structure of DNA was discovered by Francis Crick and James Watson let alone a genomic understanding of the disease. In 1940 the German neuropathologist Hans-Joachim Scherer wrote “From a biological

and clinical point of view, the secondary glioblastomas developing in astrocytomas must be distinguished from 'primary' glioblastomas. They are probably responsible for most of the glioblastomas of long clinical duration." (20). This was a profound leap at that time in the understanding of GBM as even in 1979 the World Health Organization did not consider GBM as an astrocytic tumor (20). Primary glioblastoma is termed *de novo* glioblastoma and presents as a full-blown tumor without evidence of a less-malignant precursor (20). On the contrary, secondary GBM evolves gradually from less malignant astrocytoma like low-grade diffuse astrocytoma (WHO grade II) or anaplastic astrocytoma (WHO grade III) (20). Secondary GBM accounts for only 5% of glioblastomas (21). Secondary GBM tends to occur in younger patients compared to Primary GBM with a 17 year difference in the mean age (21). Mutations in Isocitrate dehydrogenase 1 and 2 (IDH1 and IDH2) have been shown to be drivers of low-grade gliomas and secondary GBM (22). Hence IDH mutant gliomas represent a less aggressive group compared to IDH wild type.

In terms of gene expression-based molecular classification, GBM can be classified into four subtypes: Proneural, Neural, Mesenchymal, and Classical (22). The Classical subtype can be characterized by chromosome 7 amplification, chromosome 10 loss, and a high level of EGFR amplification present in 97% of classical glioblastomas (22). In the Mesenchymal subtype there is presence of focal hemizygous deletions of the region containing NF1 at 17q11.2 (22). Alterations in PDGFRA and point mutations in IDH1 were major features of the Proneural subtype (22). Likewise most secondary GBMs fall into the Proneural

subtype. Expression of neuron markers like NEFL, GABRA1, SYT1, and SLC12A5 was present in the Neural subtype (22).

Intriguingly, it was found that there is a localization difference in the origin of these different subtypes. The sub-ventricular zone (SVZ) is a region in the brain that is adjacent to the lateral wall of the lateral ventricle close to the center of the brain. Neural stem cells (NSC) and astrocyte precursors are located in the SVZ (23). NSCs migrate radially and differentiate into various progenitor cells during development (23). It is thought that genetic aberrations in these cell populations may be what give rise to GBM (24). It was found that the Proneural and Neural glioblastoma subtypes tend to occur closer the SVZ while the Mesenchymal and Classical glioblastoma subtypes tend to develop farther from the SVZ (23).

Beyond finding critical pathways and subtypes of GBM, genomic analysis has also revealed very interesting characteristics about the biology of the disease. Telomeres are caps at the end of chromosomes that protect them. Telomeres also affect the way cells age. Telomerase is an enzyme that elongates telomeres. Telomerase reverse transcriptase (TERT) is a catalytic subunit of telomerase. Genomic analysis of the TCGA datasets found that TERT promoter mutations correlated with upregulated TERT expression at the RNA level (25). However, GBM tumors that did not have TERT promoter mutations had ATRX mutations and did not have increased TERT RNA expression (25). ATRX mutations are associated with another process that lengthens telomeres called alternative telomere lengthening (ALT) (26). The genomic data regarding TERT promoter mutations and ATRX suggest that GBM pathogenesis requires telomere

maintenance either through reactivation of telomerase by TERT promoter mutations increasing the expression of TERT or through ALT resulting from ATRX mutation (25).

Introduction 1.4: Experimental Models of GBM

With such a complex and difficult disease it is imperative to have powerful experimental models that properly allow researchers to understand glioblastoma. Mouse models of glioblastoma are particularly useful in studying disease progression and tumor pathological progression at the molecular level. Mouse models also help in understanding fundamental tumor biology like the role of stroma or the tumor microenvironment. A direct application for mouse models is in the identification of therapeutic targets.

Xenograft models have been very useful in studying glioblastoma. The most popular one has been subcutaneous engraftment of human glioblastoma cell lines to the flank of immunocompromised mice (27). This is very useful in that the tumor size can be directly followed with a caliper. Due to its utility this has been very popular in drug development research. However, orthotopic or intracranial implantation has also become very popular due to its more context-specific microenvironment for tumor development. The drawback here is that it is difficult to gauge the growth of the tumors so other more indirect methods like bioluminescent imaging must be used. The major advantage of xenograft models is that cells of

human origin can be used. The discovery and identification of glioblastoma tumor initiating cells made the use of xenograft models more powerful in terms of its capacity to model patient tumors. According to the cancer stem cell hypothesis a unique rare population of cells in the tumor have stem cell-like properties and can maintain neoplastic clones (28). A CD133+ population was isolated from human brain tumors that could recapitulate a tumor histologically similar to the patient's tumor in mice (28). This was the discovery of the first glioblastoma tumor initiating cell. Great excitement was witnessed after this finding since it gave the potential to study the biology of tumors from individual patients. Remarkably, the treatment response of xenograft tumors derived from tumor initiating cells from patients mimics the treatment response of the parental GBM (29). This was true for irradiation, chemotherapy, and targeted therapy of the xenograft tumors (29). The tumors also had the same genomic characteristics of the specific parental tumor it was derived from (29). Patient-specific orthotopic GBM xenografts represent a preclinically valuable translational platform to further understand GBM and its functional patient to patient variations.

The use of genetically engineered mouse models is another powerful method to interrogate the biology of glioblastoma. The technology of generating genetically engineered mouse models allows for many different kinds of manipulations. In instances where oncogene overexpression or mutation is to be studied a cell type-specific promoter can be used to drive expression of the gene of interest (27). In cases where a tumor suppressor is to be studied, knockout mice can be generated in which a germline deletion removes all or part of the gene of

interest (27). One important technique employed in the development of mouse models is the cre-lox system. In this system the Cre recombinase deletes the sequences between two loxP sequences (27). The expression of the Cre recombinase can also be engineered to be expressed by cell type-specific promoters like the Nestin promoter for expression in neural progenitor cells. Inducible Cre recombinase is used for temporal control of its expression.

In the case of generating gliomas in mice many have taken advantage of inactivating the p53 and Rb signaling pathways since these are commonly altered in the disease (30, 31). In addition to inactivating tumor suppressors others have found that oncogenic overexpression of V-src can also drive gliomagenesis in mice (32). Overall there have been numerous mouse models of glioblastoma and glioma generated involving the inactivation of other tumor suppressor genes like CDKN2A, Ink4A/Arf, NF1, and PTEN and the activation of other driver genes like EGFRvIII, RAS, and Akt (33).

Introduction 1.5: Hypothesis and Approach in this Study

Although much research has focused on mutations that drive cancer, it is also very important to understand genes that can drive cancer simply through overexpression. There are many different triggers for overexpression from amplification and epigenetic regulation to even translocation. However, the end result is the same with overexpression of an oncogenic protein leading to a pro-growth, pro-tumor phenotype. There are numerous examples of such genes like: c-MYC, PLAU, ELMO3, and AIB1 (34-38). It is crucial to discover more of these

genes as many have the potential to become a therapeutic target. One approach to functionally interrogate potential overexpression activated drivers is to perform gain-of-function cDNA overexpression screens. Several novel drivers for various forms of cancer have been identified through this approach. For instance, in breast cancer this approach has led to the discovery of IKBKE and PAK1 as drivers, while in ovarian cancer it has revealed GAB2 to be a driver (39-41).

In this study we wanted to leverage the current genomic understanding of GBM in order to discover new drivers. We hypothesized that a context-specific gain-of-function screen of genes amplified and/or overexpressed in GBM based on the TCGA datasets would allow us to do this. In order to be context-specific, we decided to do the screen in an *in vivo* orthotopic setting using human GBM tumor initiating cells (GSCs). Here we report that WISP1 (WNT1 inducible signaling pathway protein 1), a secreted extracellular matrix protein, is a novel overexpressed driver of GBM which can exert its pro-oncogenic function non-canonically inside the cell without being secreted.

Materials and Methods

Cell Culture

All cells were cultured at 37 degrees C in a humidified chamber with 5% CO₂.

Glioma stem cells (GSCs) were cultured in DMEM/F12 50/50 (Gibco) supplemented with 1X B27 Supplement (Invitrogen #17504-044), 20ng/mL EGF (PeproTech), 20ng/mL bFGF (PeproTech), and 1% Pen/Strep. U87MG, LN340, and LN229 were cultured in DMEM (Gibco) supplemented with 10% FBS (Gibco) and 1% Pen/Strep (Gibco).

In Vitro Assays

Cell viability was measured using Cell Titer Glo 3D Cell Viability Assay (Promega) at various time points. 1000 cells were seeded into each well in triplicate in a 6 well plate for the colony formation assay (CFA). After 10-15 days the cells were fixed with 4% paraformaldehyde and stained with Crystal Violet.

Western blot

Protein lysates were electrophoresed by SDS-Page on 5-15% gradient polyacrylamide SDS gels. They were transferred onto Nitrocellulose membranes using a semi-dry transfer apparatus according to the manufacturer's instructions (Bio-rad). The membranes were blocked in 5% nonfat milk in TBST (10 mM Tris, pH 8.0, 150 mM NaCl, 0.5% Tween 20) for 60 minutes. After blocking they were incubated in primary antibody diluted in 5% nonfat milk in TBST overnight at 4 degrees C. The membranes were then washed three times in TBST for 5 minutes each and then incubated with a 1:5000 dilution of horseradish peroxidase-conjugated secondary antibodies in 5% nonfat milk in TBST for an hour at room

temperature. Finally, the membranes were washed with TBST three times and band detection was carried out by chemiluminescence reaction followed by film exposure.

Subcellular Fractionation

Subcellular fractionation was conducted using the Thermo Scientific subcellular fractionation kit (PI78840) for cultured cells. Cells were trypsinized and lysed according to the protocol to obtain cytosolic and membranous fractions.

Immunofluorescence and Confocal Microscopy

Cells were grown in chamber slides and allowed to reach confluence. The media was removed and the cells were washed in PBS three times for 5 minutes each. The cells were then fixed in 4% paraformaldehyde for 10 minutes at room temperature. After another round of washing the cells were permeabilized with 0.5% triton x-100 for 10 minutes at room temperature. They were washed again and blocked for one hour in 3% BSA + 1% normal horse serum at room temperature. After blocking the fixed cells were incubated in primary antibody diluted in blocking solution overnight at 4 degrees C. The cells were then washed again as before and incubated in secondary antibody diluted in blocking solution for 1 hour in room temperature. After another round of washing the cells were stained with DAPI (1:10000 dilution in PBS of 5mg/ml DAPI) for 5 minutes. The cells were then washed again and treated with DAKO's antifade mounting medium. The slides were then coverslipped and allowed to sit in the dark at room temperature.

Finally the coverslips were sealed with nail hardner. The images were taken on an FV1000 Olympus Confocal microscope.

ELISA

The human WISP-1/CCN4 DuoSet ELISA kit (DY1627) from R&D systems was used to measure WISP1 concentrations in the conditioned media and lysate. The protocol from the kit was followed.

Plasmids

cDNA for all the open reading frames of interest were from the Ultimate ORF collection (Invitrogen) and transferred by Gateway cloning into the bicistronic vector pHAGE-EF1 α -IRES-GFP. pLKO shRNAs targeting WISP1 expression were purchased by SIGMA.

Transduction

For the cDNA overexpression cells were transduced with fresh concentrated lentivirus. After 24 hours the media was changed to fresh media. By 72 hours after transduction the cells were ready for any downstream application. In the case of the knockdown experiments, pLKO shRNA from fresh concentrated lentivirus was used to transduce cells in the presence of 8 μ g/ml of polybrene. After 24 hours the media was replaced with fresh media. 48 hours after transduction the cells were selected with 6 μ g/ml of puromycin for six days. After selection the cells were ready for downstream applications like western blotting and/or colony formation assay.

Lentivirus Production

HEK293T cells were transfected with a mixture of plasmid and the packaging-encoding vectors PMD2.G (Addgene) and pCMVΔR-8.74 (Addgene).

Polyethylenimine (PEI) was used for transfection. Virus-containing supernatant was collected 72 hours after transfection and filtered through a 0.45μm filter (Corning). Ultracentrifugation at 23000 rpm for 1.5 hours at 4 degrees C was used to concentrate the virus. Concentrated virus was used fresh.

Immunohistochemistry

Standard procedures were used to dehydrate and paraffin embed formalin-fixed tumors. Cut slices were rehydrated and the antigen was unmasked by heating at 95 degrees C for 30 minutes with an antigen unmasking solution (Citra Plus – Biogenex). After baking and antigen unmasking the tumor samples were incubated in 3% hydrogen peroxide for 15 minutes. They were then blocked in a 3% BSA, 10% goat serum, and 0.1% triton solution. Finally the samples were incubated in primary antibody, washed, incubated in HRP-conjugated secondary antibody, washed, and developed using DAB. Haematoxinilin was used to counterstain.

Co-Culture Experiments and Flow Cytometry

Wild type U87MG cells and U87MG cells expressing WISP1_ires_GFP were transduced to express mCherry_ires_Luciferase. Cells were flow sorted using a FACS Aria Fusion cell sorter to ensure that all cells were expressing their

respective fluorophore. Cell mixtures for experimental and control groups were 1:1 and were verified by flow cytometry of the parental cells. For the *in vivo* experiments 1.5 million cells were injected per mouse and tumors were allowed to grow for 40 days. Freshly extracted xenograft tumors were dissociated into single cells using the Tumor dissociation kit from Miltenyi Biotec. The protocol according to the kit manufacturer was followed. For the *in vitro* experiments 1000 cells were seeded into 6 well plates and colonies were allowed to grow for 14 days. The cells were then trypsinized for subsequent flow cytometric analysis. GFP positive, mCherry positive, and double positive cells for these experiments were analyzed using a BD LSRFortessa analyzer. Control cells of each pre-mixture cell type expressing GFP, mCherry, or both were used for compensation control.

Animal Studies

All animal manipulations were carried out in accordance with institutional, state, and federal laws under an approved protocol. Mice were anesthetized with intraperitoneal (IP) injections of ketamine (100mg/kg)/xylazine. These experiments consisted of 4-6 week old female nude mice purchased from the Department of Experimental Radiation Oncology, The University of Texas M.D. Anderson Cancer Center (Houston, TX). A guide screw and a multiport microinfusion syringe pump (Harvard Apparatus, Holliston, MA) were used for the orthotopic intracranial injections in a method previously described (42, 43). Glioma stem cells (GSCs) were used for all intracranial injections and 50,000 cells were injected per mouse. Intracranial tumors were monitored using a Xenogen IVIS-200 imaging system since they expressed luciferase. For subcutaneous injections cells were injected in

the flank. For LN340 and LN229 cells were mixed 1:1 with matrigel (Fisher) before injection. Tumors were measured with a caliper and tumor volume was calculated using the standard formula: $\text{Volume} = .5 \times (l \times w^2)$. For the experiments comparing GFP and WISP1 in U87MG and LN340, 3 million cells were injected per mouse. For all other subcutaneous injections 1.5 million cells were injected per mouse.

Genomic DNA extraction and qPCR

Frozen tumors from the screen were cut into small pieces using a sterile scalpel. The pieces were resuspended in buffer P1 (Qiagen) supplemented with 100µg/ml RNase A (Promega). GentleMACS M tubes (Miltenyi Biotech) and the gentleMACS dissociator (Miltenyi Biotech) were used for the dissociation step. The reference cells did not undergo this dissociation step in the gentleMACS dissociator. 1/20 volume of SDS (Promega) was added to lyse the cells and they were incubated at room temperature for 30 minutes. The lysate was passed 20 times through a 22-gauge syringe needle. One volume of Phenol:Chloroform (Sigma Aldrich) was added to the lysate after which it was vortexed and centrifuged at 12000 rpm for 12 minutes. The upper phase was separated to a new tube and a subsequent extraction step was carried out with Chloroform (Sigma Aldrich). Again the upper phase after centrifugation was transferred to another tube and 0.1 volume of 3M NaCl (Sigma Aldrich) and 0.8 volumes of isopropanol (Fisher Scientific) were added to precipitate the genomic DNA. The sample was vortexed and centrifuged at 14000 rpm for 1 hour at 4 degrees C. After centrifugation the DNA pellet was washed in 70% ethanol (Fisher Scientific) and centrifuged again for 5 minutes at 14000 rpm after vortexing. The ethanol was then removed and the

DNA pellet was air-dried and dissolved in UltraPure distilled water (Invitrogen). This solution was put in a shaker at 26 degrees C overnight. NanoDrop 2000 (Thermo Scientific) was used to quantify the DNA. qPCR was done using SYBR green (Sigma-Aldrich). The program consisted of 2 minutes at 94 degrees C and 40 cycles of 15 seconds at 94 degrees C with 1 minute at 60 degrees C. Calculations and analysis were performed using the comparative $\Delta\Delta CT$ method.

Computational Analysis

Genes overexpressed and/or amplified in GBM were selected from the TCGA Cell 2013 GBM datasets through cBioPortal (44). These selected genes were used for the screen. Tissue-specific expression and metadata was obtained from the GTEx consortium (45). This dataset encompasses 2712 samples across 51 tissue types from 207 individuals. Each individual additionally had cells cultured from blood and skin samples, but these were omitted and not included in this analysis. Any samples procured from the central nervous system, including high cervical spinal cord, cerebellum, basal nuclei and cortex were classified as “Brain”. All other samples, including subcutaneous adipose tissue, tibial artery and nerve, left ventricular, lung, skeletal muscle, thyroid, skin and blood were classified as “Non-brain”. Glioma gene expression and clinical metadata was obtained from the TCGA publication page associated with the recent pan-glioma analysis paper (46,47). This dataset consists of 486 primary grade II-IV gliomas with available RNA sequencing-based gene expression, clinical data (histology and grade) and IDH status. This dataset spans different histological subtypes, including

astrocytoma (n=116), oligodendroglioma (n=144), oligoastrocytoma (n=93) and glioblastoma (n=144). Boxplots were plotted using ggplot2 (48).

Target of Antibody	Vendor and Catalog#	Application
WISP1	Santa Cruz Biotechnology sc-25441	WB, IHC, IF
WISP1	Abcam ab155654	WB
WISP1	R&D Systems 1627-WS	ELISA, WB
Vinculin	Cell Signalling Technology 4650S	WB
Histone H3	Abcam ab6002	WB
alpha-Tubulin	Abcam ab7291	WB, IF
Calnexin	Fisher Scientific NC0927163	WB
Calreticulin	Abcam ab22683	IF
AE-6 (Golgi Marker)	Santa Cruz Biotechnology sc-58770	IF
EEA1 (Endosomal Marker)	Santa Cruz Biotechnology sc-365652	IF
GFAP	Abcam ab7260	IHC
Ki67	Abcam ab15580	IHC
Beta III Tubulin	Abcam ab18207	IHC

shRNA	Vector Backbone	shRNA Target	Vendor	Catalog#
sh70	pLKO	WISP1	Sigma	TRCN0000373970
sh91	pLKO	WISP1	Sigma	TRCN0000373891
sh50	pLKO	WISP1	Sigma	TRCN0000033350
sh51	pLKO	WISP1	Sigma	TRCN0000033351
sh52	pLKO	WISP1	Sigma	TRCN0000033352
shNT	pLKO	scrambled (negative control)	Addgene	Plasmid #1864

Results

Results 1.1: In Vivo Context-Specific Gain-of-Function Screen Identifies WISP1 as a Potential Driver in GBM

In order to identify novel genetic drivers of GBM, we started with the rationale that some of the genes amplified and/or overexpressed in GBM will represent drivers. Analysis of the GBM TCGA datasets allowed us to produce a list of amplified and/or overexpressed genes in GBM comprising 74 genes. To find novel functional drivers among these genes we decided to do a context-specific *in vivo* functional genomic gain-of-function screen. We hypothesized that overexpression of driver genes would reduce the latency of tumor formation. In order to best appreciate a potential difference in latency, we chose the glioblastoma tumor initiating cell line GSC 7-11 for its slow 8-9 month latency (Fig 1). In the GSC and GBM lines used in this study we kept in mind the genomic alterations such as copy number and mutation status (Appendix 1). We overexpressed our gene(s) of interest using a bicistronic IRES vector in pHAGE such that GFP would also be expressed along with our gene(s) of interest. The EF-1 α promoter was used to drive constitutive expression. Lentivirus-mediated transduction was employed to overexpress the gene(s) of interest. In addition to the 74 genes we included isoforms of some of these genes giving a total of 87 open reading frames (ORFs) for the screen. EGFRvIII was used as the positive control as it is a known driver of GBM while GFP was used as the negative control (49). We used a pooled strategy where cells were transduced with roughly 6-7 ORFs per pool. We made sure that the ORFs in each pool were of similar size.

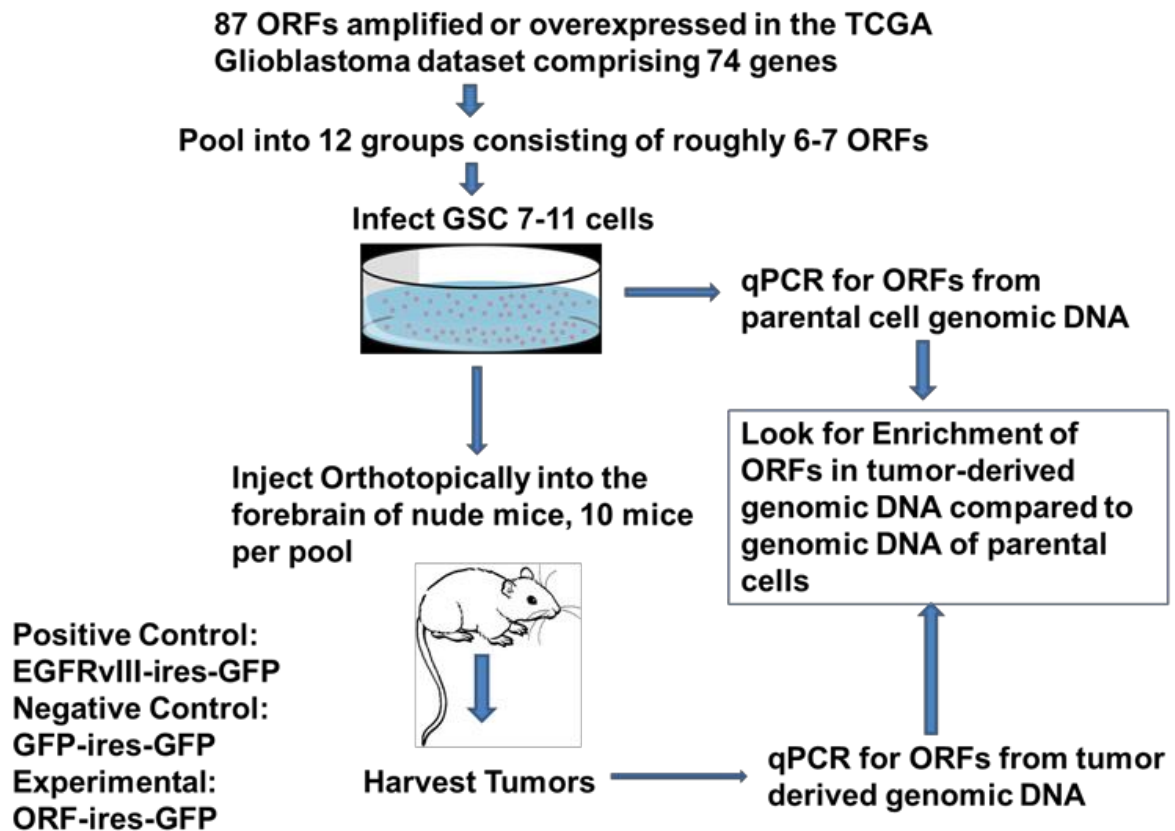


Figure 1. Flow chart outline depicting the design and details of the screen.

There were 12 such pools to cover the 87 ORFs. Each pool consisted of roughly 10 mice. The cells were injected orthotopically into the forebrains of nude mice and allowed to grow as tumors. Before injection some of the same cells were kept as parental reference cells. We hypothesized that cells transduced to overexpress a driver would begin to dominate the population of cells in the tumors with reduced latency such that qPCR of genomic DNA of the tumor compared to that of the parental cells would indicate significant fold enrichment for the driver gene. We used a qPCR strategy where the forward primer was the same for all the ORFs as it was complementary to a portion of the EF1- α promoter but the reverse primer was unique to each ORF. For normalization two primers outside the long terminal repeat (LTR) sequences were used to amplify a portion of the plasmid which served as the control (Fig 2).

The injected cells were also transduced to express mCherry_ires_Luciferase which allowed us to image the mice for tumor development using bioluminescent imaging. As predicted some of the pools had a reduced latency compared to the GFP control indicating the presence of a potential driver. Among these were pools 1, 2, 9, and 12. Mice in these pools developed tumors faster and displayed reduced survival (Figure 3). We harvested the tumors from these mice and extracted the genomic DNA for qPCR analysis. In the analysis we considered any enrichment of greater than two fold to be indicative of a potential driver. In this definition there were five potential drivers from the screen: prostate stem cell antigen (PSCA), Ly6/PLAUR Domain Containing 2 (LYPD2), chromatin

accessibility complex 1 (CHRA1), TatD Dnase Domain Containing 1 (TATDN1),
and WNT1 inducible



Figure 2. A diagram depicting the qPCR strategy used.

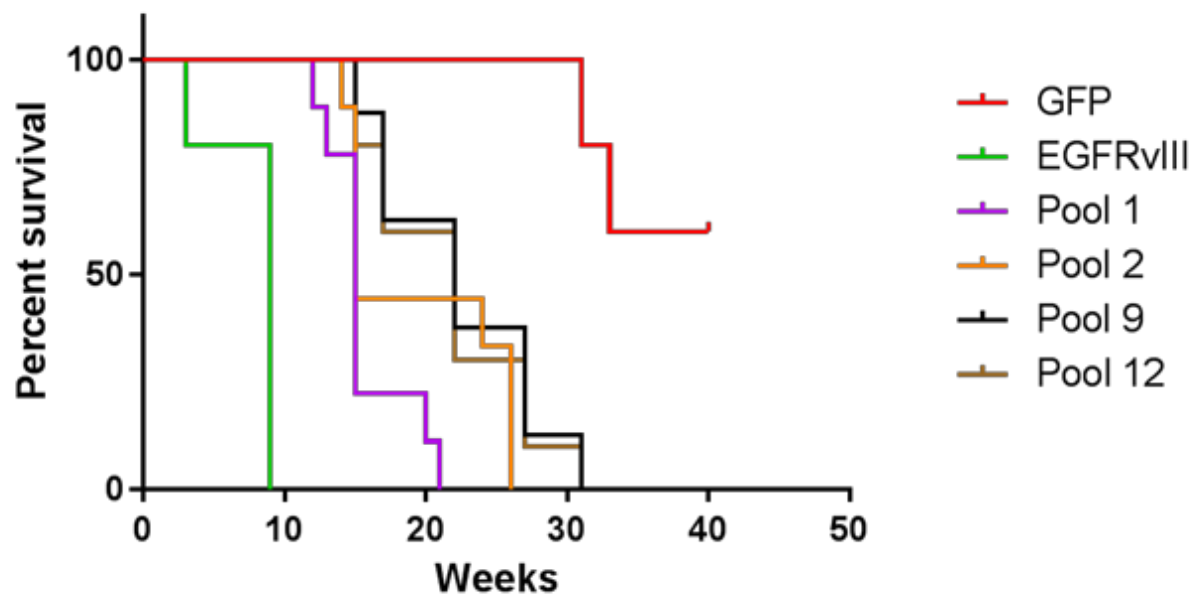


Figure 3. Survival curves for the pools from the screen that had a reduced latency. LogRank (Mantel-Cox) test shows statistical significance for the survival of each pool relative to the GFP negative control: Pool 1 (n=9) $p=.0005$, Pool 2 (n=9) $p=.0009$, Pool 9 (n=8) $p=.0018$, Pool 12 (n=10) $p=.001$, n=5 for GFP control.

signaling pathway protein 1 (WISP1) (Fig 4-7). Even though pool 1 had a reduced latency none of the overexpressed ORFs in pool 1 had a two-fold or greater enrichment in the qPCR analysis. This is most likely explained by synergistic effects of that particular combination of genes rather than due to a certain driver gene(s). Among these five genes we were interested to know which one was the most promising potential driver. In order to compare these genes for their relevance in GBM and glioma we analyzed various datasets. Using tissue-specific expression and metadata from the GTEx consortium we found that all of these genes except TATDN1 showed significantly lower expression in brain versus non-brain tissue (Fig 8). We next compared gene expression in TCGA glioma samples according to glioma grade. For all the genes except LYPD2, expression was associated with tumor grade but a positive association was found to exist for CHRAC1 and WISP1. Both of these genes showed higher expression in grade four tumors relative to grade II-III, and this difference is visually the greatest for WISP1 (Fig 9). WISP1 is known to have very little expression in the brain but based on this analysis we have found that WISP1 is overexpressed in GBM as its expression is progressively higher in higher grades of glioma with GBM (grade IV) having the highest level relative to grade III and grade II glioma (50, Fig 9). IDH wild type gliomas are more aggressive while IDH mutant gliomas are less aggressive (51). We therefore wanted to see which of these genes are expressed higher in IDH wild-type versus IDH mutant tumors. Comparison of gene

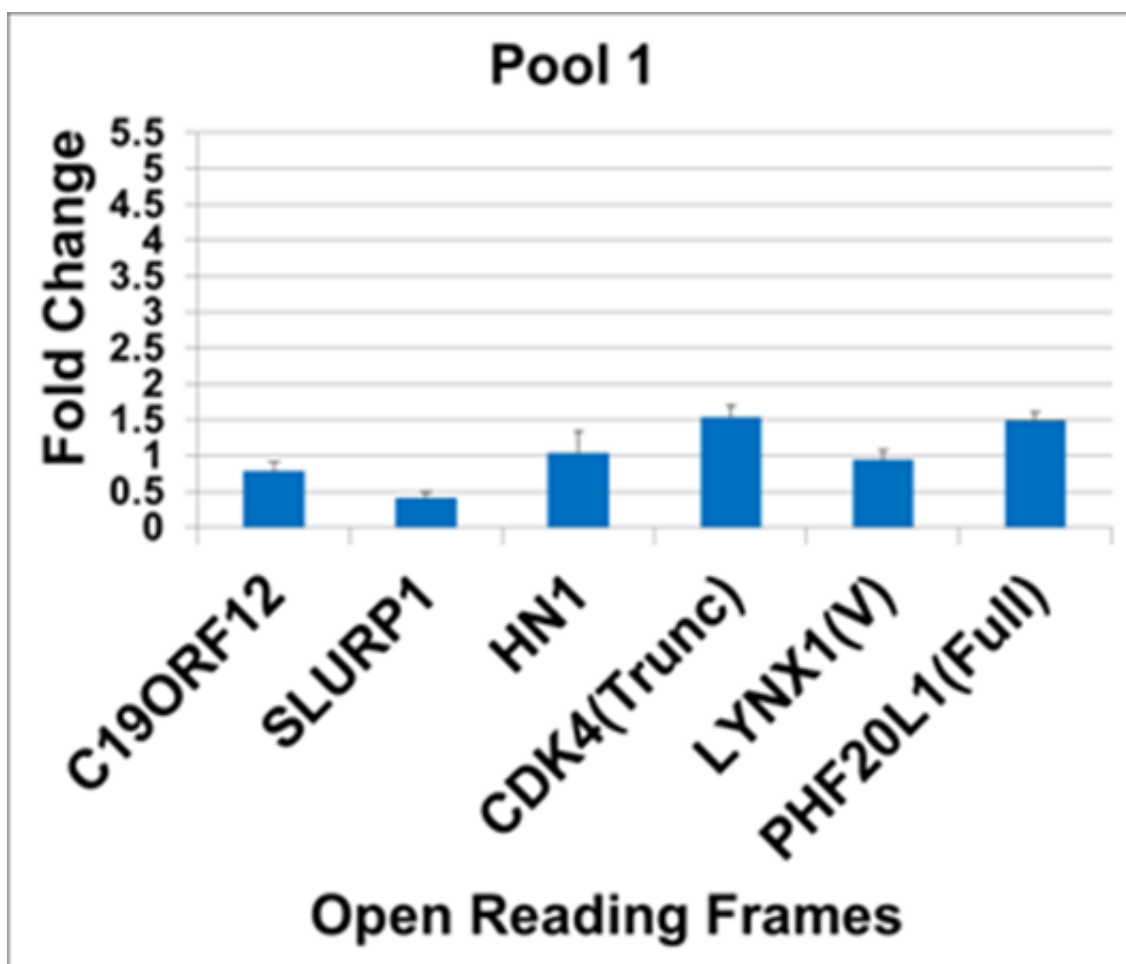


Figure 4. qPCR fold changes for Pool 1 are shown for each ORF relative to the reference. The mean represents the average fold change for each ORF from 5 tumors derived from the first 5 mice in each pool to be sacrificed. The error bars represent the standard error of the mean. The ORFs are also specified in parentheses as either: TRUNC-truncated versions, V-variants, Full-full length form, C-ORF clones. The “hit” genes with a fold change above 2 are in red while the rest are in blue.

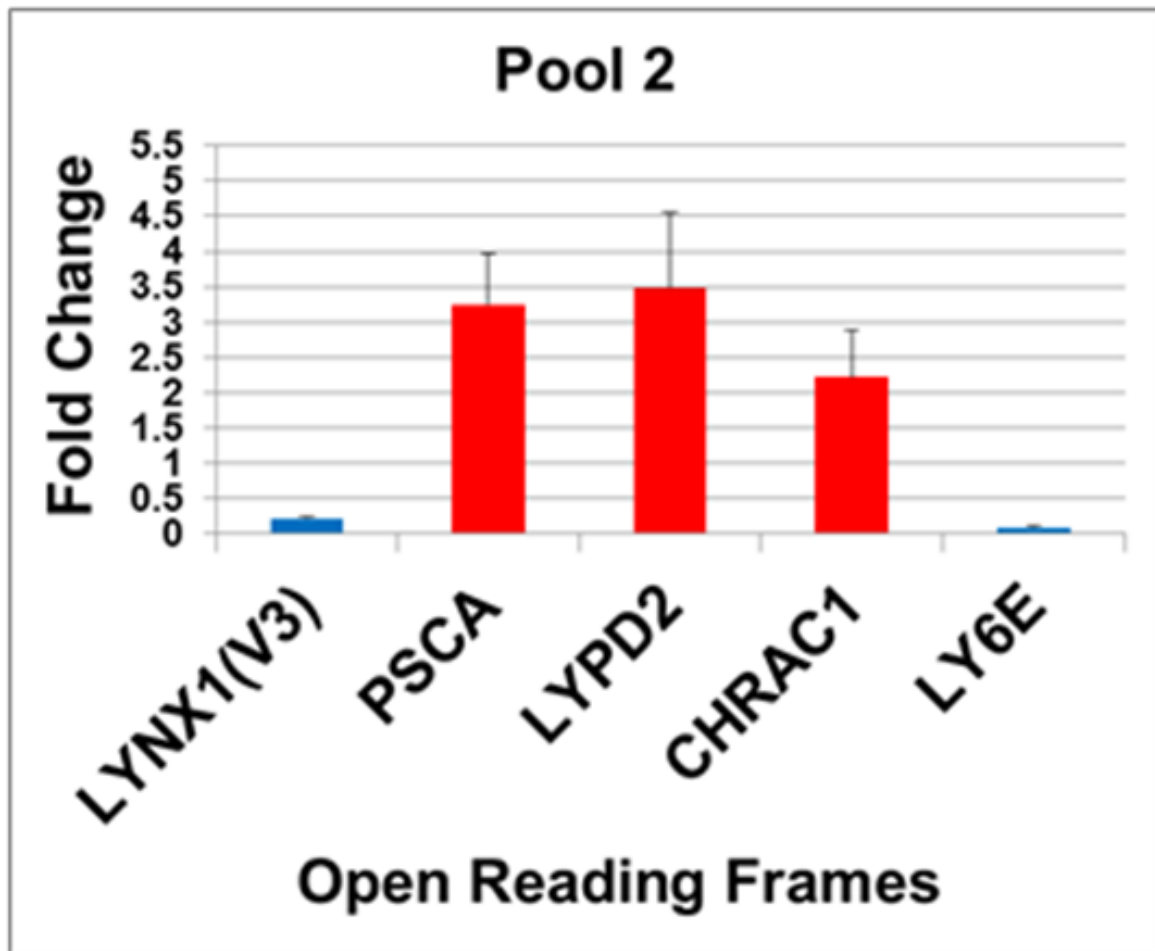


Figure 5. qPCR fold changes for Pool 2 are shown for each ORF relative to the reference. The mean represents the average fold change for each ORF from 5 tumors derived from the first 5 mice in each pool to be sacrificed. The error bars represent the standard error of the mean. The ORFs are also specified in parentheses as either: TRUNC-truncated versions, V-variants, Full-full length form, C-ORF clones. The “hit” genes with a fold change above 2 are in red while the rest are in blue.

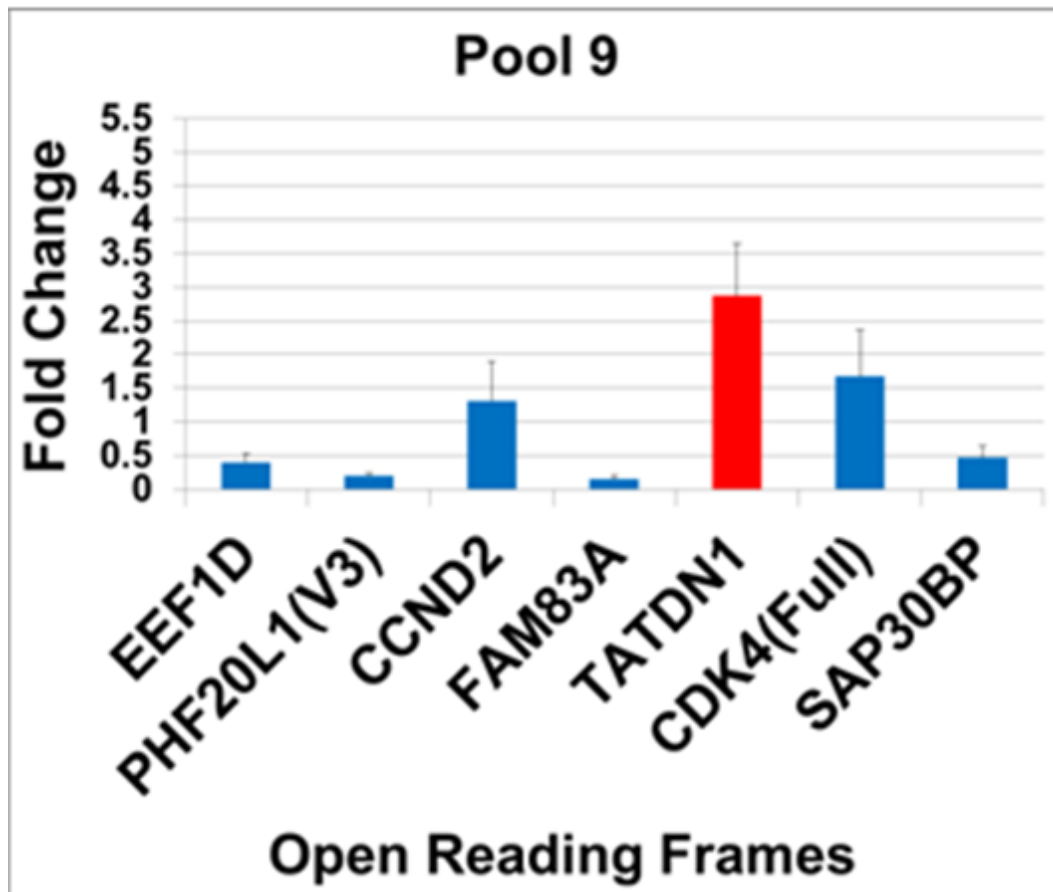


Figure 6. qPCR fold changes for Pool 9 are shown for each ORF relative to the reference. The mean represents the average fold change for each ORF from 5 tumors derived from the first 5 mice in each pool to be sacrificed. The error bars represent the standard error of the mean. The ORFs are also specified in parentheses as either: TRUNC-truncated versions, V-variants, Full-full length form, C-ORF clones. The “hit” genes with a fold change above 2 are in red while the rest are in blue.

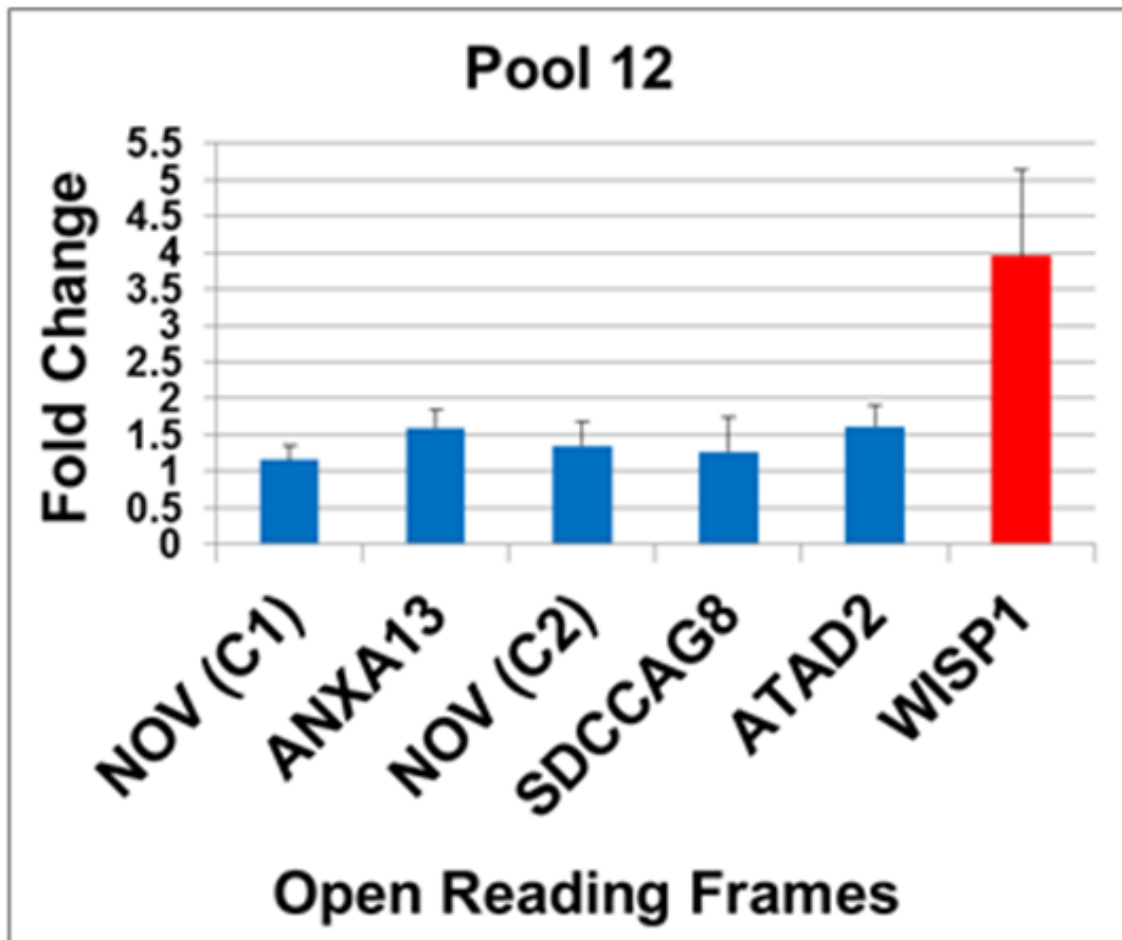


Figure 7. qPCR fold changes for Pool 12 are shown for each ORF relative to the reference. The mean represents the average fold change for each ORF from 5 tumors derived from the first 5 mice in each pool to be sacrificed. The error bars represent the standard error of the mean. The ORFs are also specified in parentheses as either: TRUNC-truncated versions, V-variants, Full-full length form, C-ORF clones. The “hit” genes with a fold change above 2 are in red while the rest are in blue.

expression in TCGA glioma samples according to IDH status revealed that expression of all these genes except LYPD2 associated with IDH status. CHRAC1 and WISP1 both showed decreased expression in IDH mutant tumors relative to IDH wild-type tumors, and this difference was again visually the greatest for WISP1 (Fig 10). We were also interested to see expression differences among the different Verhaak transcriptional subtypes (22). The expression of all these genes except LYPD2 and CHRAC1 associated with the tumor subtype (Fig 11). WISP1 showed increased expression in mesenchymal and classical tumors compared to the neural and proneural subtypes (Fig 11). This is intriguing as the proneural subtype tends to have a longer survival compared to the other subtypes.

Though the GSC 7-11 line had an amplification in the region containing the WISP1 gene, we found that the GSC 7-11 line had the lowest protein expression of WISP1 of any of our GSC lines (Appendix 2). It was even lower than in lines not harboring an amplification (Appendix 2). Therefore, use of the GSC 7-11 line to identify WISP1 through an overexpression screen was rationalized. Taken together, WISP1 demonstrated to be the most promising potential driver and the most relevant gene among these five in glioma.

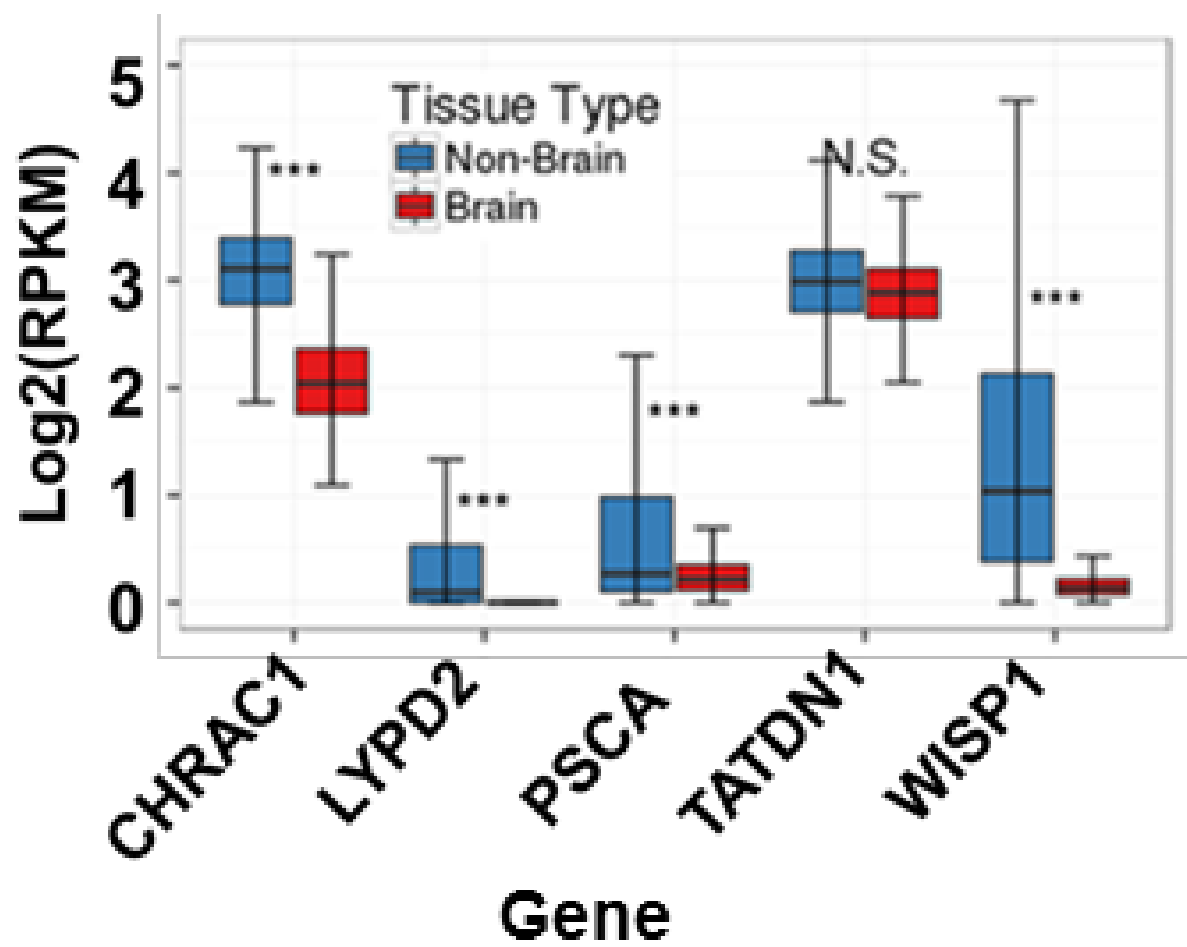


Figure 8. Comparison of gene expression in GTEx tissue samples (n=2,712, Methods) grouped according to whether the sample was procured from brain tissue (n=357) or non-brain tissue (n=2,355). RNA sequencing RPKM values for the five hits from the preliminary screen are shown. Groups were compared for each gene individually using a two-sided t-test. N.S. not significant; * $P < 0.05$; ** $P < 0.001$; *** $P < 0.0001$.

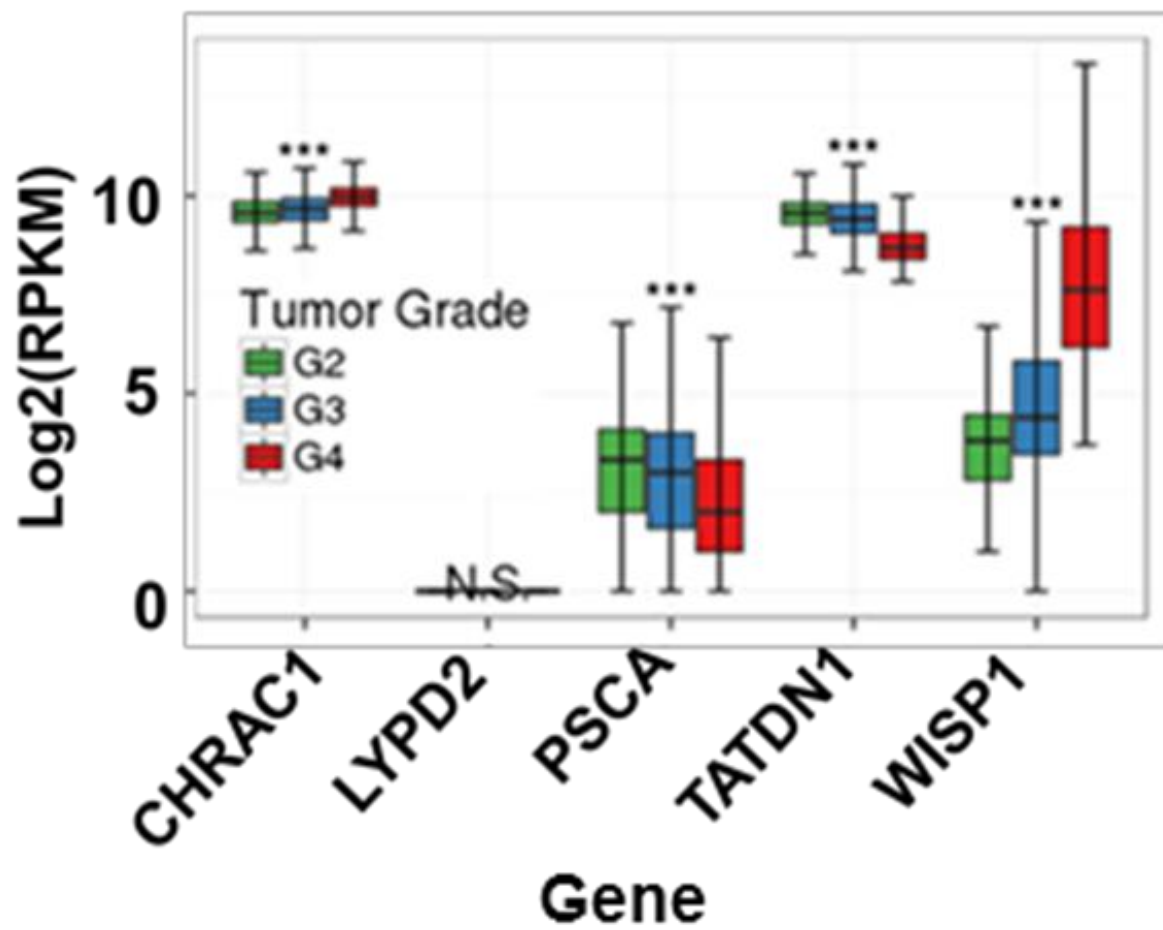


Figure 9. Comparison of gene expression in TCGA glioma samples (n=486, Methods) according to glioma grade. RNA sequencing RPKM values for the five hits from the preliminary screen are shown. Groups were compared for each gene individually using a one-way ANOVA. N.S. not significant; * $P < 0.05$; ** $P < 0.001$; *** $P < 0.0001$.

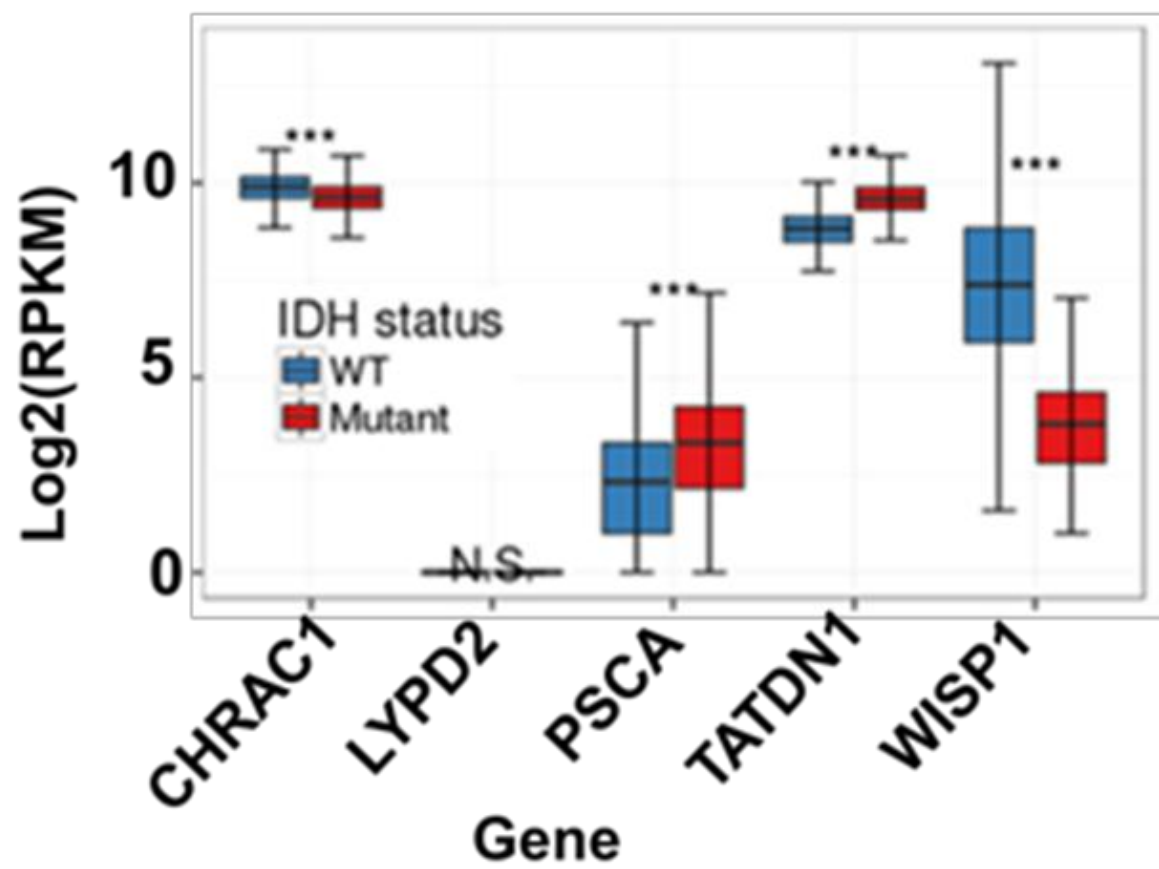


Figure 10. Comparison of gene expression in TCGA glioma samples (n=486, Methods) according to IDH status. RNA sequencing RPKM values for the five hits from the preliminary screen are shown. Groups were compared for each gene individually using a two-sided t-test. N.S. not significant; * $P < 0.05$; ** $P < 0.001$; *** $P < 0.0001$.

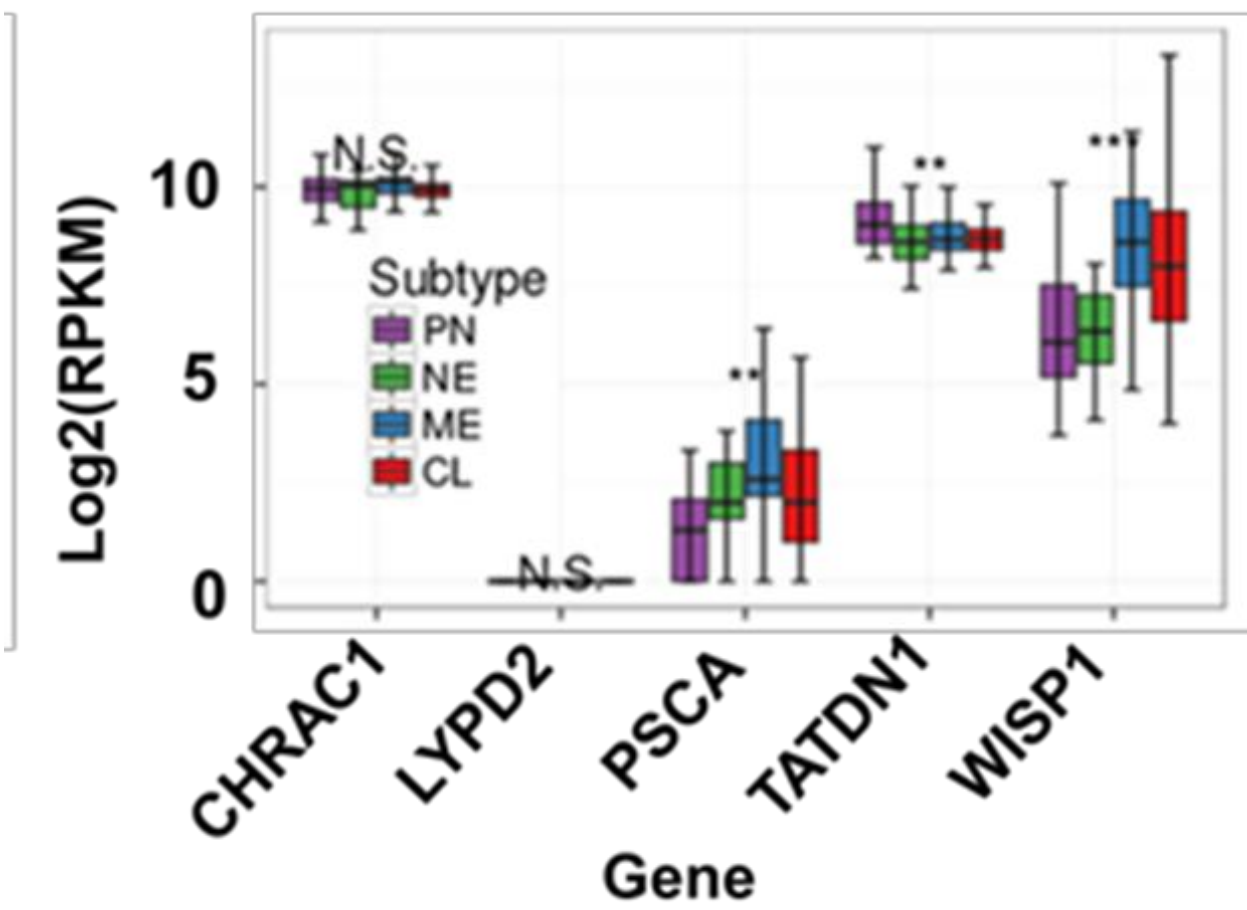


Figure 11. Comparison of gene expression in TCGA glioma samples (n=486, Methods) according to transcriptional subtype. RNA sequencing RPKM values for the five hits from the preliminary screen are shown. Groups were compared for each gene individually using a one-way ANOVA. N.S. not significant; * $P < 0.05$; ** $P < 0.001$; *** $P < 0.0001$.

Results 1.2: WISP1 overexpression drives tumor growth in GBM

We next sought to validate WISP1 as a driver of glioblastoma. Like before, GSC 7-11 cells were transduced to overexpress WISP1 in the same way but this time WISP1 was the only ORF. Again EGFRvIII expression and GFP expression were used as positive and negative controls. The cells were injected orthotopically again into the forebrains of nude mice and the latency of tumor development was compared to that of the GFP control. WISP1 overexpression alone was able to drive tumor growth resulting in a reduced latency (Fig 12). We also conducted this experiment in GSC 8-11 and found that WISP1 reduced the latency again (Fig 13). Now that we saw the effect of WISP1 overexpression in this orthotopic model, we were curious to see the effect in a more tangible subcutaneous model where we could easily see and assess tumor growth directly. The U87MG cell line was transduced to overexpress either WISP1_ires_GFP or GFP_ires_GFP and injected subcutaneously in the flanks of nude mice. The tumors overexpressing WISP1 grew significantly faster resulting in much larger tumors at the same time (Fig 14). They also had a higher percentage of Ki67 positive cells based on immunohistochemistry of the tumor tissue (Fig 15). These results indicated that WISP1 is able to drive tumor growth but we were also curious if WISP1 overexpression could induce tumor formation in a GBM line that does not readily form tumors subcutaneously. Again we found that WISP1 overexpression resulted in 40% tumor formation while it was 0% in the GFP expressing control using the

GBM line LN340 (Fig 16). These tumors were followed for close to 50 weeks but the results were the same since day 45 after implantation.

GSC 7-11

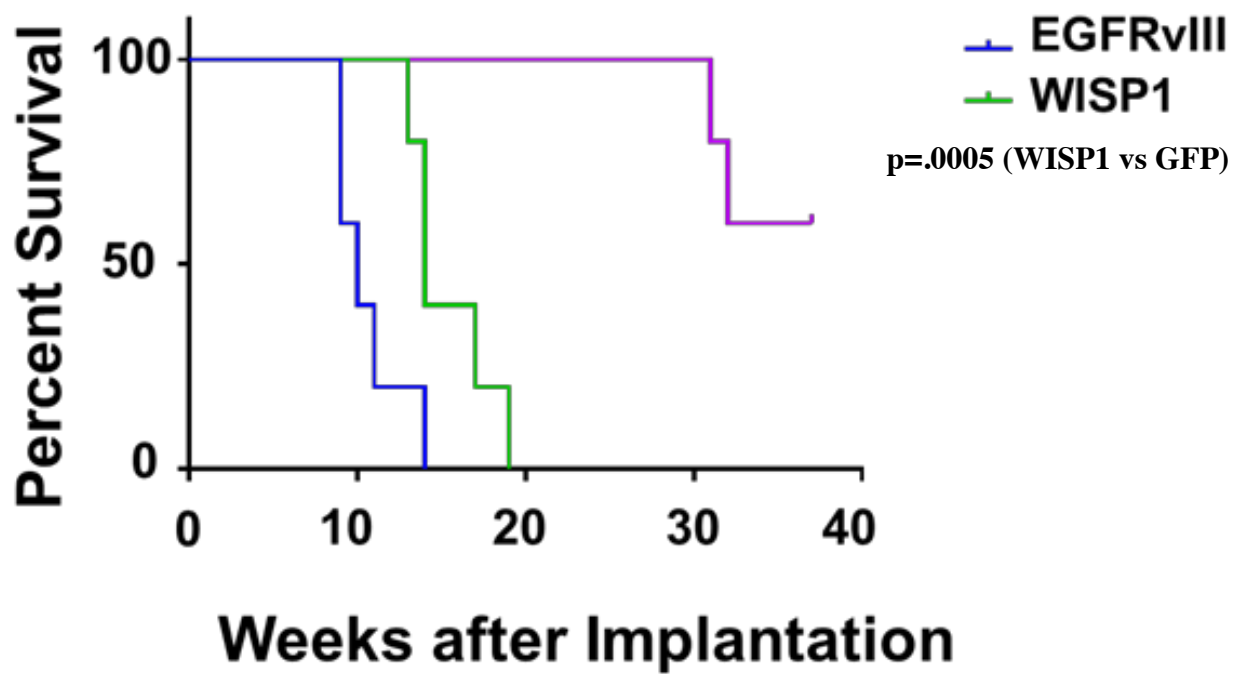


Figure 12. Survival curves for mice orthotopically injected with transduced GSC 7-11 cells. cells n=5 and the reduction in tumor latency after WISP1 overexpression compared to GFP control was statistically significant with $p=.0005$ based on LogRank (Mantel-Cox) test.

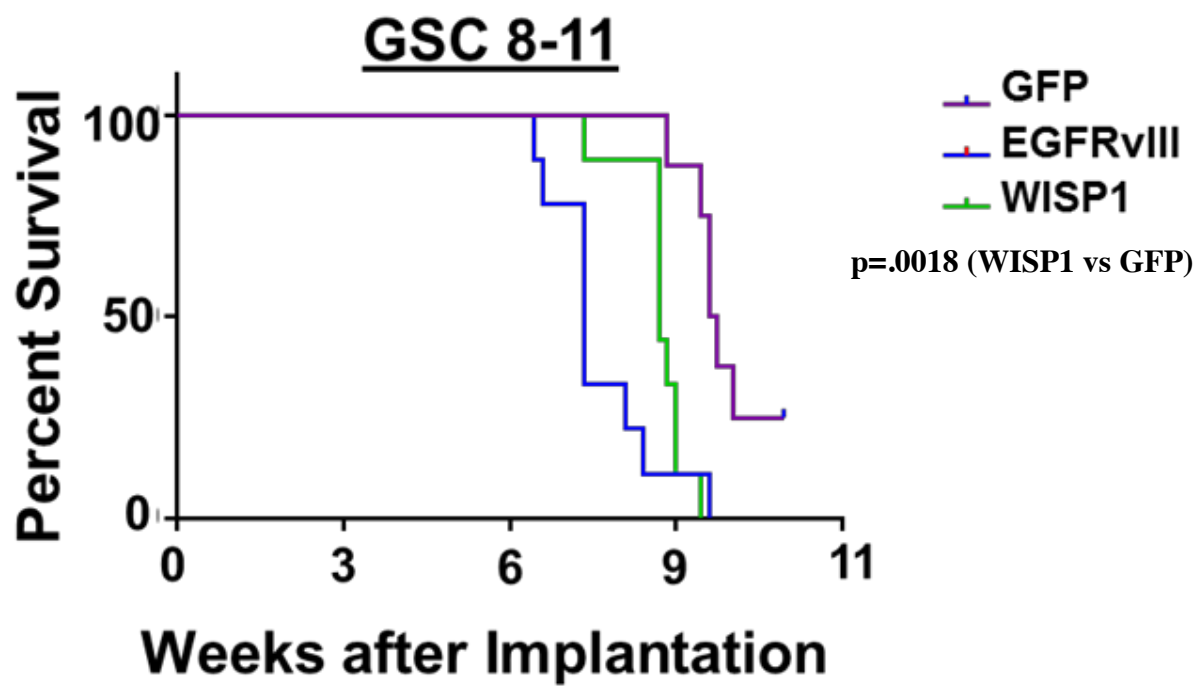
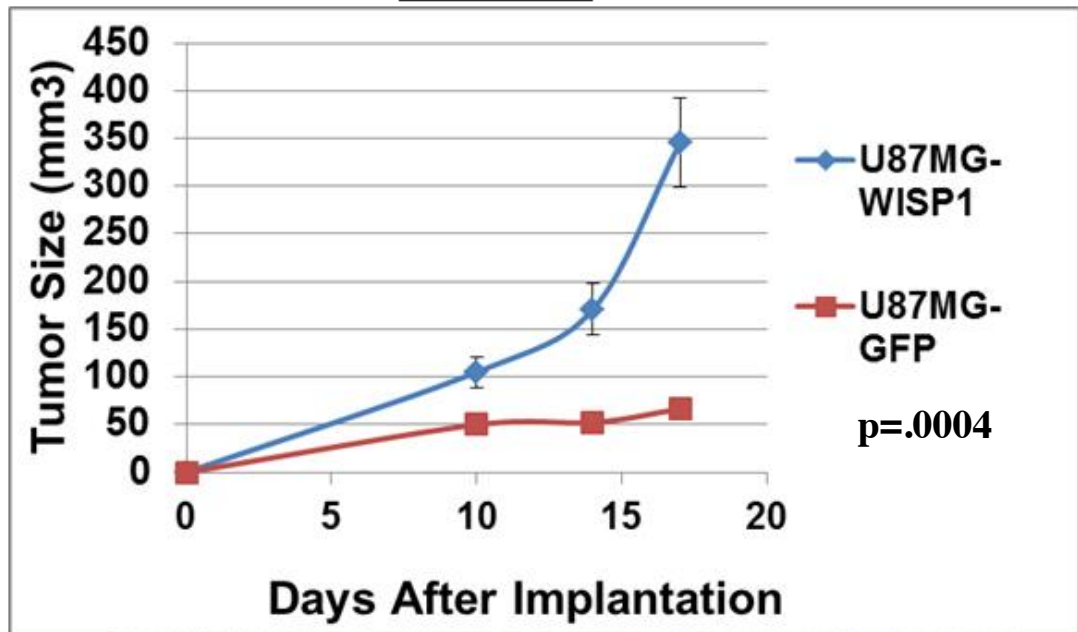


Figure 13. Survival curves for mice orthotopically injected with transduced GSC 8-11 cells. n=9 (WISP1 group) and n=8 (GFP group). The reduction in tumor latency after WISP1 overexpression compared to GFP control was statistically significant with $p=.0018$ based on LogRank (Mantel-Cox) test.

U87MG

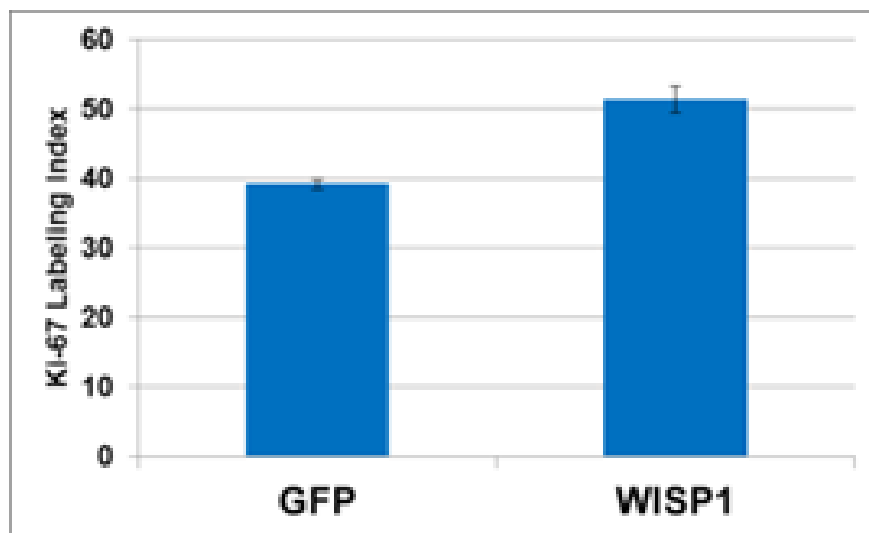
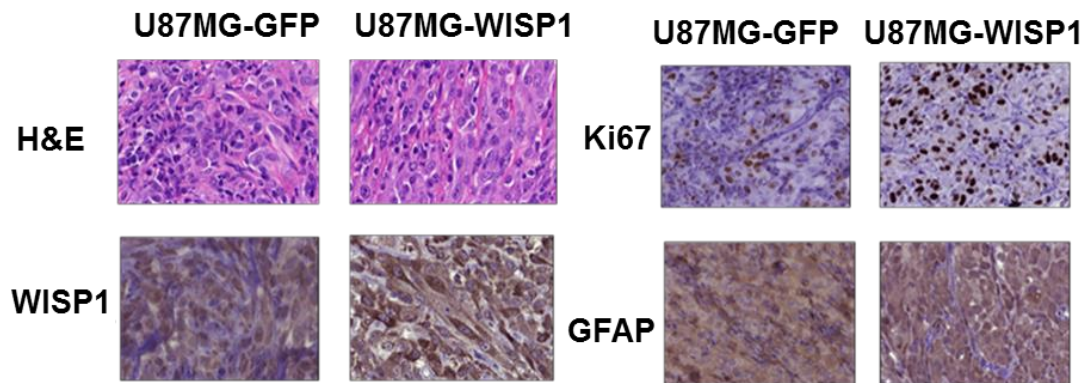


WISP1

GFP



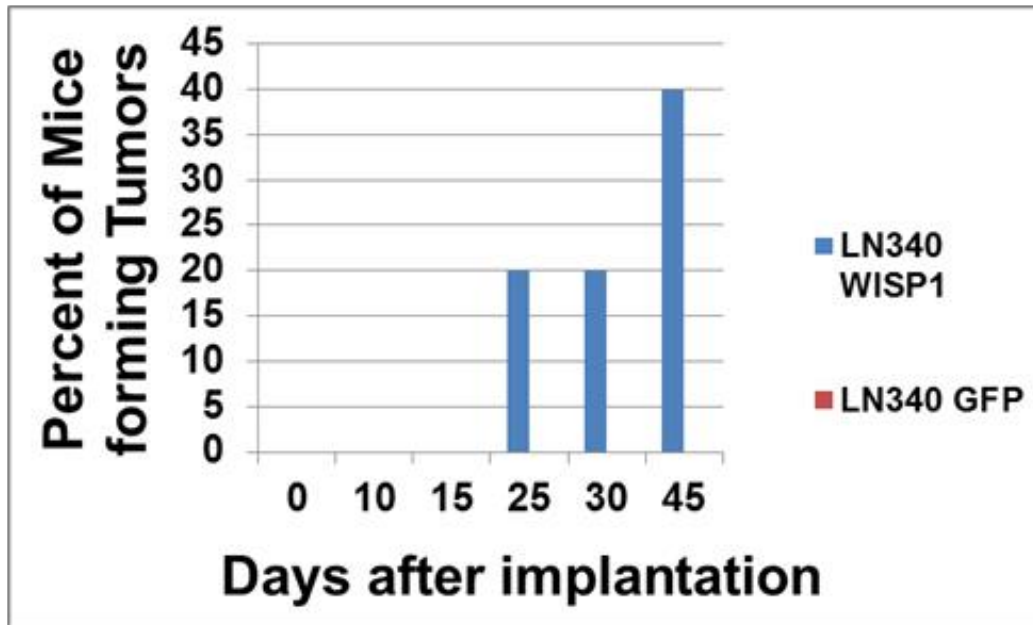
Figure 14. Tumor growth after subcutaneous injection with U87MG cells transduced to overexpress WISP1 or GFP. n=10 for each group of mice. The error bars represent the standard error of the mean. 3 million cells were injected per mouse. The photo is of the tumors at the last time point of the experiment. $p=.0004$ at the last time point based on two sided t test.



$p=.0001$

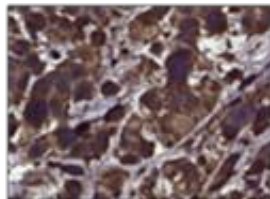
Figure 15. Immunohistochemistry of the tumors derived from the U87MG cells. The Ki67 labeling index was measured for both groups. The error bars represent standard deviation. $p=.0001$ based on two sided t test.

LN340



LN340 WISP1

GFAP



β III
Tubulin

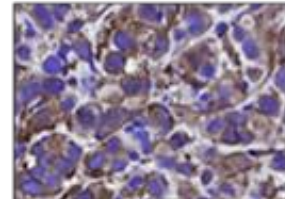


Figure 16. Percent of tumor formation over time after subcutaneous injection with LN340 cells transduced to overexpress WISP1 or GFP. n=10 for each group of mice. 3 million cells were injected per mouse. Immunohistochemistry of the resulting tumors after WISP1 overexpression (bottom).

Results 1.3: WISP1 knockdown reduces growth in GBM

We next sought to understand if WISP1 suppression had a pronounced phenotype as this would be very interesting from a potential therapeutic perspective. We conducted colony formation assays and knocked down the expression of WISP1 using two shRNAs targeting the 3'UTR of WISP1 mRNA in LN340 and LN229. Compared to the non-targeting shRNA control (shNT), knockdown of WISP1 resulted in fewer colonies *in vitro* (Fig 17, 18). In order to confirm that the observed effects were on target, we went ahead to rescue the impaired ability to form colonies after WISP1 knockdown. Expression of WISP1 cDNA that lacks the 3'UTR targeted by sh70 was able to rescue the impairment in colony formation induced by WISP1 knockdown in both LN340 and LN229 (Fig 19, 20). Knockdown of WISP1 in the GSC 6-27 line using four shRNAs led to a reduction in growth as measured by a cell viability assay that measures ATP (Fig 21). Sh50 and sh52 targeted the coding region while sh70 and sh91 targeted the 3'UTR of the endogenous WISP1 mRNA. Photos taken on the last day of the growth assay also indicated reduced growth (Fig 21).

We next wanted to see if WISP1 knockdown could reduce tumor growth *in vivo*. Again we knocked down expression of WISP1 in U87MG cells using the sh91 shRNA. The cells were injected subcutaneously. No tumors resulted after knockdown of WISP1 while the control non-targeting shRNA (shNT) expressing tumors grew predictably as U87MG does (Fig 22). These experiments nominate WISP1 as a potential target of interest for future GBM therapy.

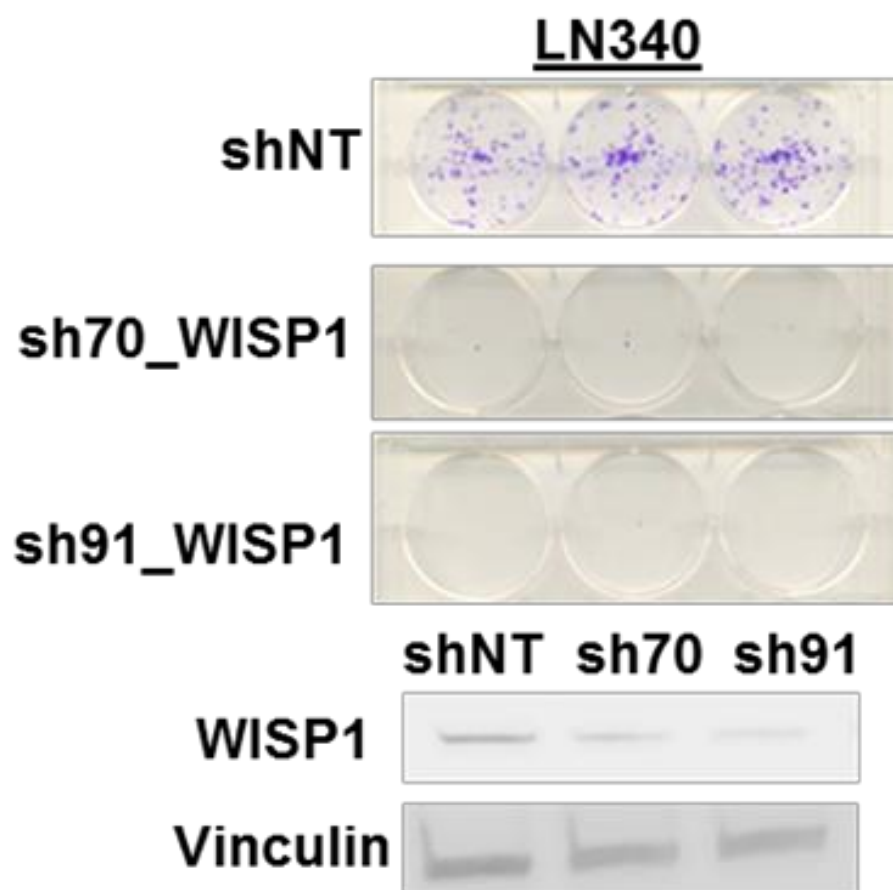
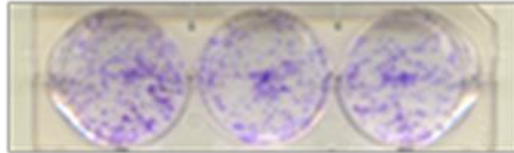


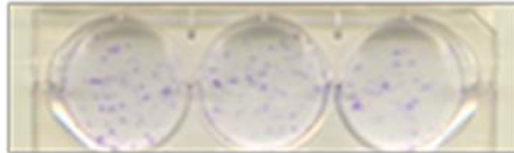
Figure 17. Colony formation assay after WISP1 knockdown with two different shRNAs in LN340 cells. Immunoblot is for WISP1 in control and knockdown lines.

LN229

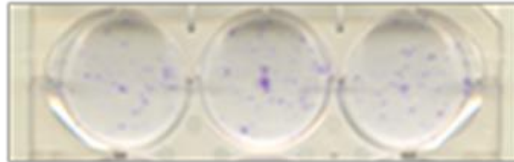
shNT



sh70_WISP1



sh91_WISP1



shNT sh70 sh91

WISP1



Vinculin



Figure 18. Colony formation assay after WISP1 knockdown with two different shRNAs in LN229 cells. Western blot for WISP1 in control and knockdown lines.

LN340

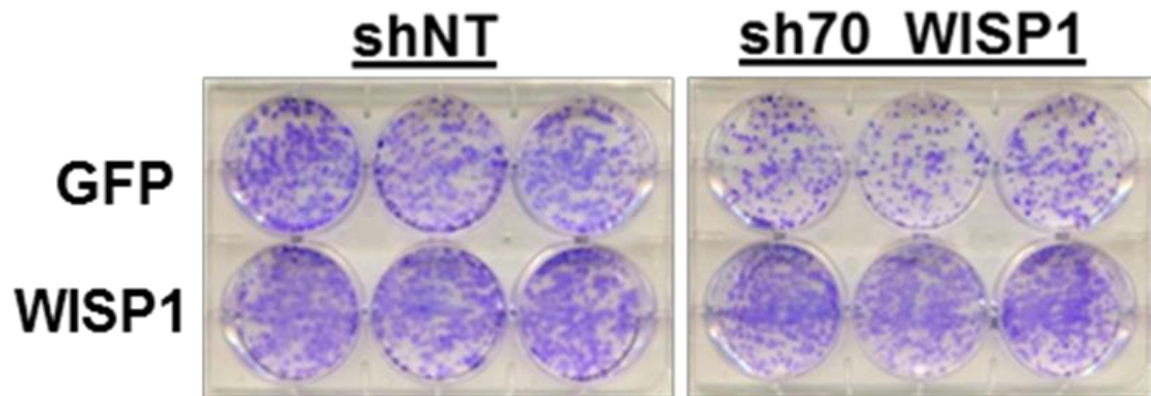


Figure 19. Rescue experiment showing colony formation assay in LN340 cells expressing either pHAGE-WISP1_ires_GFP or pHAGE-GFP_ires_GFP. The cells also expressed either an shRNA targeting WISP1 (sh70) or a control shRNA (shNT). Protein expression is shown in the immunoblot for each condition.

LN229

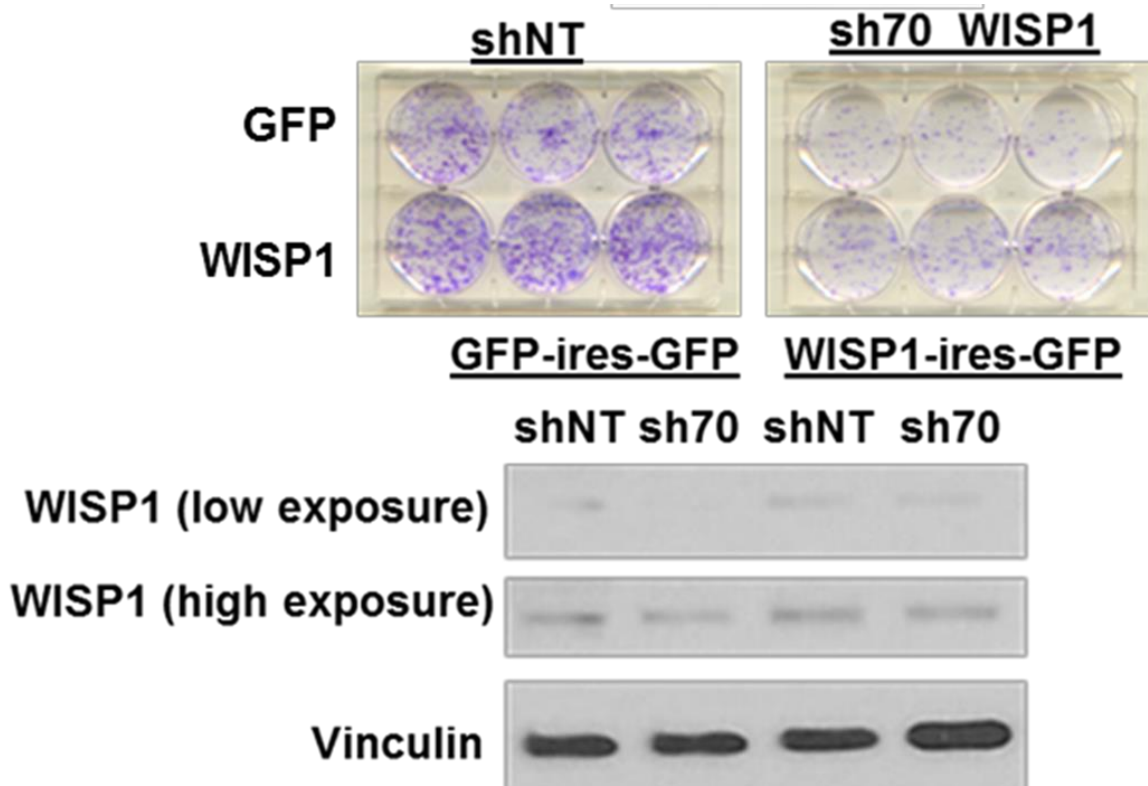


Figure 20. Rescue experiment showing colony formation assay in LN229 cells expressing either pHAGE-WISP1_ires_GFP or pHAGE-GFP_ires_GFP. The cells also expressed either an shRNA targeting WISP1 (sh70) or a control shRNA (shNT). Protein expression is shown in the immunoblot for each condition.

GSC 6-27

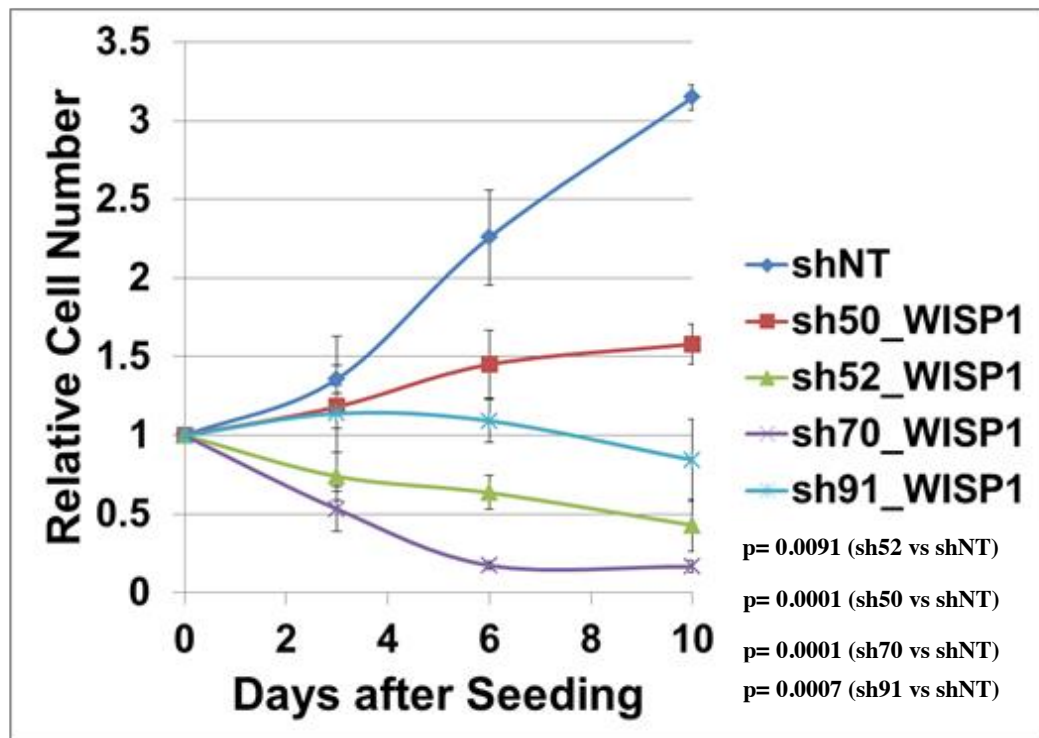
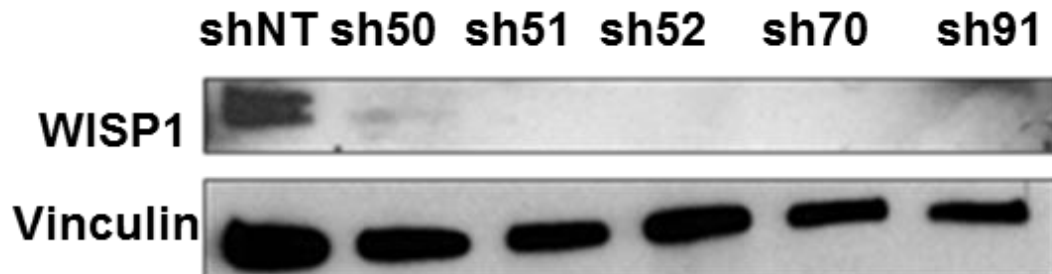
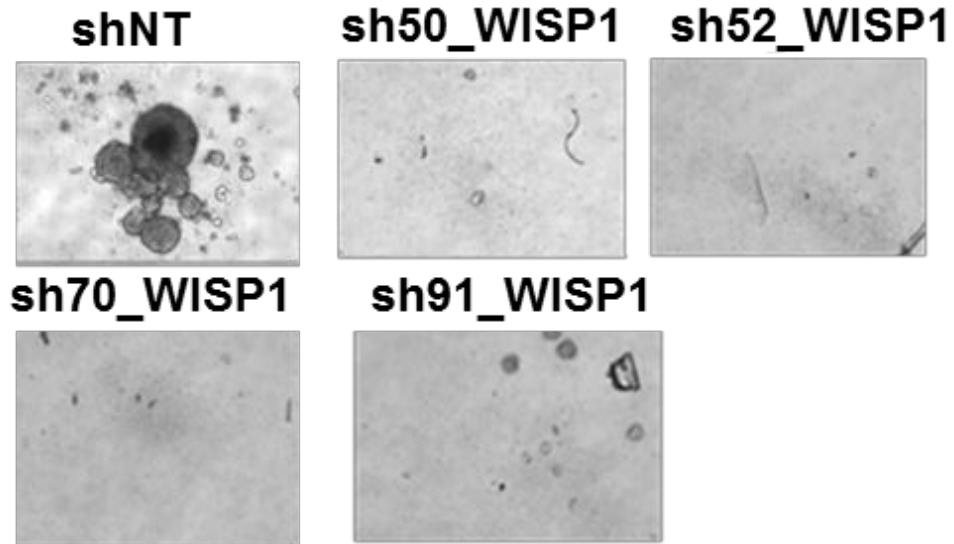


Figure 21. Growth of GSC 6-27 cells in culture after knockdown of WISP1. Values are relative cell growth based on CellTiterGlo measurements of viability over time normalized to day 0. The error bars represent standard deviation. The pictures were taken on the last time point. Western blots for WISP1 in control and knockdown lines are also shown. $p=0.0001$ (sh50 vs shNT), $p=0.0091$ (sh52 vs shNT), $p=0.0001$ (sh70 vs shNT), $p=0.0007$ (sh91 vs shNT)

U87MG

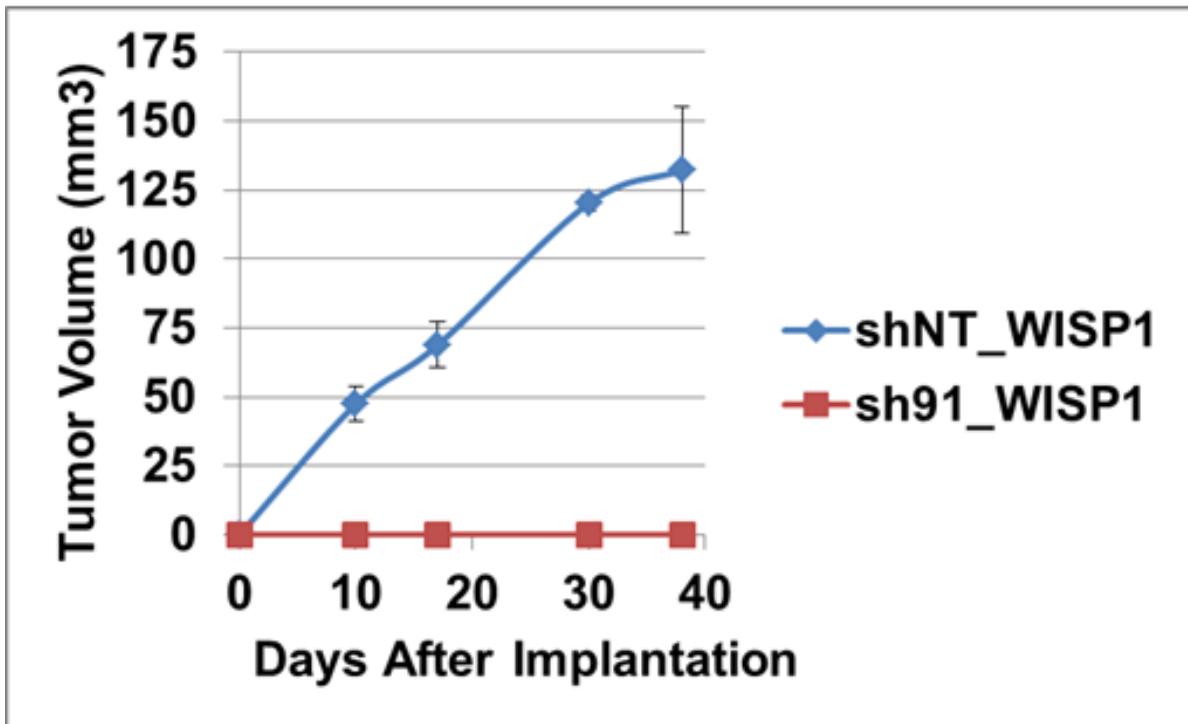


Figure 22. Subcutaneous tumor growth after injection with U87MG cells expressing either control shRNA (shNT) or shRNA targeting WISP1 (sh91). n=4 for the number of mice in the shNT control group and n=5 in the sh91 knockdown group. The error bars indicate the standard error of the mean.

Results 1.4: Generation of truncated forms of WISP1 lacking specific modules

WISP1 is a secreted matricellular protein. It is composed of 367 amino acids and in addition to the signal peptide (SP) module it contains four structural modules (23). The structural modules are IGFBP, VWC, TSP, and CT. The IGFBP module is structurally related to the insulin-like growth factor binding domain while the VWC module comprises the von Willebrand factor type C domain. The TSP module is homologous to the thrombospondin type I repeat and the CT module is structurally related to the carboxyl-terminal domain (52). We were interested in understanding which of these modules are necessary for the tumor driving phenotype in glioblastoma. In order to tackle this problem, we developed constructs of WISP1 in pHAGE lacking each of these 5 modules using the bicistronic vector as before (Fig 23). There is a natural variant of WISP1 which lacks the VWC module. We used that variant as the delta VWC since it is naturally occurring. U87MG cells were transduced to overexpress either GFP, EGFRvIII, WISP1, or one of the WISP1s designed to lack one of the five modules. The U87MG line was chosen because it gave a very dramatic *in vivo* difference in previous experiments allowing us to now use this system to identify portions of WISP1 that are necessary for the phenotype. We performed western blot analysis on these cells to confirm the presence of these truncated forms of WISP1 (Fig 24). Since the CT module overlaps with the epitope for the WISP1 antibody we had to use another WISP1 antibody whose epitope overlaps with the VWC module

instead. This allowed us to detect the CT module (Fig 24). We also sequence confirmed expression of the respective truncated form of WISP1 expressed in each

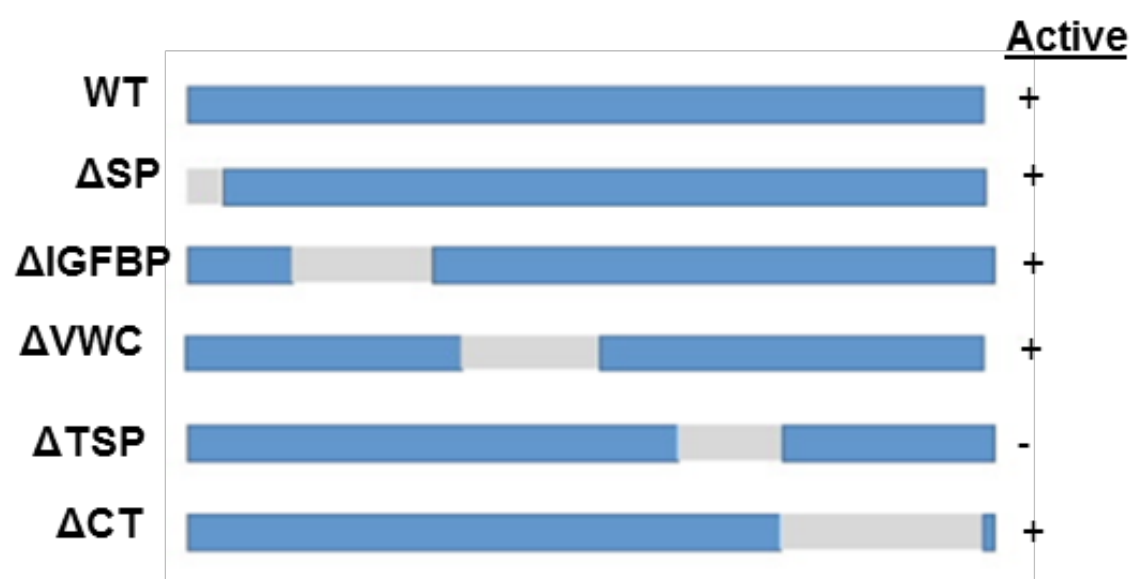


Figure 23. Diagram depicting the truncated forms of WISP1 made for these experiments. The in vivo growth promoting activity found here (Figure 5) is also indicated for each truncated form.

U87MG Cell Lysate

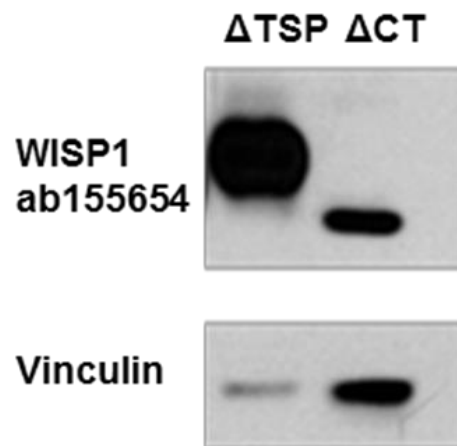
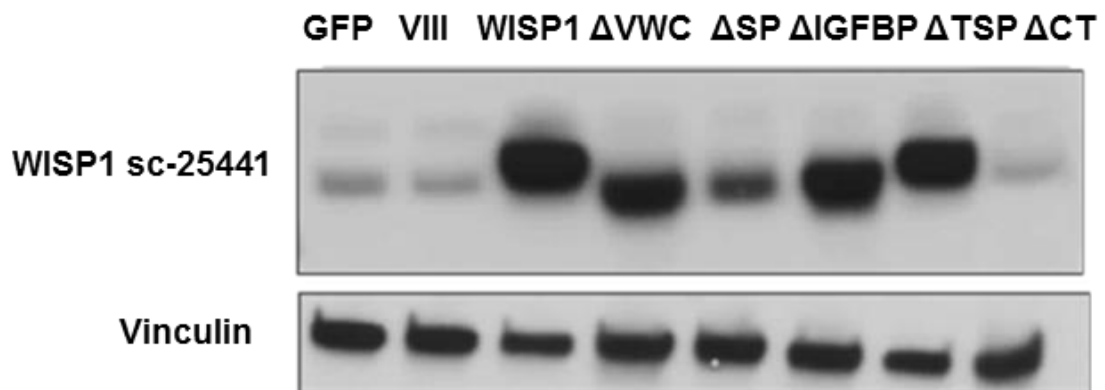


Figure 24. Immunoblots from lysates of U87MG cells expressing each truncated form and the controls (GFP, EGFRvIII, WISP1). Two different antibodies were used since the Δ CT WISP1 is not picked up by the antibody that recognizes an epitope from amino acids 311-367 (sc-25441) while the Δ VWC WISP1 is not picked up by the antibody that recognizes an epitope from amino acids 135-230 (ab155654). An immunoblot membrane using the same antibody against WISP1 used for the ELISA experiments (1627-WS) confirms that the antibody recognizes all the truncated forms except for Δ CT WISP1.



Figure 25. An immunoblot membrane using the same antibody against WISP1 used for the ELISA experiments (1627-WS) confirms that the antibody recognizes all the truncated forms except for Δ CT WISP1.

transduced line. The SP module is a tag that targets a protein for secretion. The delta SP WISP1 should thus not be secreted. ELISA was performed on the media of each of these respective cell lines expressing either a truncated form of WISP1, wild type WISP1, GFP, or EGFRvIII. The particular antibody used in this ELISA does not detect the delta CT WISP1 so we could not measure the concentration of delta CT WISP1 in the media (Fig 25). We found that the wild type WISP1, delta VWC WISP1, and delta IGFBP WISP1 had high concentrations in the media of their respective cells (Fig 26). The concentration of delta SP WISP1 and delta TSP WISP1 in the media were comparable to that of endogenous WISP1 in the media of GFP and EGFRvIII expressing cells. However, delta SP WISP1 and delta TSP WISP1 were detectable by immunoblotting when using the same antibody that was used for the ELISA. This indicated that delta SP WISP1 and delta TSP WISP1 are not secreted (Fig 25, 26). We wanted to further confirm that these truncated forms of WISP1 are truly not secreted so we performed ELISA on the cell lysate and the cell media using the same protein concentration for both. The concentration of WISP1 in the media of delta SP WISP1 and delta TSP WISP1 overexpressing cells matched that of the endogenous protein in the media of control cells expressing GFP or EGFRvIII. However, higher levels of delta SP WISP1 and delta TSP WISP1 were detected in the lysate as would be predicted (Fig 27, 28). This further confirmed that delta SP WISP1 and delta TSP WISP1 were not present in the media proving that they were indeed not secreted.

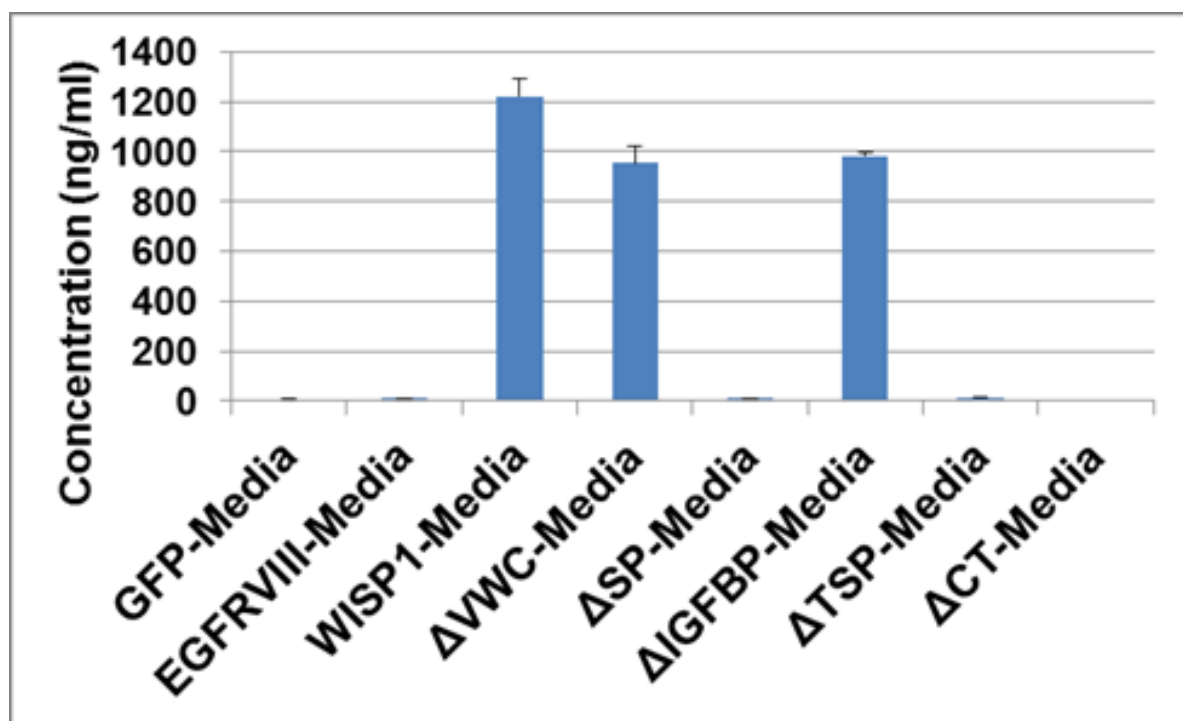


Figure 26. ELISA for WISP1 of media from the cells expressing the truncated forms of WISP1 and the controls (GFP, EGFRvIII, WISP1)

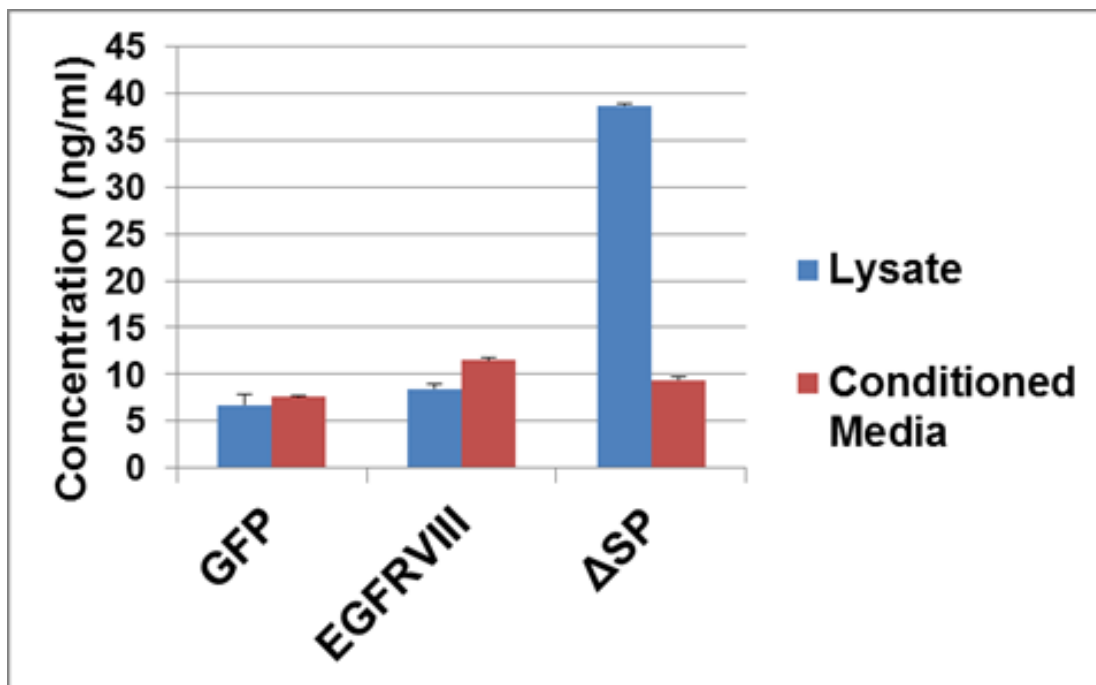


Figure 27. Media are from the same number of cells in the same volume of media for the same amount of time. ELISA for WISP1 comparing the same amount of total protein from cell lysate and conditioned media for cells expressing either GFP, EGFRvIII, or Δ SP WISP1

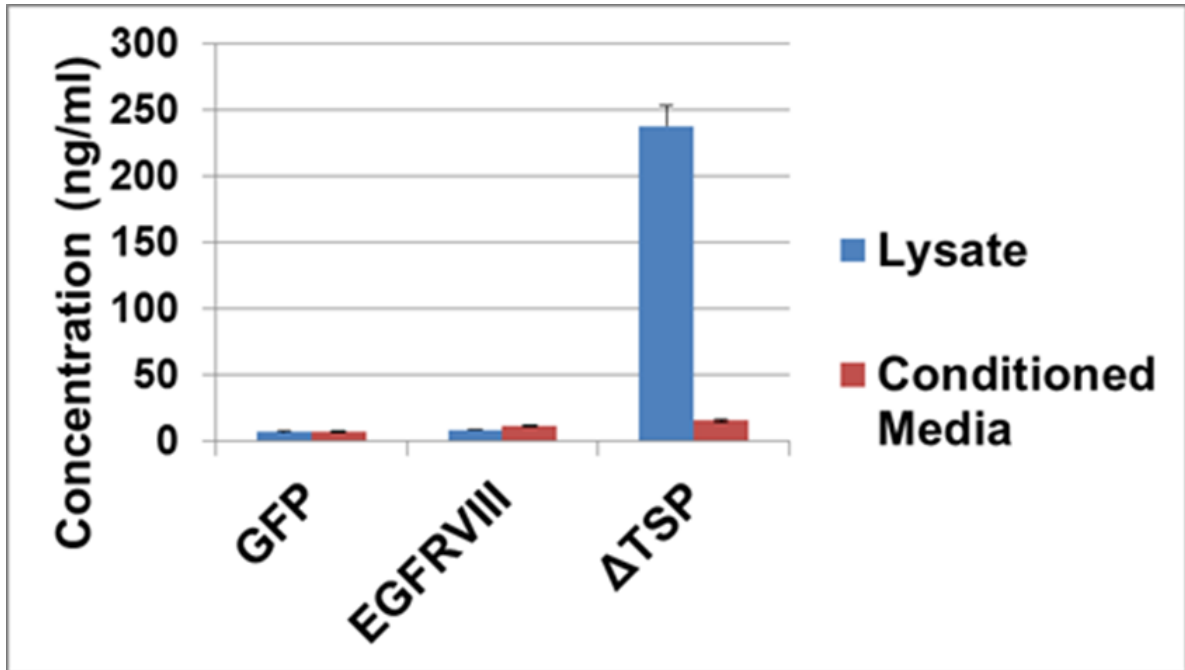


Figure 28. ELISA for WISP1 comparing the same amount of total protein from cell lysate and conditioned media for cells expressing either GFP, EGFRvIII, or Δ TSP WISP1

Results 1.5: Structural functional analysis indicates that non-secreted Δ SP WISP1 is able to drive growth while Δ TSP WISP1 fails to produce any tumors *in vivo*.

We then injected these cells subcutaneously into the flanks of nude mice. WISP1 is known to function as a secreted protein. However, contrary to conventional wisdom, expression of the delta SP WISP1 was able to drive tumor growth even better than any other form of WISP1 (Fig 29-32). Intriguingly, expression of the delta TSP WISP1 resulted in the formation of no tumors (Fig 30). Expression of the rest of the truncated forms of WISP1 including overexpression of the wild type form gave a similar phenotype (Fig 29-32). We repeated this *in vivo* experiment again and got the same exact results. We performed western blots on the protein extracted from these tumors and confirmed the presence of the truncated forms of WISP1 (Fig 33). These results indicate that WISP1 is able to drive tumor growth inside the cell without being secreted and that the TSP module is necessary for the phenotype.

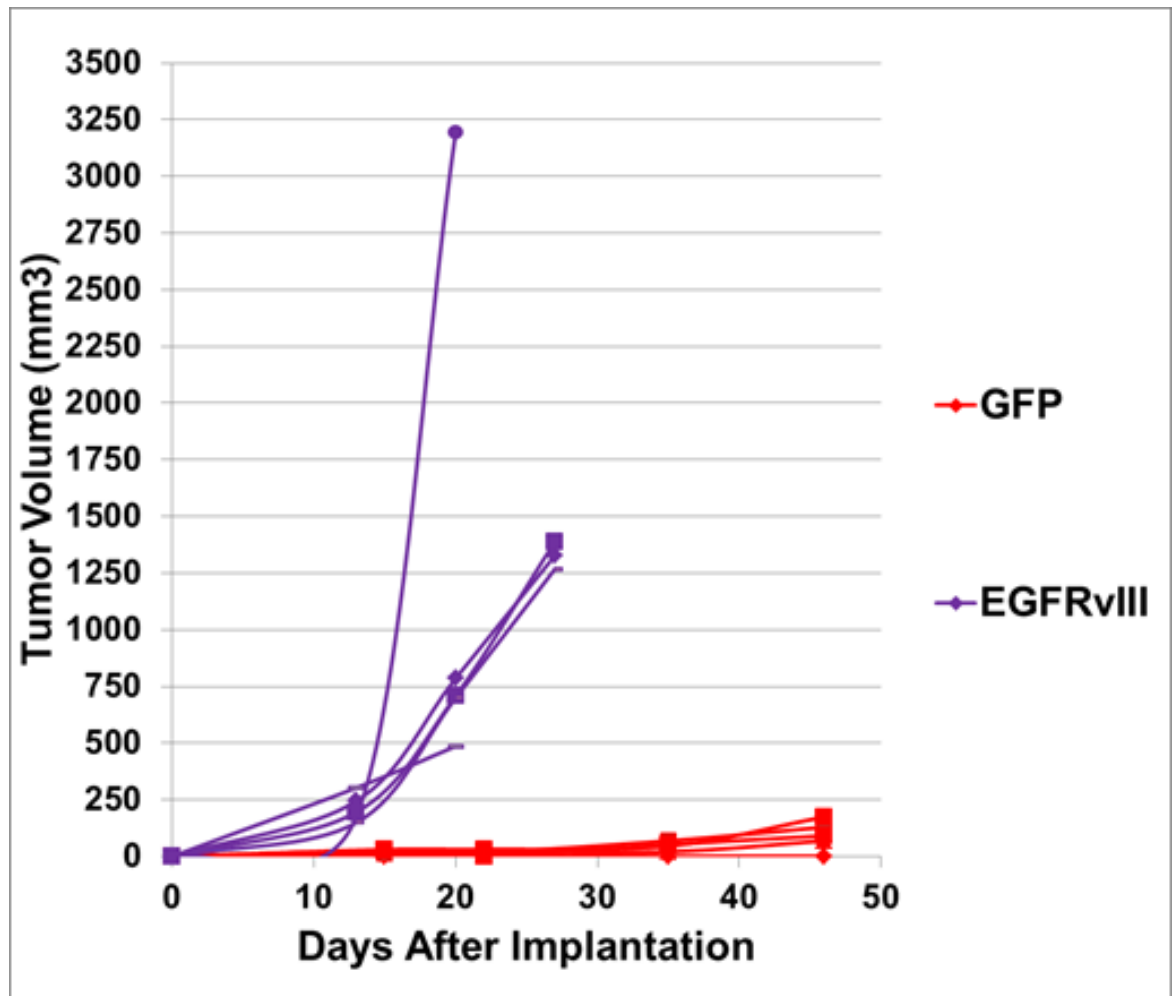


Figure 29. Subcutaneous tumor growth after injection with U87MG cells expressing each truncated form of WISP1 and the controls (GFP, EGFRvIII, WISP1).. Here the GFP and EGFRvIII control groups are shown. n=5 for the number of mice in each group. Each line indicates the growth of an individual mouse. The color of the line indicates the group of the mouse which is indicated in the legend on the right. 1.5 million cells were injected per mouse.

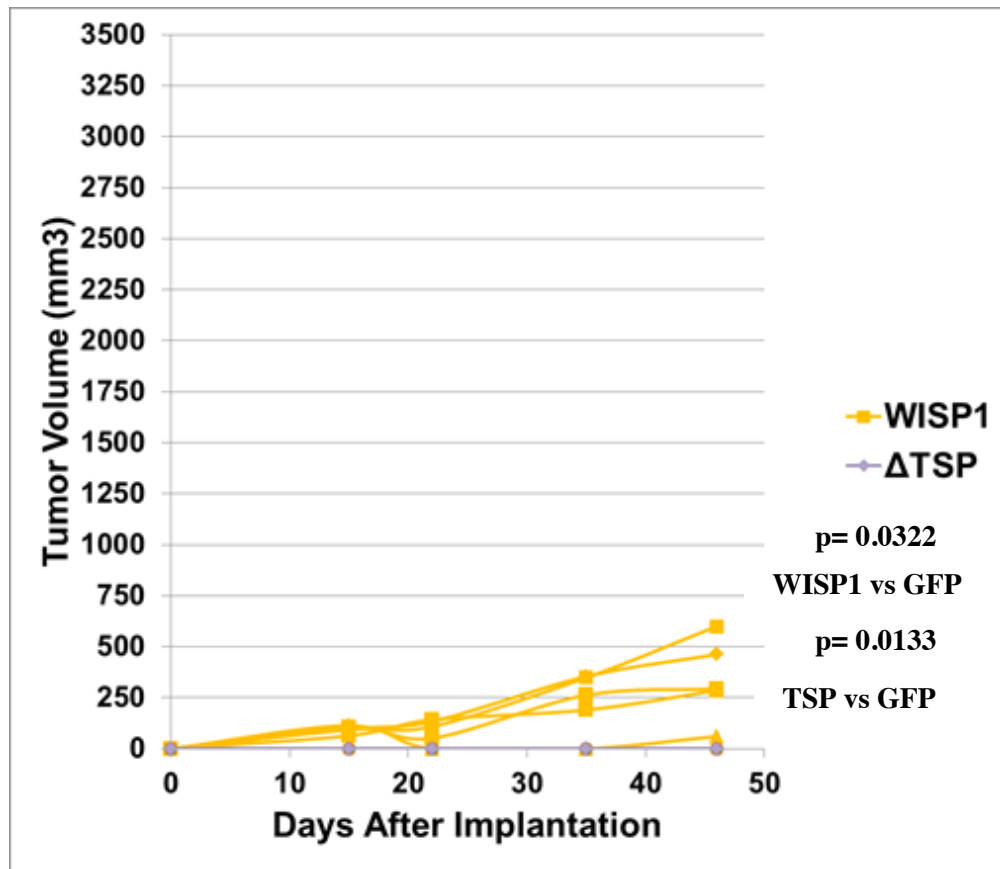


Figure 30. Subcutaneous tumor growth after injection with U87MG cells expressing each truncated form of WISP1 and the controls (GFP, EGFRvIII, WISP1).. Here the WISP1 and Δ TSP control groups are shown. n=5 for the number of mice in each group. Each line indicates the growth of an individual mouse. The color of the line indicates the group of the mouse which is indicated in the legend on the right. 1.5 million cells were injected per mouse. p= 0.0322 (WISP1 vs GFP); p= 0.0133 (TSP vs GFP). Statistics are based on two tailed t test of the measurements from the last time point.

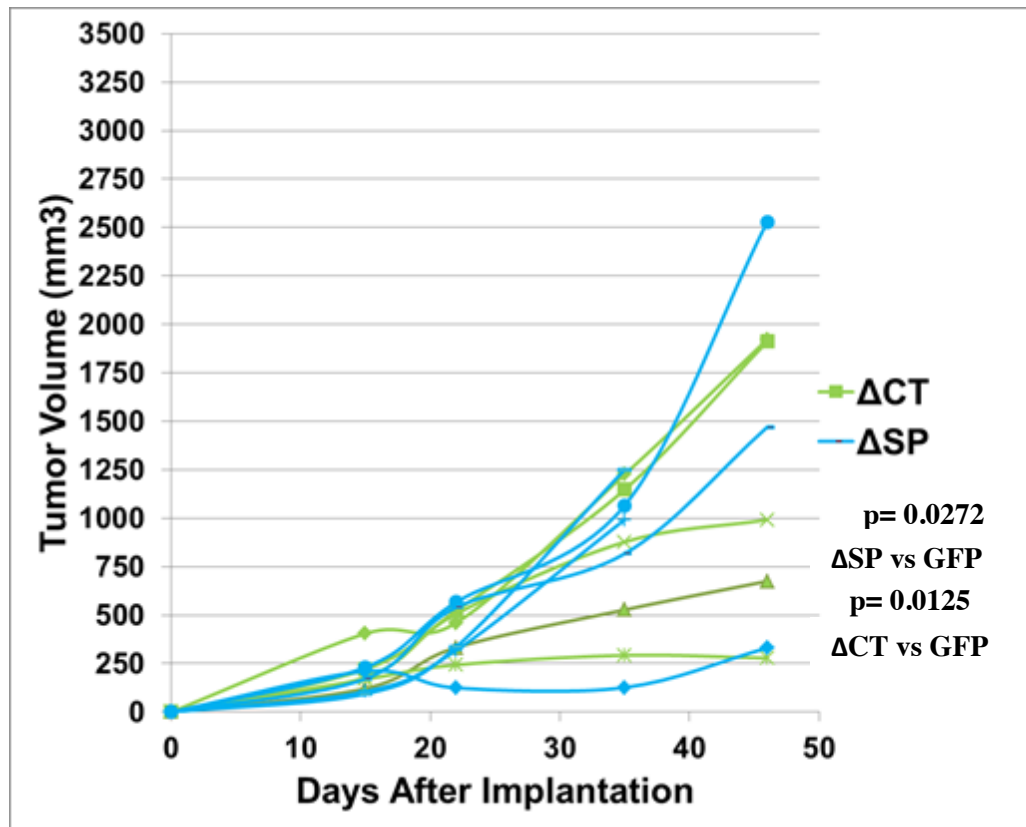


Figure 31. Subcutaneous tumor growth after injection with U87MG cells expressing each truncated form of WISP1 and the controls (GFP, EGFRvIII, WISP1).. Here the Δ CT and Δ SP control groups are shown. n=5 for the number of mice in each group. Each line indicates the growth of an individual mouse. The color of the line indicates the group of the mouse which is indicated in the legend on the right. 1.5 million cells were injected per mouse. p= 0.0272 (Δ SP vs GFP) ; p= 0.0125 (Δ CT vs GFP). Statistics are based on two tailed t test of the measurements from the last time point.

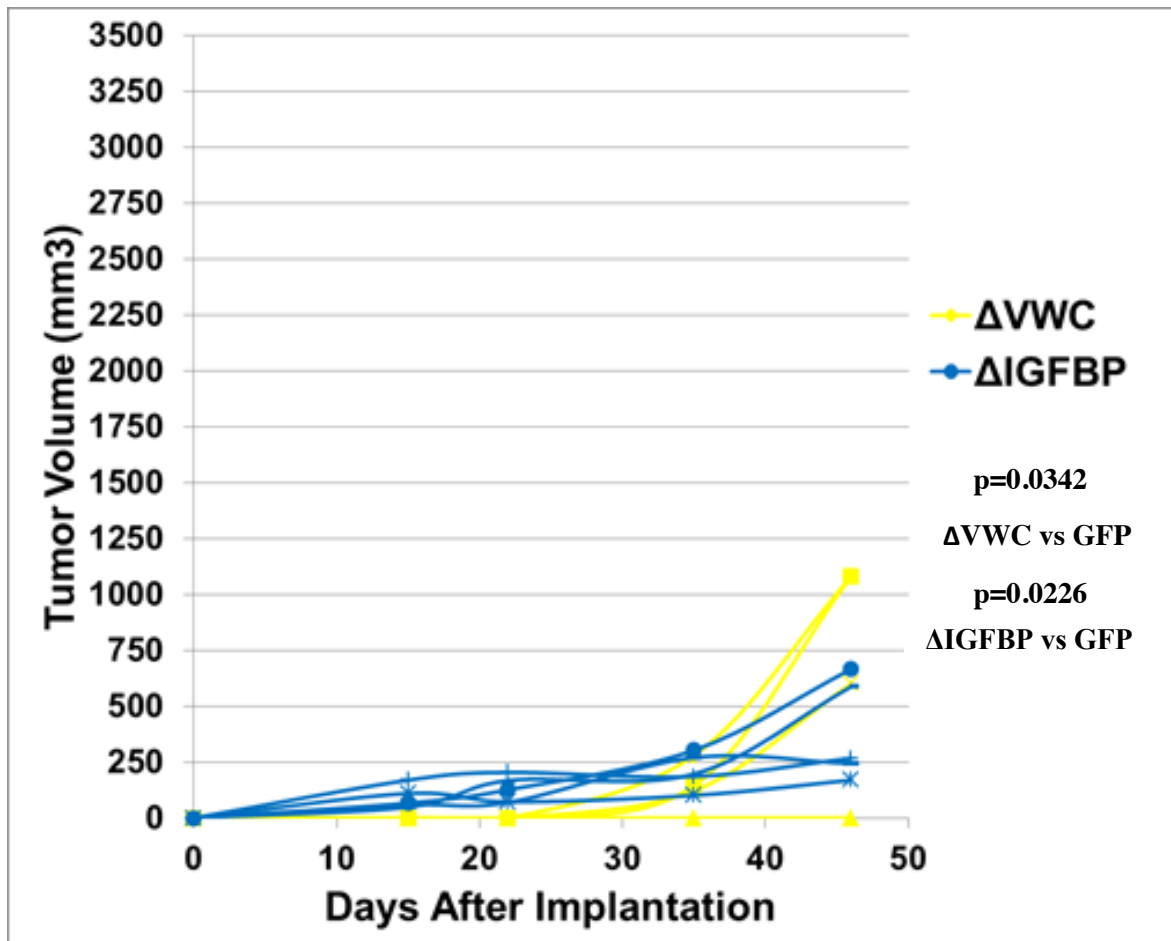


Figure 32. Subcutaneous tumor growth after injection with U87MG cells expressing each truncated form of WISP1 and the controls (GFP, EGFRvIII, WISP1). Here the Δ VWC and Δ IGFBP control groups are shown. n=5 for the number of mice in each group. Each line indicates the growth of an individual mouse. The color of the line indicates the group of the mouse which is indicated in the legend on the right. 1.5 million cells were injected per mouse. p= 0.0342 (Δ VWC vs GFP); p= 0.0226 (Δ IGFBP vs GFP). Statistics are based on two tailed t test of the measurements from the last time point.

U87MG Tumor Lysate

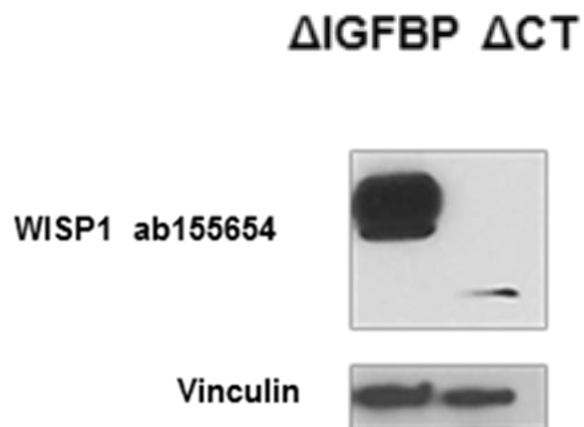
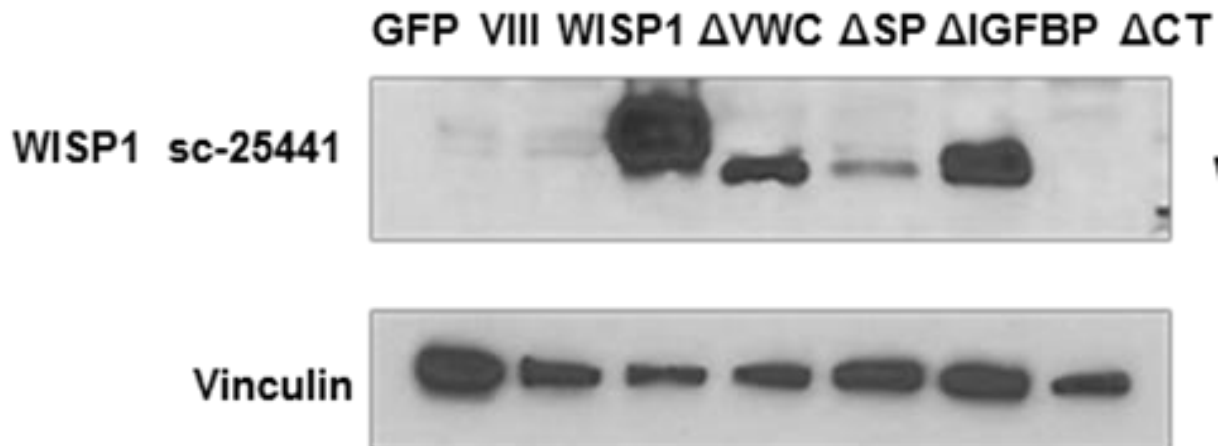


Figure 33. Immunoblots from lysates of the resulting U87MG subcutaneous tumors expressing each truncated form and the controls (GFP, EGFRvIII, WISP1). Again two different antibodies were used since the Δ CT WISP1 is not picked up by the antibody that recognizes an epitope from amino acids 311-367 (sc-25441) while the Δ VWC WISP1 is not picked up by the antibody that recognizes an epitope from amino acids 135-230 (ab155654). .

Results 1.6: Secreted WISP1 fails to drive growth in GBM

We were interested in understanding whether WISP1 drives tumor growth in a novel secretion independent fashion. In order to do this we needed to assess whether the secreted WISP1 is able to act as a driver. To investigate this we developed three cell lines for co-culture experiments. Using U87MG we developed a line expressing mCherry_ires_Luciferase, a line expressing both mCherry_ires_Luciferase and WISP1_ires_GFP, and a line expressing only WISP1_ires_GFP. The line overexpressing WISP1 and expressing mCherry was made from the same cells that were only expressing WISP1_ires_GFP to ensure that they overexpressed WISP1 at the same level. These three lines were flow sorted to make sure that all the cells either express GFP, mCherry, or both (Fig 34). The line expressing only WISP1_ires_GFP was mixed with either the line expressing both WISP1_ires_GFP and mCherry_ires_Luciferase or the one expressing only mCherry_ires_Luciferase. We mixed these cells in a 1:1 ratio and then confirmed the proportions by flow cytometry analysis. This generated two mixtures with the experimental mixture as a combination of green and red cells (WISP1_ires_GFP expressing cells and mCherry_ires_Luciferase expressing cells) and the control mixture as a combination of green and double positive cells (WISP1_ires_GFP expressing cells and WISP1_ires_GFP + mCherry_ires_Luciferase expressing cells). These cells were then either seeded for colony formation assay *in vitro* or injected subcutaneously *in vivo* (Fig 34). Our hypothesis behind this experiment was that if WISP1 drives growth through secretion then the line only expressing mCherry_ires_Luciferase should be

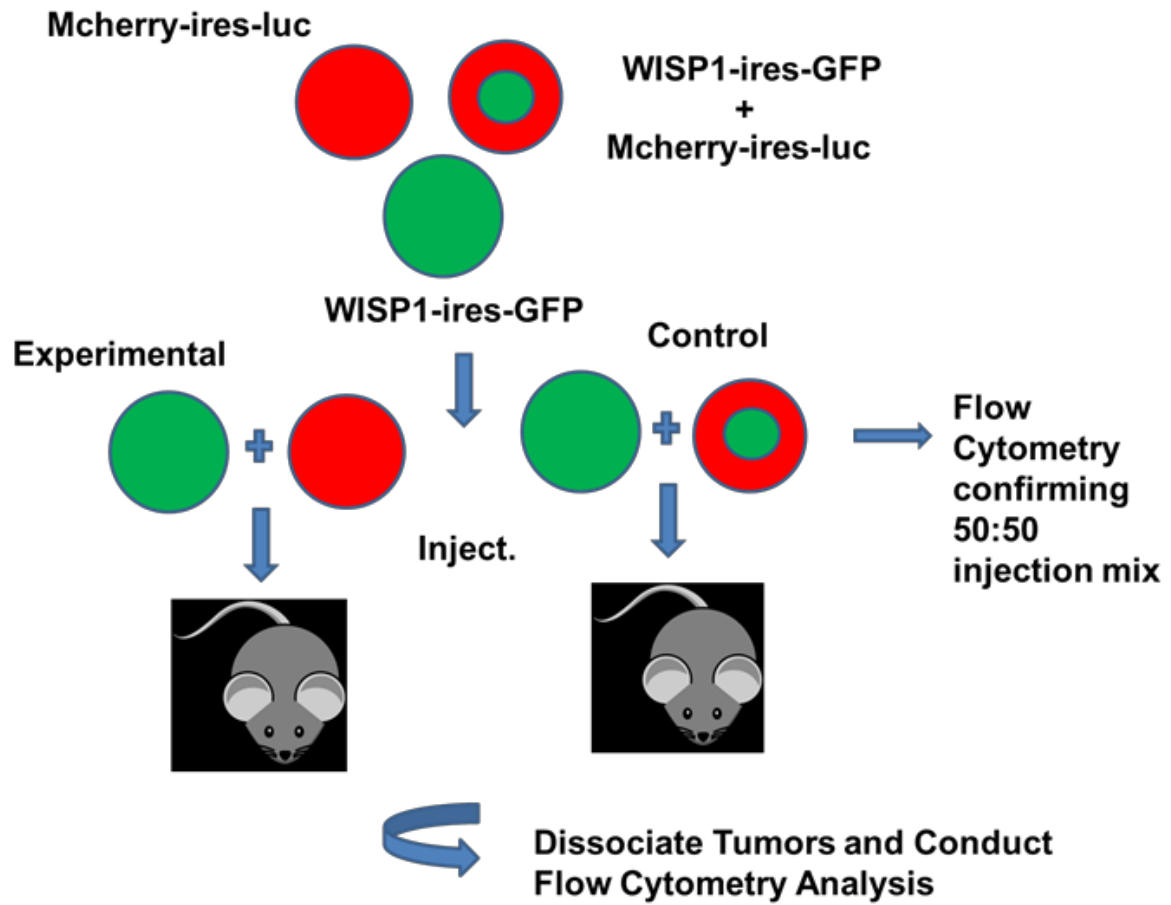
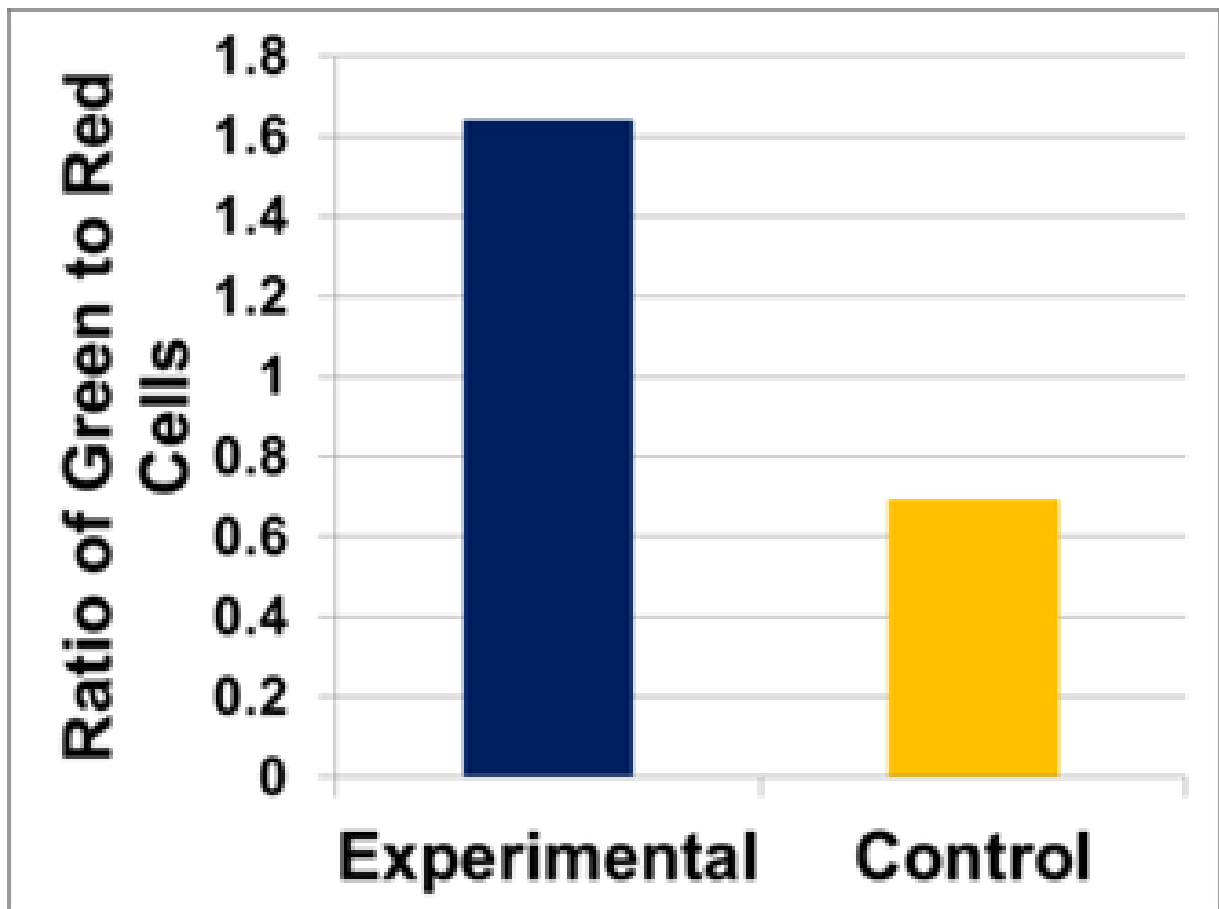
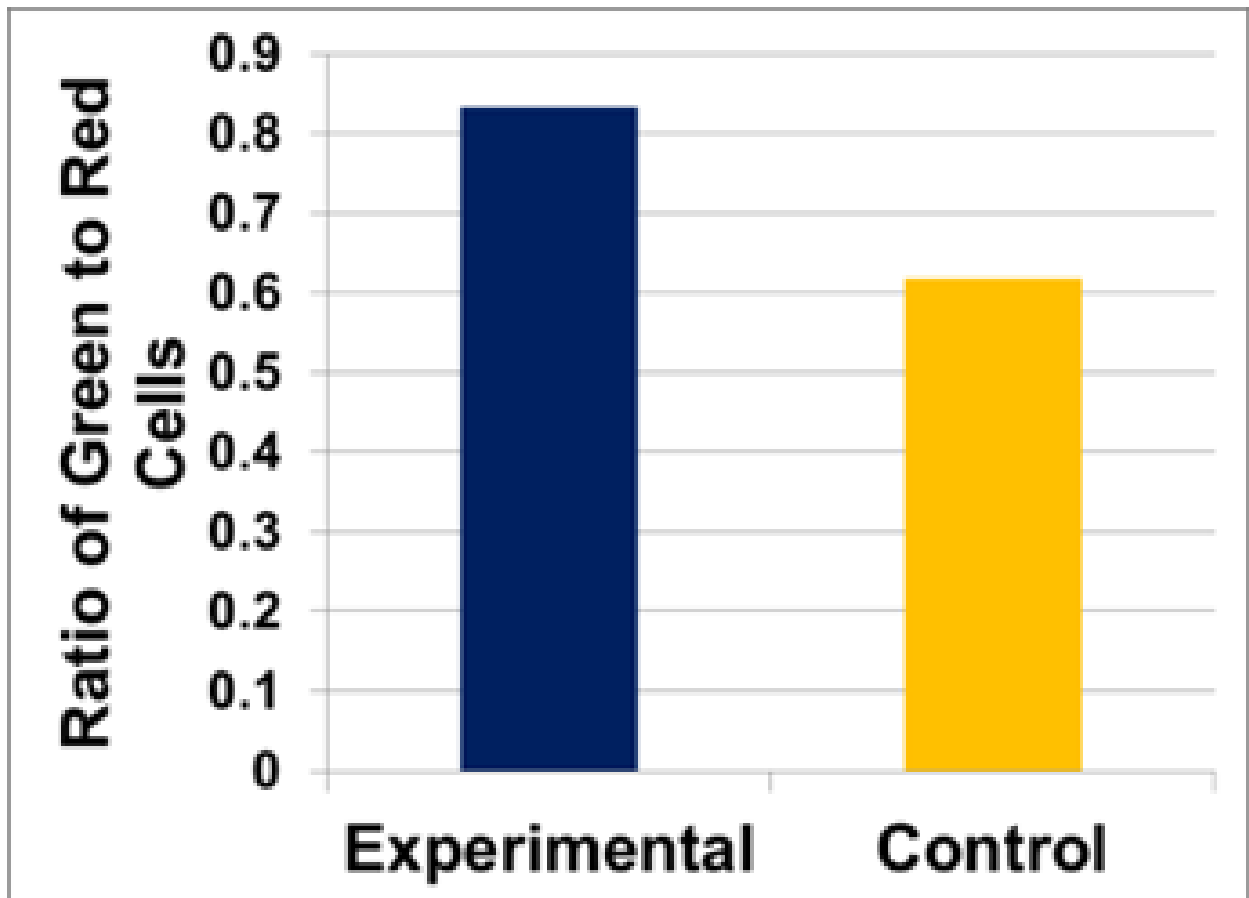


Figure 34. Schematic diagram describing the co-culture experimental design..

A



B



C

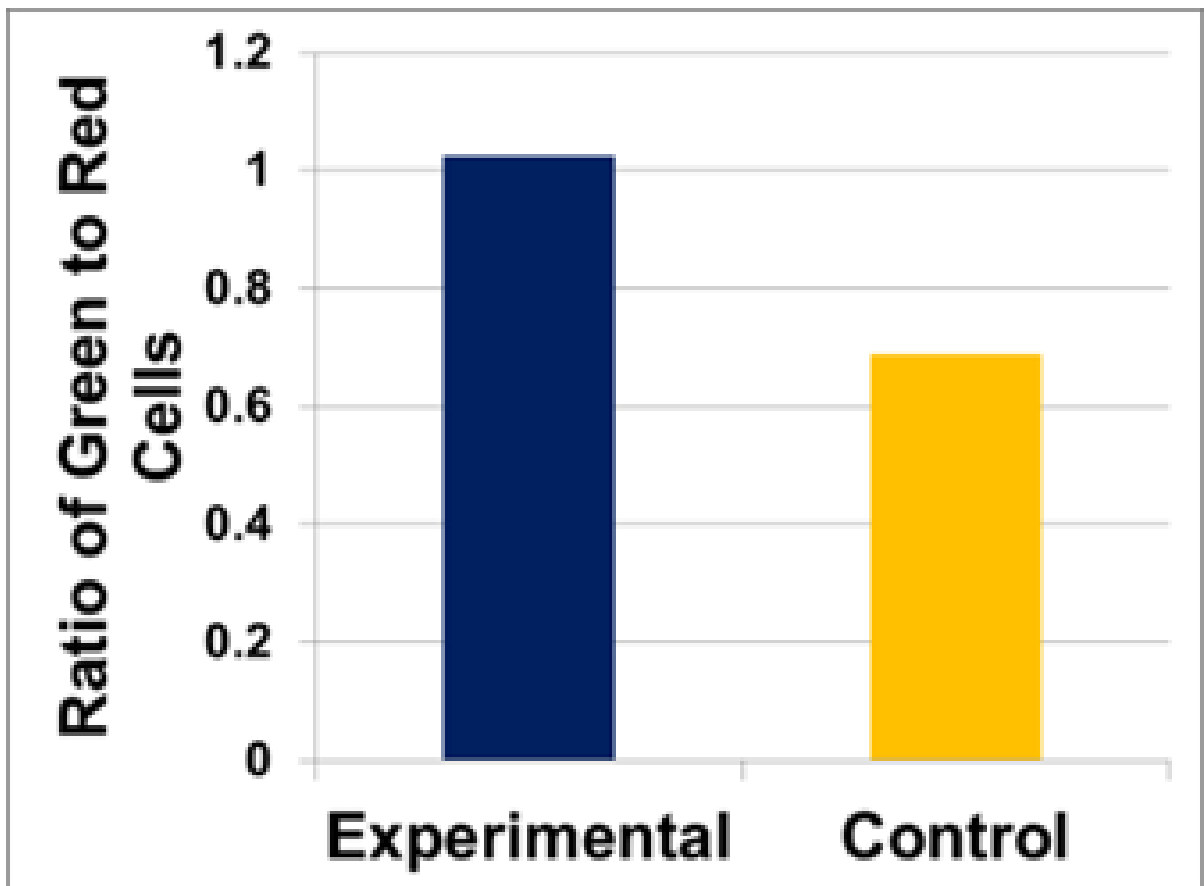
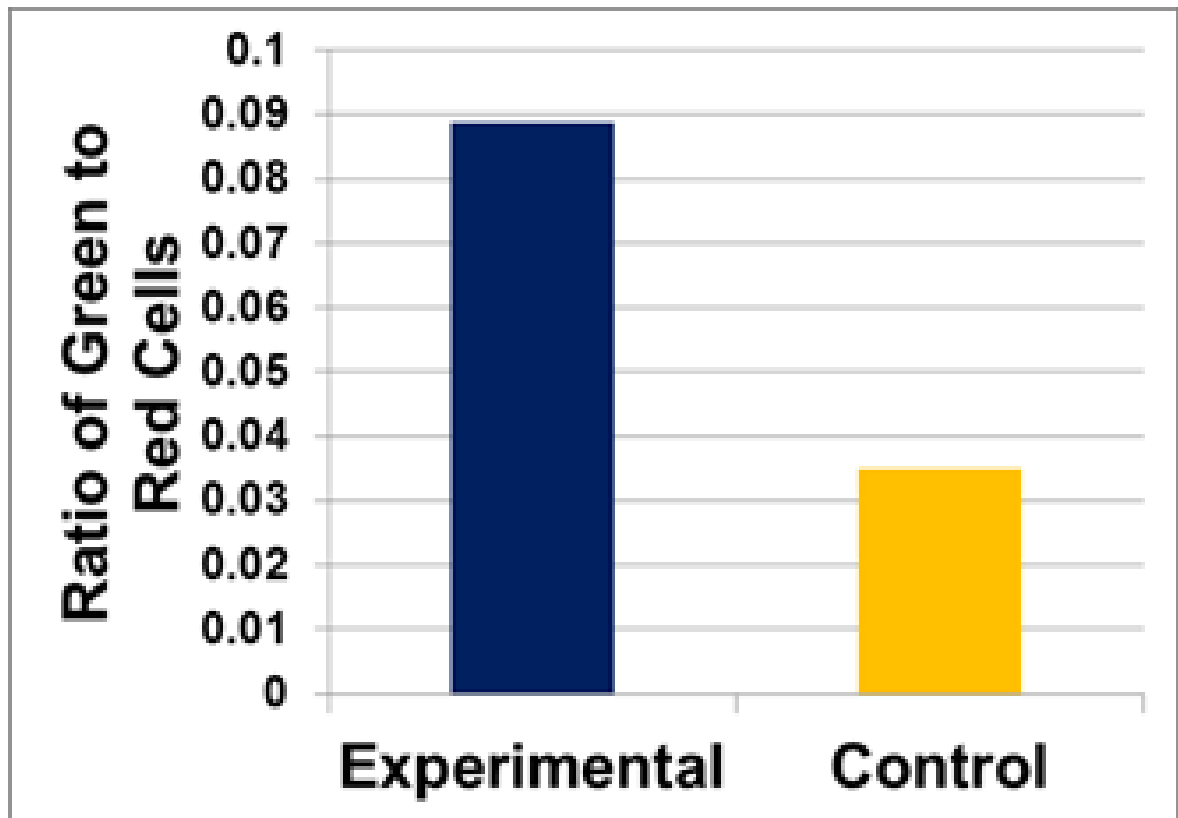


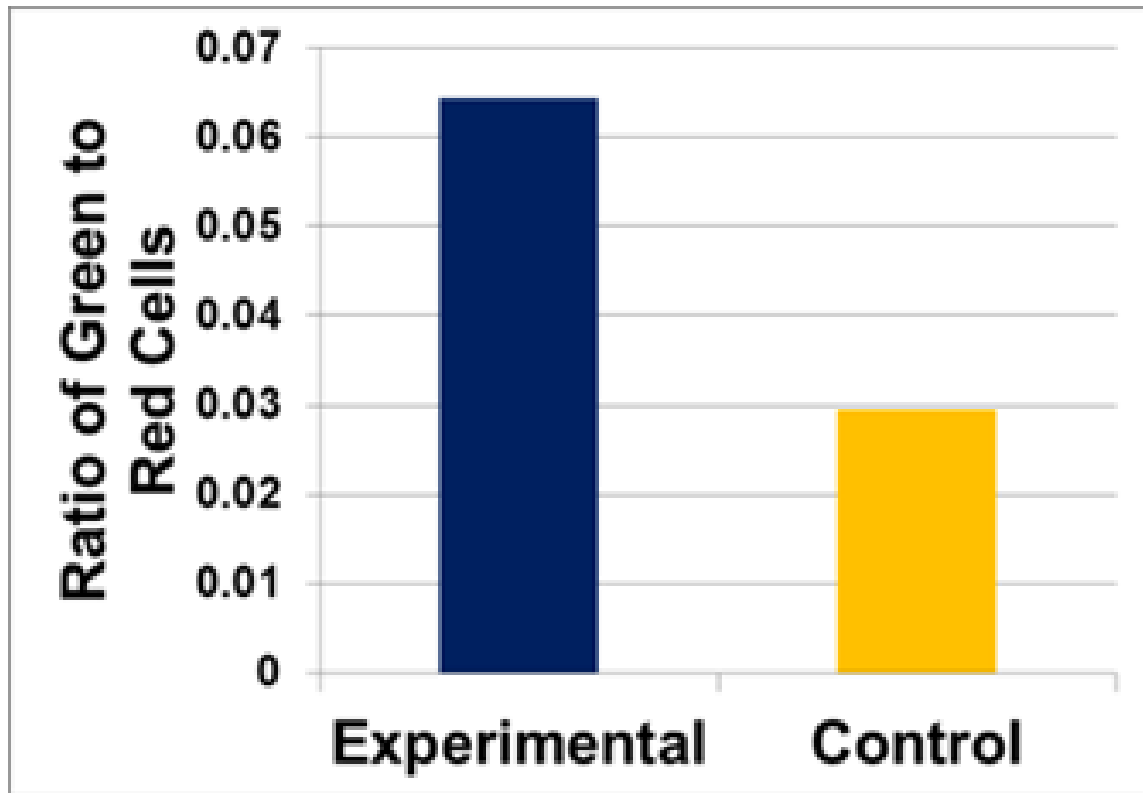
Figure 35. In vitro co-culture results after colony formation assay showing the ratio of green cells to red cells in experimental groups and the ratio of green only cells to double positive cells in control groups. Each graph A-C represents cells from two different colony formation assay wells for each condition (experimental or control).

stimulated by the WISP1 secreted by the WISP1_ires_GFP expressing cells in the mixture. If this is the case, then the final proportions of GFP+ cells after colony formation or tumor formation should be the same in both the experimental mixture and the control mixture. If the secreted WISP1 is not able to induce growth then one would expect the proportion of GFP+ cells to be higher in the experimental mixture compared to the control mixture. This would indicate that the WISP1 is acting within the cell to promote growth. After development of colonies the cells were trypsinized for flow cytometry analysis. Likewise after tumor development the tumors were dissociated into single cells for flow cytometry analysis. The ratio of cells that are only GFP+ to mCherry+ cells was much higher in the experimental groups compared to that of the controls (Fig 35A-C). Each graph represents cells from two wells of a 6 well plate after 2 weeks of colony formation. It seems that there is a tendency for the mCherry_ires_Luciferase expressing cells to grow faster based on the shift towards mCherry+ cells in the control mixture (Fig 35A-C). However, the WISP1_ires_GFP expressing cells were still able to overcome that and dominate the experimental mixture. The push towards mCherry+ cells was even stronger *in vivo* but still the tumors derived from the experimental mixture had an even higher ratio of only GFP+ cells to mcherry+ cells compared to that of controls (Fig 36A-C). Each graph represents the results of a single tumor. These results support the notion that WISP1 does not drive growth through secretion but rather drives growth inside the cell.

A



B



C

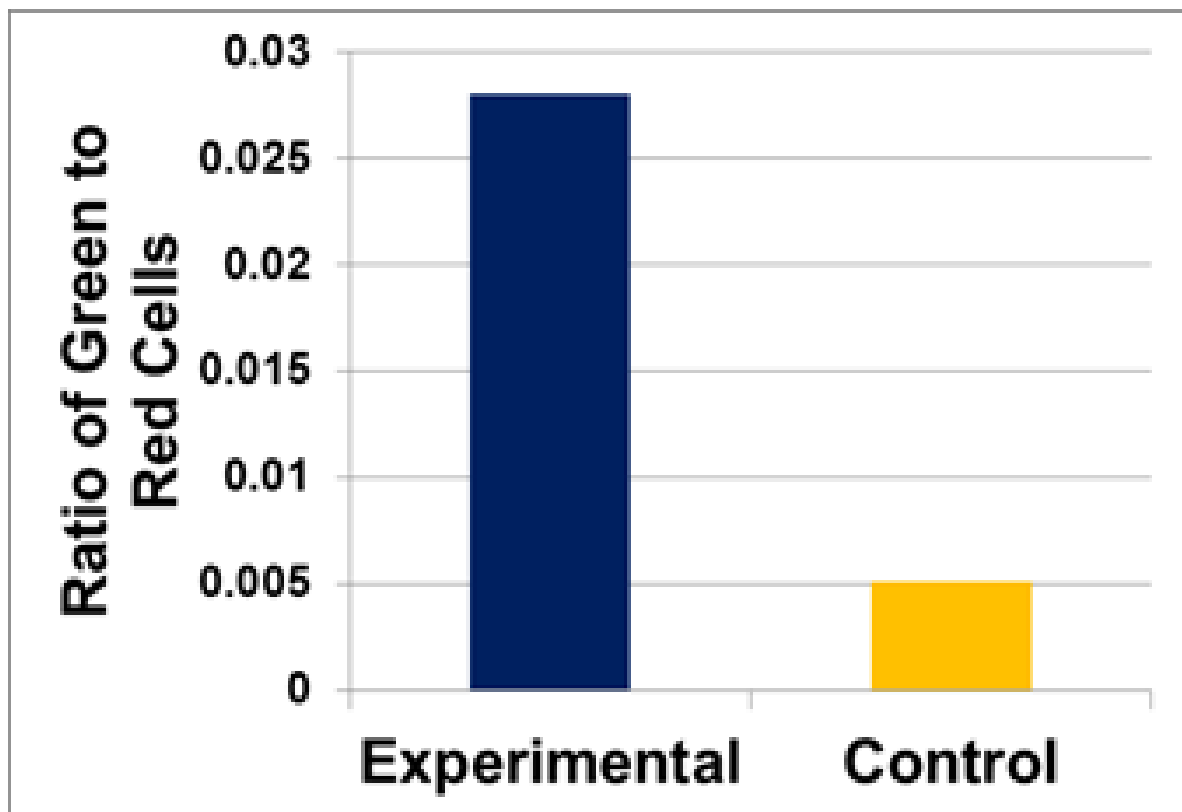


Figure 36 In vivo co-culture results after tumor development showing the ratio of green cells to red cells in experimental groups and the ratio of green only cells to double positive cells in control groups. Each graph A-C represents cells from a tumor for each condition (experimental or control).

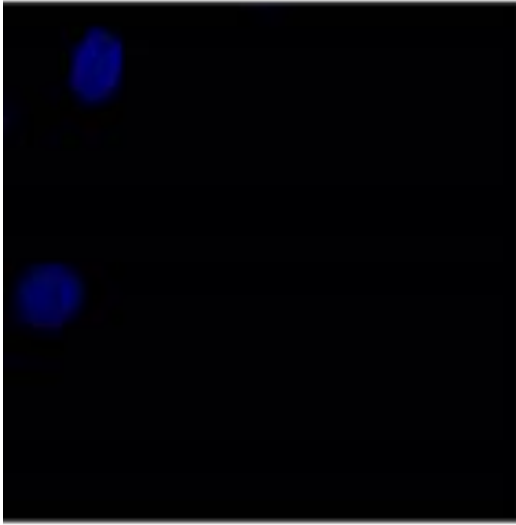
Results 1.7: There is ectopic expression of endogenous WISP1 in the cytosol in GBM

Our next interest was to gain a deeper understanding of WISP1's localization within the cell. Since WISP1 is a secreted protein we expected to be able to find it possibly in the endoplasmic reticulum (ER), Golgi, or endosomes. We performed immunofluorescence and confocal microscopy of U87MG cells using EEA1 as an endosomal marker, AE6 as a Golgi marker, and Calreticulin as an ER marker. We did not see localization in the Golgi or endosomes (Fig 37-38). However, we did find that WISP1 co-localized with Calreticulin indicating localization in the ER (Fig 39). We interpret this to mean that there is a much more substantial portion of WISP1 in the ER than possibly in the Golgi or endosomes. We also noticed that WISP1 did not seem to be present in the nucleus (Fig 37-41). We were intrigued by the functional studies demonstrating that expression of the delta SP WISP1 could drive tumor growth. Normally translation begins in the cytosol and the signal peptide directs the protein to the ER to join in the secretory pathway (53). However, the delta SP WISP1 should not be directed to the ER since it lacks the signal peptide and instead should probably remain in the cytosol. The presence of delta SP WISP1 in the cytosol would implicate the cytosol as an important area for WISP1 function in GBM. For the cytosol to be relevant endogenous WISP1 would also need to be present there. To investigate this we conducted immunofluorescence and confocal microscopy of both U87MG and U87MG expressing the delta SP WISP1. Alpha tubulin was used as the cytosolic

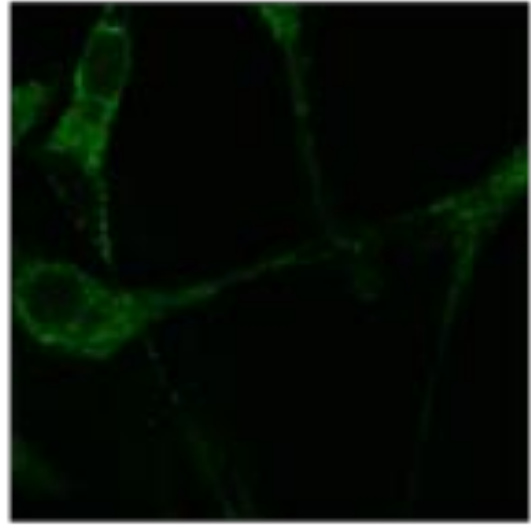
marker. Though the antibody against WISP1 will detect both endogenous and delta SP WISP1 we still wanted to compare the localization. Endogenous WISP1 was indeed found to be present in the cytosol and delta SP WISP1 was in the cytosol as well (Fig 40-42).

U87MG

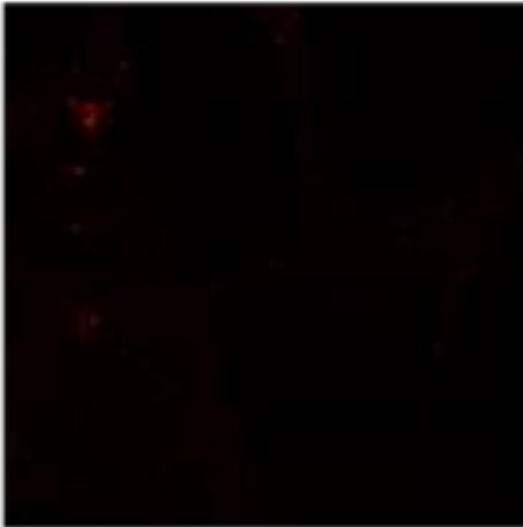
DAPI



WISP1



EEA1



Merge

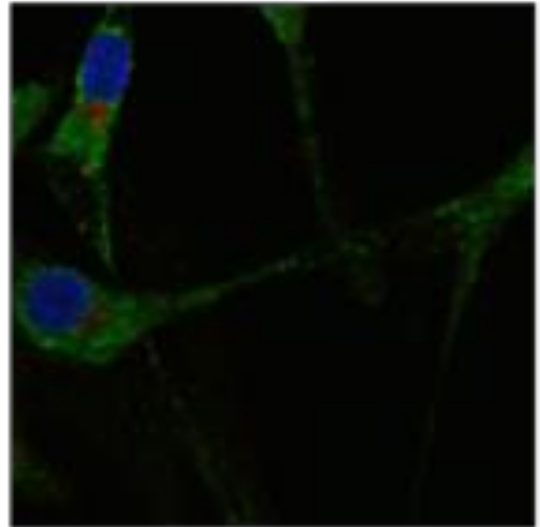
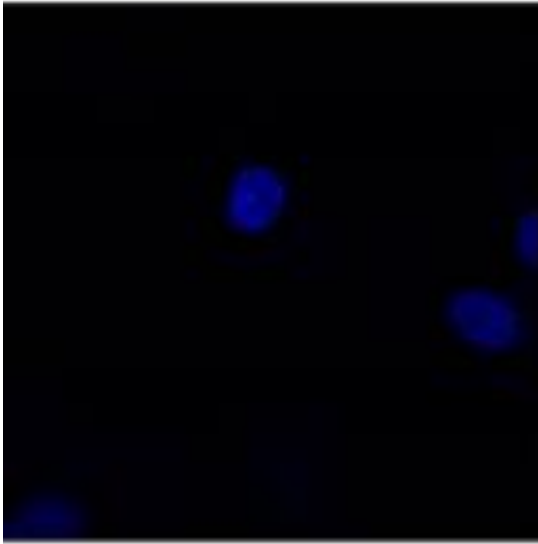


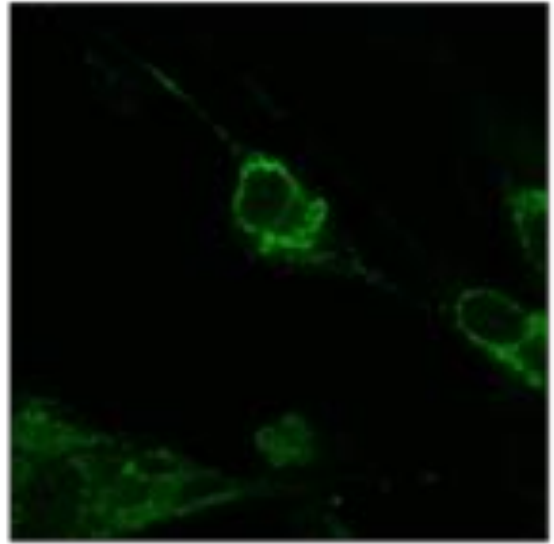
Figure 37 Immunofluorescence of U87MG cells for DAPI, WISP1, and the endosomal marker EEA1. Images were captured by an FV1000 Olympus Confocal microscope.

U87MG

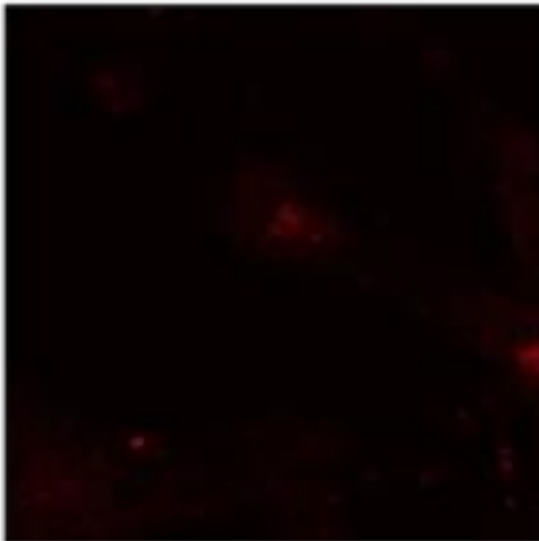
DAPI



WISP1



AE6



Merge

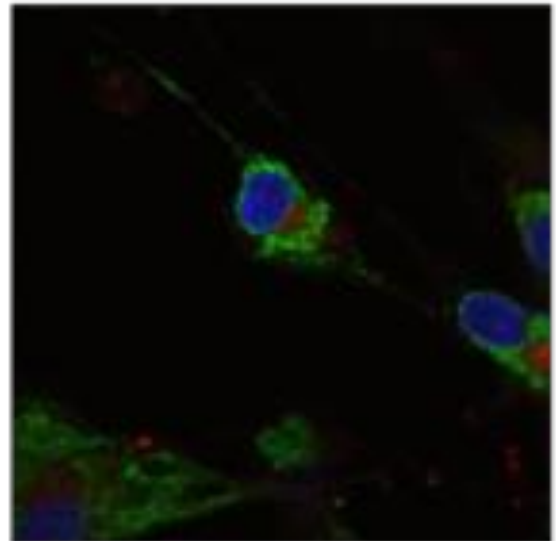
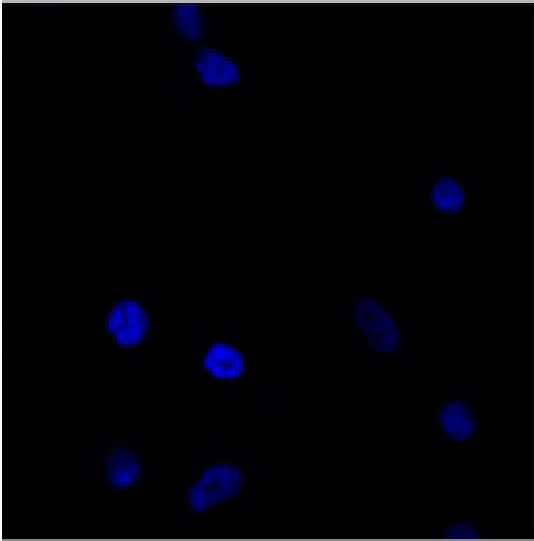


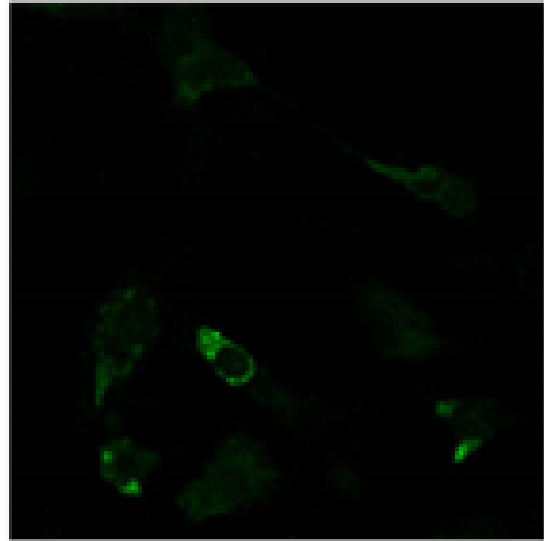
Figure 38 Immunofluorescence of U87MG cells for DAPI, WISP1, and the golgi marker AE6. Images were captured by an FV1000 Olympus Confocal microscope.

U87MG

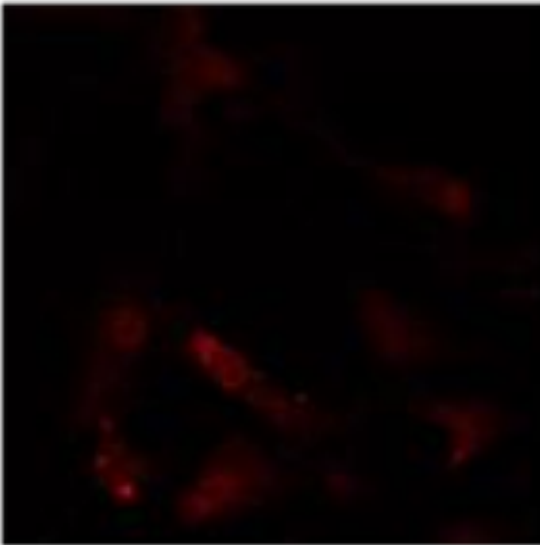
DAPI



WISP1



Calreticulin



Merge

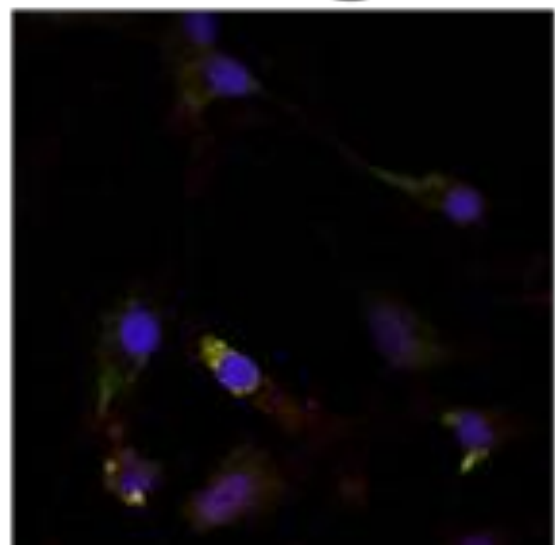
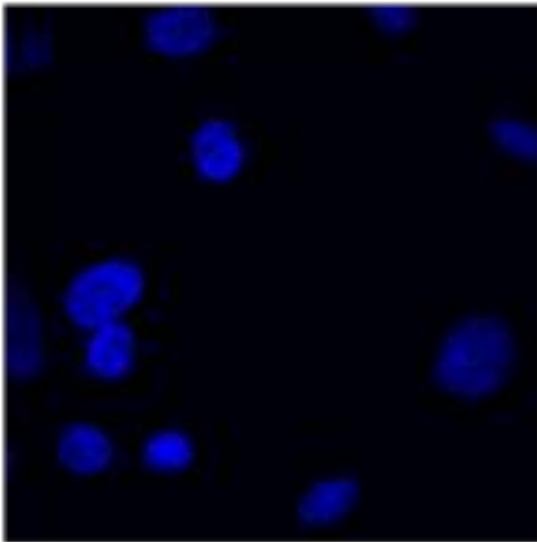


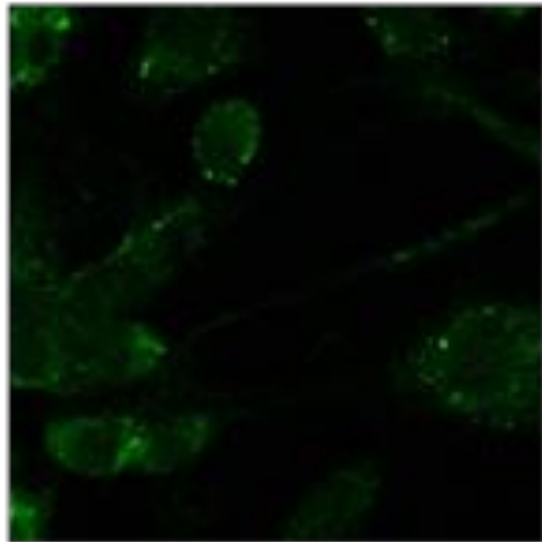
Figure 39 Immunofluorescence of U87MG cells for DAPI, WISP1, and the endoplasmic reticulum marker Calreticulin. Images were captured by an FV1000 Olympus Confocal microscope.

U87MG

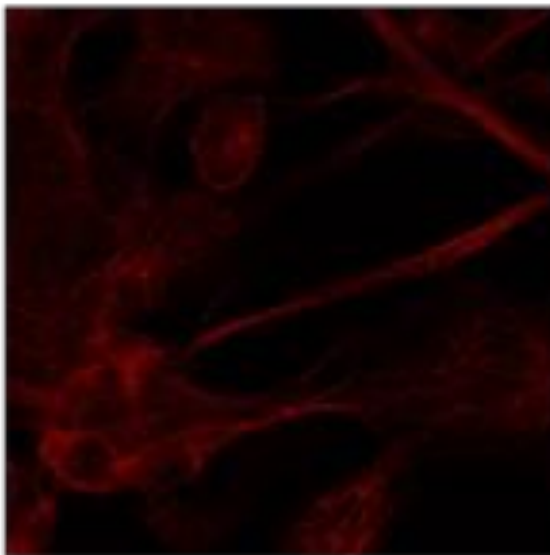
DAPI



WISP1



α Tubulin



Merge

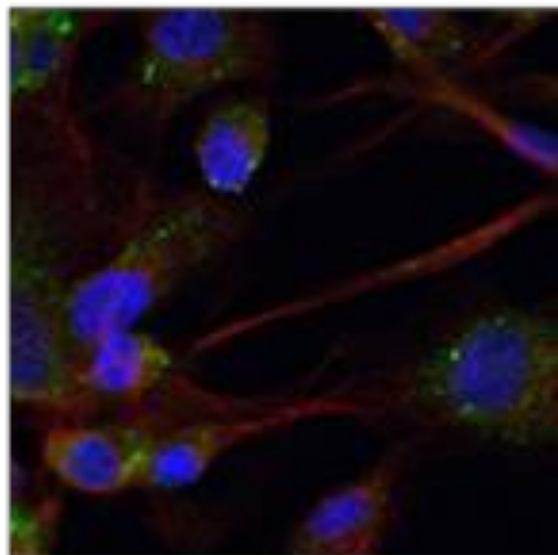
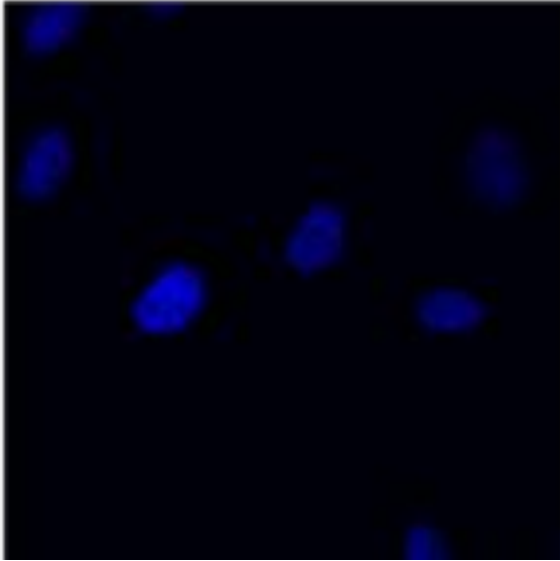


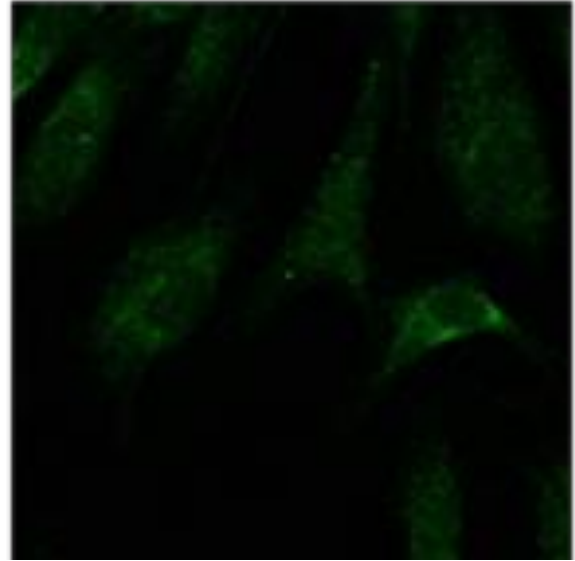
Figure 40. Immunofluorescence of U87MG cells for DAPI, WISP1, and the cytosolic marker α -Tubulin. Images were captured by an FV1000 Olympus Confocal microscope.

**Δ SP WISP1
U87MG**

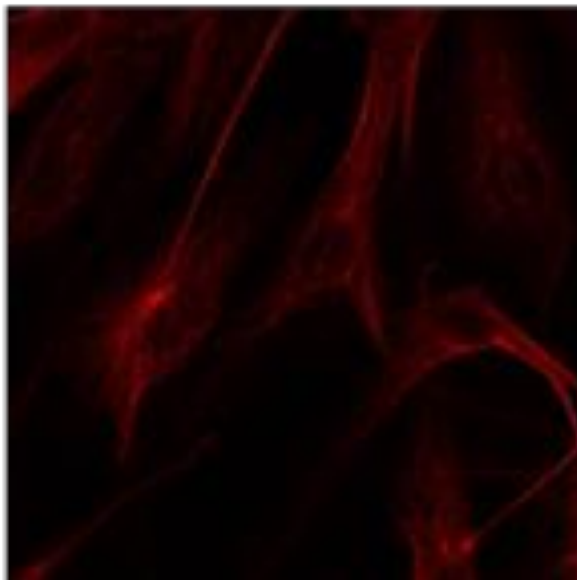
DAPI



WISP1



α Tubulin



Merge

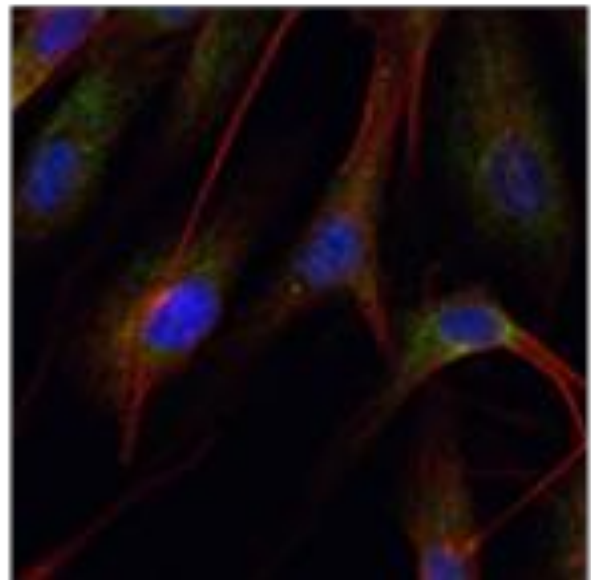


Figure 41. Immunofluorescence of U87MG cells expressing Δ SP WISP1 for DAPI, WISP1, and the cytosolic marker α -Tubulin. Images were captured by an FV1000 Olympus Confocal microscope.

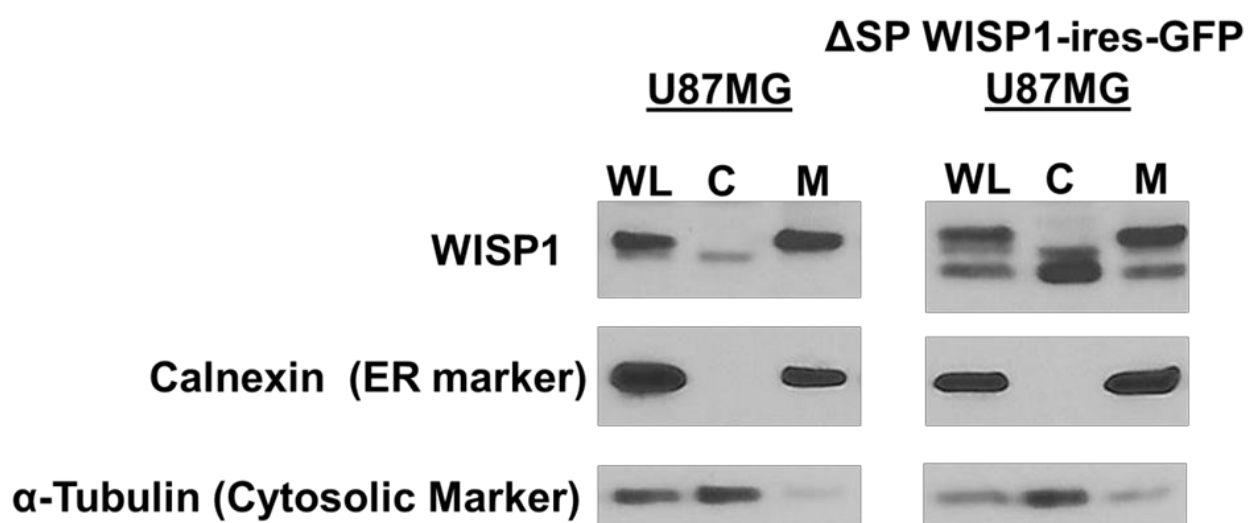


Figure 42. Immunoblot of lysate from U87MG cells (left) and U87MG cells expressing Δ SP WISP1 (right) that was fractionated into cytosolic (C) and membranous (M) fractions. Unfractionated whole lysate (WL) was also immunoblotted.

The delta SP WISP1 seemed to be more dispersed throughout the cytoplasm while the major concentration of the endogenous WISP1 seemed to be perinuclear where the ER is located. We also utilized another method to investigate the localization. We performed fractionation and immunoblotting to more precisely see the various levels of the protein in different subcellular fractions of the lysate. We compared the levels of WISP1 and delta SP WISP1 in the whole lysate, cytosolic fraction, and the membranous fraction which comprises organelles like the ER. The ER marker Calnexin was used as a control for the membranous fraction while alpha-Tubulin was used as a control for the cytosolic fraction. The Delta SP WISP1 appeared as a band just under the endogenous WISP1 in the immunoblot (Fig 42). We found that the endogenous WISP1 is primarily in the membranous fraction which makes sense as it is secreted and should be targeted to the ER. Intriguingly, there was also a portion of the endogenous WISP1 in the cytosol confirming the immunofluorescence results (Fig 42). This further confirmed that the cytosol is relevant since endogenous WISP1 is present there. As predicted the delta SP WISP1 was primarily in the cytosolic fraction while a small portion of it was seen in the ER (Fig 42). These results make it quite plausible that WISP1 functions in the cytosol as a driver in GBM.

WISP1 functions in a non-canonical manner in the cytosol

An interesting question is whether cytosolic WISP1 functions through a different pathway than its secreted canonical counterpart. Secreted WISP1 is known to activate Akt by inducing its phosphorylation. The RTK/RAS/PI-3K pathway which encompasses Akt is an important altered pathway in GBM. Conventional thought would have implicated activation of Akt as the reason behind WISP1's activity in GBM. Astonishingly, though we find that WISP1 overexpression induces phosphorylation of Akt in GBM which is consistent with its known function in other cell types, overexpression of the delta SP form of WISP1 does not activate Akt (Fig 43). This supports the possibility that WISP1 drives growth through a non-canonical pathway inside the cell in GBM. It is interesting that the phenotype of overexpression of the delta SP form of WISP1 was even more robust than that of wild type WISP1 without such Akt activation. Whatever WISP1 is doing in the cytosol must be even more oncogenic than the Akt activation induced by secreted WISP1.

To look for downstream changes induced by WISP1 and delta SP WISP1 we conducted an RPPA of the lysates from tumors derived from U87MG cells transduced with either GFP_ires_GFP, WISP_ires_GFP, or delta SP WISP1_ires_GFP. A decrease in Merlin (coded by the NF2 gene) was a very interesting observation (Fig 44). Merlin is a cytoskeletal protein coded by the *NF2* gene. It regulates several signaling pathways controlling cell shape, cell growth, and cell adhesion. Intriguingly, Merlin is also a known tumor suppressor in GBM (54, 55). Overexpression of NF2 in U87MG cells was found to reduce tumor

growth while knockdown of NF2 in U251 was found to increase tumor growth (55). Mutations in NF2 also lead to neurofibromatosis type II which leads to an increased risk for glioma and glioblastoma. We validated the RPPA result by western blotting and found that Merlin was lower after WISP1 overexpression compared to the GFP control (Fig 45). Consistently, expression of delta SP WISP1 resulted in even lower levels of Merlin as compared to WISP1 overexpression (Fig 45). These results are very interesting as they support a possibility that cytosolic WISP1 reduces Merlin leading to greater tumor growth. This could be one of the ways in which WISP1 works as a driver in GBM.

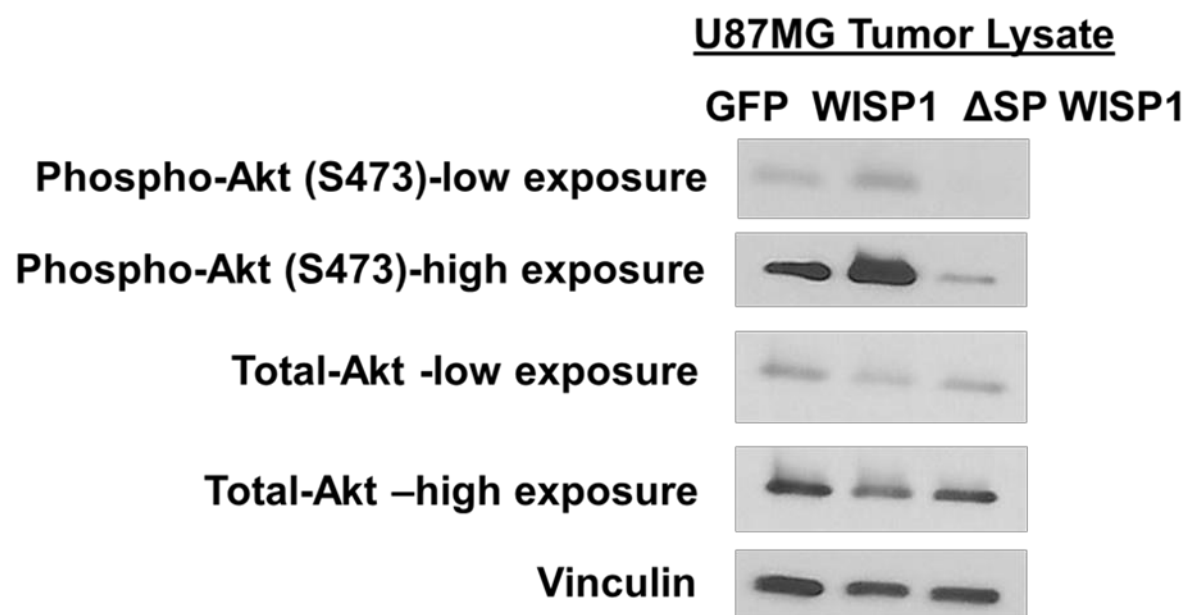


Figure 43. Immunoblot for pAkt (S473) and total Akt of lysates from tumors derived from U87MG cells expressing either GFP, WISP1, or Δ SP WISP1.

U87MG Tumor Lysate RPPA

Merlin-R-C



Δ SP WISP1

GFP

WISP1

Figure 44. RPPA heatmap of lysates from tumors derived from U87MG cells expressing either GFP, WISP1, or Δ SP WISP1. The heatmap shows the differences in Merlin (NF2)

U87MG Tumor Lysate

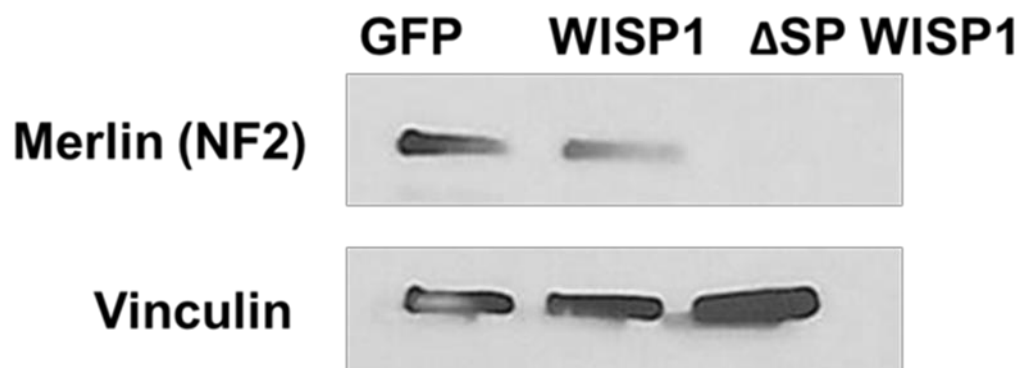


Figure 45. Immunoblot for Merlin (NF2) of lysates from tumors derived from U87MG cells expressing either GFP, WISP1, or Δ SP WISP1.

Discussion

Despite the current multimodal treatment for GBM, there is a tremendous need for new effective therapies. The current genomic understanding of the disease opens up new avenues to find unknown drivers of GBM. Here we have leveraged the TCGA datasets to conduct a functional genomic screen of “high-priority” genes that are overexpressed and/or amplified in GBM. In order to be context-specific, the screen was performed *in vivo* using a human glioma stem cell orthotopic mouse model. WISP1 emerged as the most relevant and intriguing gene “hit” from the screen. Based on available datasets we found that WISP1 is expressed at low levels in the brain but is overexpressed in glioblastoma. The expression was found to increase with increasing grade of glioma. This implicates WISP1 in the development of the disease. Furthermore, we found that the more aggressive IDH wild type forms of glioma had higher levels of WISP1 expression. Consistently, even less aggressive subtypes of glioma had a lower expression level of WISP1. Therefore, we chose to investigate WISP1 further.

Until now the role of WISP1 in glioblastoma had been unknown. We found that overexpression of WISP1 is able to drive tumor growth. WISP1 overexpression was able to reduce the latency of tumor formation in orthotopic models using GSCs. Likewise in subcutaneous xenograft models using GBM lines, overexpression led to faster tumor growth. In one line that does not readily form tumors, overexpression of WISP1 was able to induce tumor formation. This demonstrates that WISP1 is able to drive tumor growth and formation in GBM. Intriguingly, based on the datasets we found that the level of WISP1 is low in the brain relative to its expression in other tissues. However, the increase in WISP1

expression in glioma and its progressive increase in higher grades of glioma suggest that WISP1 plays a functional role in making the tumors more aggressive. This is further supported by the functional evidence we show demonstrating WISP1's ability to drive tumor growth. Together, this points to WISP1 as a newly discovered overexpressed driver of GBM.

Understanding genetic drivers of a disease are important for potential therapy. We conducted knockdown studies to explore the potential therapeutic potential of WISP1 as a driver. Knockdown of WISP1 reduced colony formation *in vitro* and slowed down tumor growth *in vivo*. We can attribute these effects to that of genetic knockdown rather than to off-target effects of the shRNA based on our rescue experiments. These studies not only support WISP1 as a driver with potential therapeutic application in GBM but also substantiate its role in driving the disease.

WISP1 is a secreted extracellular matrix protein and belongs to the CCN protein family (56). It has no specific identified receptor but most evidence points towards interaction with integrins as its primary means of activity (57). WISP1 has been shown to physically interact with the $\alpha 5\beta 1$ integrin with a functional role in osteogenic bone marrow stromal cells (58). Other studies have found evidence supporting that WISP1 functions through the $\alpha V\beta 5$ integrin (59, 60). Many have studied the effects of WISP1 on Akt since integrins are known to be able to signal downstream to targets like Akt (61-63). Extracellular WISP1 has been found to be able to activate Akt leading to greater phospho-Akt (64, 65). WISP1 induced

activation of Akt has a functional role. For instance, one study found that it results in myocyte hypertrophy (65).

We were interested in functionally characterizing the WISP1 protein in GBM. Structurally, the protein is composed of 5 modules: SP (signal peptide), IGFBP, VWC, TSP, and CT (55). The signal peptide is a tag that tells the cell that a protein is destined for secretion. If a protein does not have the signal peptide then translation of the protein remains in the cytosol. However, if a protein has a signal peptide then it locates to the ER to embark onto the secretory pathway. The signal peptide is then cleaved so the secreted protein does not have the signal peptide. Strikingly, we found that overexpression of WISP1 lacking the signal peptide module was able to result in a strong growth promoting phenotype. This is interesting based on the current understanding of WISP1 since it is a secreted protein and it is thought to function extracellularly while the delta SP form of WISP1 is able to drive growth intracellularly. We also found that the TSP module is necessary for the phenotype. This raises a possibility that the TSP module may have an essential function inside the cell to drive GBM. It is surprising that overexpression of the delta TSP form of WISP1 prevented the formation of any tumors. We speculate that this could be due to a dominant negative effect where the delta TSP form of WISP1 prevents the wildtype WISP1 to function. One possibility is that the TSP module is involved in mediating a crucial protein-protein interaction that is necessary for the phenotype. Another possibility is that the lack of the TSP module alters the tertiary structure of the protein preventing it from functioning.

The ability of the delta SP form of WISP1 to drive growth sparked our interest in understanding if the phenotype is secretion independent. The results of our *in vitro* and *in vivo* co-culture experiments indicate that secreted WISP1 is not able to drive growth. If WISP1 drove growth through secretion then we would expect that the ratio of green cells to red cells in the experimental group would be the same as that of the ratio of green cells to double positive (GFP+ and mCherry+) cells in the control group. This is because the green and red cells in the experimental group should be exposed to the same secreted WISP1. If WISP1 only acts through secretion then both populations of green cells and red cells should be stimulated similarly. As an alternative method to test the same hypothesis we tried to use conditioned medium to rescue colony formation after WISP1 knockdown. Conditioned medium failed to rescue, while only genetic expression of WISP1 cDNA was able to rescue colony formation. Together, these experiments support an alternative means of WISP1 activity in GBM where it functions inside the cell rather than through secretion.

A key question that next emerged was whether intracellular WISP1 was biologically relevant. In order to better understand if intracellular WISP1 is biologically relevant we engaged ourselves to learn about its localization inside the cell in GBM. We found that WISP1 naturally can be found in the ER and the cytoplasm. From our fractionation experiments it became clear that though most of the WISP1 in a cell is in the membranous fraction like in the ER there is still a portion of it in the cytosol. Whereas, the delta SP form of WISP1 is mostly in the

cytosol with less in the membranous fraction. This is consistent with what should happen when the signal peptide is not present.

The notion that WISP1 functions intracellularly in the cytosol even though it is a secreted extracellular matrix protein represents a paradigm shift in our understanding of WISP1. Gradually some extracellular matrix proteins like osteopontin or fibulin-1D are starting to be reported to have non-canonical intracellular locations and functions like what we find here for WISP1 (66). This is a very intriguing concept from many standpoints. From an evolutionary perspective it is quite puzzling that a protein evolved to be secreted and function in the extracellular matrix will have such an impactful role in the cytosol. Another key question is why a protein will localize ectopically to the cytosol when it should be secreted. One potential answer to this that we believe may apply to WISP1 is alternative translation initiation. Just as alternative splicing leads to a multiplicity of functional protein isoforms, alternative translation initiation does the same. It can occur due to leaky scanning by 40S ribosomal subunits which miss the proper AUG translation initiation site and end up scanning farther in the 3'-direction until recognizing a downstream AUG codon as a translation initiation site (67). Thus, part of the protein does not get translated leading to a truncated isoform. It is thought that some properties of the mRNA can influence the AUG recognition. For instance, the stability of the secondary structure can change the pace of the 40S during translation, leading to leakiness and translation initiation from an alternative site (68). Osteopontin is an example of such a protein that is secreted but due to

alternative translation initiation an isoform of it results lacking the signal peptide (69). Remarkably, it then has a different function inside the cell.

We believe that alternative translation initiation is a possibility for WISP1 in GBM. In the mRNA transcript of WISP1 we intriguingly found an in-frame AUG codon after the first 27 codons. If translation initiates from this downstream AUG site then it would result in a truncated form of WISP1 lacking the signal peptide. In our fractionation experiments we noticed two bands for WISP1 in the whole lysate of U87MG. There was a strong band and a slightly lower molecular weight light band. Surprisingly, it is this light band that remains in the cytosolic fraction while in the membranous fraction we only see the strong higher molecular weight band. It is quite conceivable that the slightly lower molecular weight WISP1 present in the cytosolic fraction possibly represents a truncated isoform lacking the signal peptide due to alternative translation initiation.

The downregulation of Merlin by cytosolic WISP1 was a very interesting observation. Merlin is a known tumor suppressor in GBM which makes this a plausible mechanism through which WISP1 may be functioning. Clinically patients with mutant Merlin are at much greater risk of developing GBM. Based on the lack of Akt activation by the delta SP WISP1 it seems that WISP1 is involved in a different pattern of signaling inside the cell which is very effective in driving GBM growth. WISP1 may be functioning through Merlin suppression to exert its oncogenic activity in glioblastoma. Together, this suggests a model where WISP1 functions through an alternative non-canonical pathway of signaling to promote glioblastoma growth (Fig 46).

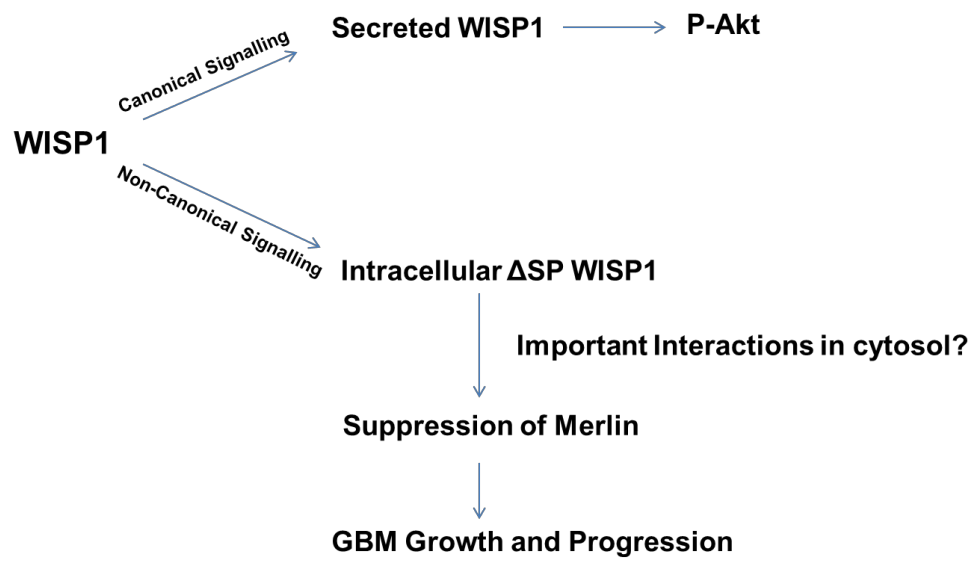


Figure 46. Hypothetical model of one possibility for what WISP1 may be doing to drive GBM

Future Directions

This work opens up numerous possibilities and many new questions. The first striking question that emerges is how exactly WISP1 is able to drive GBM. This is even more interesting in light of the new found understanding that WISP1 can work intracellularly in GBM. It is quite intriguing that a protein made to work outside the cell could elicit such a powerful function inside the cell. One hypothesis I would propose is that WISP1 functions through binding another protein. This seems quite plausible based on the data I got after expression of the delta TSP WISP1. The lack of this module resulted in what looks like a dominant negative effect. It was a striking result to see the lack of any tumor development after expression of the delta TSP WISP1. This is a similar phenotype as WISP1 knockdown. This makes me think that the delta TSP WISP1 obstructs the wild type WISP1 from interacting with its partner. For this to be true it also means that the TSP module must be the binding site. More research is needed to find what this TSP module binds to. Again another possibility is that the lack of the TSP module results in important changes in the tertiary structure of the protein rendering it non-functional. This possibility should also be investigated.

The result that Merlin goes down after WISP1 overexpression and after expression of delta SP WISP1 also gives insight into a potential mechanism. Perhaps the binding of WISP1 to its interacting partner in the cytosol leads to Merlin downregulation. It would be very interesting if the change in the level of Merlin is the major contributor towards WISP1's ability to drive GBM. This could potentially open up greater interest and attention towards understanding the role of Merlin in GBM. Most of the research with Merlin has dealt with its primary role in

Neurofibromatosis type II. A deeper understanding of Merlin in GBM could potentially also have translational impact in the future.

Another interesting question that comes to my mind is why *WISP1* is overexpressed in GBM in the first place. There could be an activating event that leads to *WISP1* overexpression. Since *WISP1* is normally so low in the brain, I believe that a primary culprit in GBM is whatever is causing the overexpression in the first place. More research in finding the reason behind its overexpression is necessary. There could be an epigenetic reason for this, as one possibility for *WISP1* upregulation could be demethylation of the *WISP1* promoter. One study found decreased DNA methylation levels in the *WISP1* promoter in primary oral squamous cell carcinoma of patients with lymph node metastases (70). This decreased DNA methylation was also found to correlate with increased *WISP1* expression (70). It could be that there is a demethylation in the *WISP1* promoter in GBM which leads to the upregulation of *WISP1* expression.

Though the overexpression of *WISP1* may be due to another factor, I still believe that *WISP1* itself may prove to be a very interesting therapeutic target. The results of the knockdown experiments I got reveal that potentially inhibiting *WISP1* should lead to a reduction in GBM growth. In this regard, at least from a translational standpoint, it is more important to understand how to inhibit *WISP1* in the cytosol rather than understand why it is overexpressed in GBM.

As I mentioned in the Discussion section, I believe that the ectopic expression of *WISP1* in the cytosol may be due to alternative translation initiation.

I am really curious as to why a portion of WISP1 ends up in the cytosol. This is another interesting area of future research from a more fundamental molecular biology standpoint. A deeper understanding of this will also generate a greater appreciation for the diversity and complexity that can be generated by a relatively limited number of human genes.

Conclusion

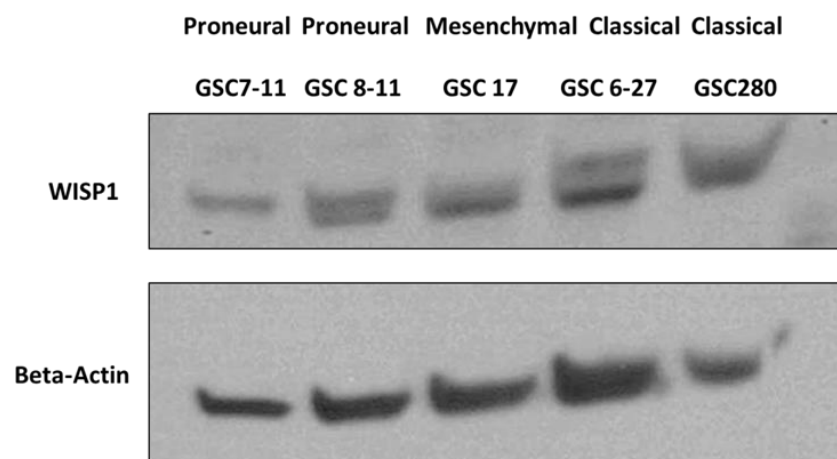
My dissertation work has revealed WISP1 to be a driver of GBM with possible therapeutic potential as a target. Our current understanding of WISP1 as a secreted extracellular matrix protein has changed as I have shown here that it can drive GBM in the cytosol most likely through a non-canonical pathway. This has opened up new avenues for investigation both in understanding further what specifically WISP1 is doing in the cytosol to drive GBM and in exploring this unique paradoxical class of secreted extracellular matrix proteins that have important non-canonical roles inside the cell.

Just like the ancient Egyptians who wrote over 5 millennia ago that breast cancer has no known cure, today we must say the same for GBM. However, breast cancer currently has a far, far better prognosis than ever before imagined in those days. It took the combined effort of countless scientists from countless fields over this vast stretch of time to bring us here today. One scientific advance must base itself on another in this endless journey towards the discovery of greater scientific truth. Perhaps one day we will look back at us today just as we can now look back at the time of the ancient Egyptians and think to ourselves how far we have come in a world where glioblastoma is no longer such a devastating disease.

Appendix

		GSC 7-11	GSC 8-11	GSC 6-27	U-87 MG	LN340
Copy number	WISP1	Gain	Neutral	Neutral	Neutral	Neutral
	EGFR	Neutral	Neutral	Neutral	Neutral	Gain
	PTEN	Neutral	Neutral	Loss	Neutral	Neutral
	CDK4	Neutral	Neutral	Neutral	Neutral	Neutral
	RB1	Neutral	Loss	Neutral	Loss	Loss
	CDKN2A/B	Neutral	Loss	Loss	Loss	Loss
	MDM2	Neutral	Neutral	Neutral	Neutral	Neutral
	MDM4	Neutral	Neutral	Neutral	Neutral	Neutral
	PDGFRA	Neutral	Neutral	Neutral	Neutral	Neutral
Mutation	WISP1	Wild-type	Wild-type	Wild-type	Wild-type	
	IDH1/2	Wild-type	Wild-type	Wild-type	Wild-type	
	EGFR	Wild-type	Wild-type	Wild-type	Wild-type	
	TP53	Missense	Missense	Wild-type	Wild-type	
	RB1	Splice site	Missense	Wild-type	Wild-type	
	PTEN	Missense	Splice site	Wild-type	Splice site	
	NF1	Wild-type	Wild-type	Wild-type	Frameshift	
	PDGFRA	Missense	Wild-type	Wild-type	Wild-type	

Appendix 1: Genomic background of the GSC and GBM lines showing the mutation and copy number states.



Appendix 2: Immunoblot of various GSC lines.

Bibliography

1. Jr, Jiri Polivka, Jiri Polivka, Lubos Holubec, Tereza Kubikova, Vladimir Priban, Ondrej Hes, Kristyna Pivovarcikova, and Inka Treskova. (2017). Advances in Experimental Targeted Therapy and Immunotherapy for Patients with Glioblastoma Multiforme. *Anticancer Research* 37.1, 21-33.
2. Dolecek T.A., Propp J.M., Stroup N.E., Kruchko, C. (2012). CBTRUS statistical report: primary brain and central nervous system tumors diagnosed in the United States in 2005-2009. *Neuro-Oncol* 14, v1-49.
3. Louis DN, Ohgaki H, Wiestler OD, Cavenee WK, Burger PC, Jouvet A, Scheithauer BW, Kleihues, P. (2007). The 2007 WHO Classification of Tumours of the Central Nervous System. *Acta Neuropathol* 114, 97-109.
4. Ostrom QT, Gittleman H, Liao P, Rouse C, Chen Y, Dowling J, Wolinsky Y, Kruchko C, Barnholtz-Sloan J. (2014). CBTRUS statistical report: primary brain and central nervous system tumors diagnosed in the United States in 2007-2011. *Neuro-Oncol* 16, iv1-63.
5. Polivka J Jr., Polivka J, Rohan V, Topolcan O, Ferda J. (2012). New molecularly targeted therapies for glioblastoma multiforme. *Anticancer Res* 32: 2935-2946.
6. Thakkar JP, Dolecek TA, Horbinski C, Ostrom QT, Lightner DD, Barnholtz-Sloan JS, and Villano JL. Epidemiologic and molecular prognostic review of glioblastoma. *Cancer Epidemiol Biomarkers Prev.* 2014;23(10):1985-96.

7. Alcantara Ilaguno SR, Parada LF. Cell of origin of glioma: biological and clinical implications. *Br J Cancer*. 2016;115(12):1445-1450.
8. Krex D, Klink B, Hartmann C, von Deimling A, Pietsch T, Simon M, Sabel M, Steinbach JP, Heese O, Reifenberger G, Weller M, Schackert G, German Glioma Network. (2007). Long-term survival with glioblastoma multiforme. *Brain J Neurol* 130, 2596-2606.
9. Furnari FB, Fenton T, Bachoo RM, Mukasa A, Stommel JM, Stegh A, Hahn WC, Ligon KL, Louis DN, Brennan C, Chin L, DePinho RA, and Cavenee WK. Malignant astrocytic glioma: genetics, biology, and paths to treatment. *Genes Dev*. 2007;21(21):2683-710.
10. Wen PY, Kesari S. Malignant gliomas in adults. *N Engl J Med*. 2008;359(5):492-507.
11. Jessen KR, Mirsky R. Glial cells in the enteric nervous system contain glial fibrillary acidic protein. *Nature*. 1980;286(5774):736-7.
12. Davis ME. Glioblastoma: Overview of Disease and Treatment. *Clin J Oncol Nurs*. 2016;20(5):S2-8.
13. Phillips HS, Kharbanda S, Chen R, Forrest WF, Soriano RH, Wu TD, Misra A, Nigro JM, Colman H, Soroceanu L, Williams PM, Modrusan Z, Feuerstein BG, and Aldape K. Molecular subclasses of high-grade glioma predict prognosis, delineate a pattern of disease progression, and resemble stages in neurogenesis. *Cancer Cell*. 2006;9(3):157-73.

14. Ellor SV, Pagano-young TA, Avgeropoulos NG. Glioblastoma: background, standard treatment paradigms, and supportive care considerations. *J Law Med Ethics*. 2014;42(2):171-82.
15. Stupp R, Mason WP, Van den bent MJ, Weller M, Fisher B, Taphoorn MJ, Belanger K, Brandes AA, Marosi C, Bogdahn U, Curschmann J, Janzer RC, Ludwin SK, Gorlia T, Allgeier A, Lacombe D, Cairncross JG, Eisenhauer E, and Mirimanoff RO. Radiotherapy plus concomitant and adjuvant temozolomide for glioblastoma. *N Engl J Med*. 2005;352(10):987-96.
16. Stupp R, Taillibert S, Kanner AA, Kesari S, Steinberg DM, Toms SA, Taylor LP, Lieberman F, Silvani A, Fink KL, Barnett GH, Zhu JJ, Henson JW, Engelhard HH, Chen TC, Tran DD, Sroubek J, Tran ND, Hottinger AF, Landolfi J, Desai R, Caroli M, Kew Y, Honnorat J, Idbaih A, Kirson ED, Weinberg U, Palti Y, Hegi ME, and Ram Z. Maintenance Therapy With Tumor-Treating Fields Plus Temozolomide vs Temozolomide Alone for Glioblastoma: A Randomized Clinical Trial. *JAMA*. 2015;314(23):2535-43.
17. Sellers WR. A blueprint for advancing genetics-based cancer therapy. *Cell*. 2011 Sep 30; 147(1):26–31.
18. Sawyers CL. Shifting paradigms: the seeds of oncogene addiction. *Nat Med*. 2009 Oct; 15(10): 1158–1161.
19. Cancer Genome Atlas Research Network: Comprehensive genomic characterization defines human glioblastoma genes and core pathways. (2008). *Nature* 455: 1061-1068.

20. Ohgaki H, Kleihues P. Genetic pathways to primary and secondary glioblastoma. *Am J Pathol.* 2007;170(5):1445-53.
21. Ohgaki H, Kleihues P. Population-based studies on incidence, survival rates, and genetic alterations in astrocytic and oligodendroglial gliomas. *J Neuropathol Exp Neurol.* 2005;64(6):479-89.
22. Verhaak RG, Hoadley KA, Purdom E, Wang V, Qi Y, Wilkerson MD, Miller CR, Ding L, Golub T, Mesirov JP, Alexe G, Lawrence M, O'Kelly M, Tamayo P, Weir BA, Gabriel S, Winckler W, Gupta S, Jakkula L, Feiler HS, Hodgson JG, James CD, Sarkaria JN, Brennan C, Kahn A, Spellman PT, Wilson RK, Speed TP, Gray JW, Meyerson M, Getz G, Perou CM, and Hayes DN; Cancer Genome Atlas Research Network. Integrated genomic analysis identifies clinically relevant subtypes of glioblastoma characterized by abnormalities in PDGFRA, IDH1, EGFR, and NF1. *Cancer Cell.* 2010;17(1):98-110.
23. Steed TC, Treiber JM, Patel K, Ramakrishnan V, Merk A, Smith AR, Carter BS, Dale AM, Chow LM, and Chen CC. Differential localization of glioblastoma subtype: implications on glioblastoma pathogenesis. *Oncotarget.* 2016;7(18):24899-907.
24. Sanai N, Alvarez-buylla A, Berger MS. Neural stem cells and the origin of gliomas. *N Engl J Med.* 2005;353(8):811-22.
25. Brennan CW, Verhaak RG, Mckenna A, Campos B, Noushmehr H, Salama SR, Zheng S, Chakravarty D, Sanborn JZ, Berman SH, Beroukhim R, Bernard B, Wu CJ, Genovese G, Shmulevich I, Barnholtz-Sloan J, Zou L,

- Vegesna R, Shukla SA, Ciriello G, Yung WK, Zhang W, Sougnez C, Mikkelsen T, Aldape K, Bigner DD, Van Meir EG, Prados M, Sloan A, Black KL, Eschbacher J, Finocchiaro G, Friedman W, Andrews DW, Guha A, Iacocca M, O'Neill BP, Foltz G, Myers J, Weisenberger DJ, Penny R, Kucherlapati R, Perou CM, Hayes DN, Gibbs R, Marra M, Mills GB, Lander E, Spellman P, Wilson R, Sander C, Weinstein J, Meyerson M, Gabriel S, Laird PW, Haussler D, Getz G, and Chin L; TCGA Research Network. The somatic genomic landscape of glioblastoma. *Cell*. 2013;155(2):462-77.
26. Lovejoy CA, Li W, Reisenweber S, Thongthip S, Bruno J, de Lange T, De S, Petrini JH, Sung PA, Jasin M, Rosenbluh J, Zwang Y, Weir BA, Hatton C, Ivanova E, Macconail L, Hanna M, Hahn WC, Lue NF, Reddel RR, Jiao Y, Kinzler K, Vogelstein B, Papadopoulos N, and Meeker AK. Loss of ATRX, genome instability, and an altered DNA damage response are hallmarks of the alternative lengthening of telomeres pathway. *PLoS Genet*. 2012;8(7):e1002772.
27. Rankin SL, Zhu G, Baker SJ. Review: insights gained from modelling high-grade glioma in the mouse. *Neuropathol Appl Neurobiol*. 2012;38(3):254-70.
28. Singh SK, Hawkins C, Clarke ID, Squire JA, Bayani J, Hide T, Henkelman RM, Cusimano MD, and Dirks PB. Identification of human brain tumour initiating cells. *Nature*. 2004;432(7015):396-401.
29. Joo KM, Kim J, Jin J, Kim M, Seol HJ, Muradov J, Yang H, Choi YL, Park WY, Kong DS, Lee JI, Ko YH, Woo HG, Lee J, Kim S, and Nam DH. Patient-specific orthotopic glioblastoma xenograft models recapitulate the

- histopathology and biology of human glioblastomas in situ. *Cell Rep.* 2013;3(1):260-73.
30. Wiesner SM, Decker SA, Larson JD, Ericson K, Forster C, Gallardo JL, Long C, Demorest ZL, Zamora EA, Low WC, SantaCruz K, Largaespada DA, and Ohlfest JR. De novo induction of genetically engineered brain tumors in mice using plasmid DNA. *Cancer Res.* 2009;69(2):431-9.
31. Xiao A, Wu H, Pandolfi PP, Louis DN, and Van dyke T. Astrocyte inactivation of the pRb pathway predisposes mice to malignant astrocytoma development that is accelerated by PTEN mutation. *Cancer Cell.* 2002;1(2):157-68.
32. Smilowitz HM, Weissenberger J, Weis J, Brown JD, O'Neill RJ, and Laissue JA. Orthotopic transplantation of v-src-expressing glioma cell lines into immunocompetent mice: establishment of a new transplantable in vivo model for malignant glioma. *J Neurosurg.* 2007;106(4):652-9.
33. Kegelman TP, Hu B, Emdad L, Das SK, Sarkar D, Fisher PB. In vivo modeling of malignant glioma: the road to effective therapy. *Adv Cancer Res.* 2014;121:261-330.
34. Roix JJ, McQueen PG, Munson PJ, Parada LA and Misteli T. Spatial proximity of translocation-prone gene loci in human lymphomas. *Nat Genet.* 2011;34:287–291.
35. Pulukuri SM, Estes N, Patel J, Rao JS. Demethylation-linked activation of urokinase plasminogen activator is involved in progression of prostate cancer. *Cancer Res.* 2007;67:930–939.

36. Søres S, Daugaard IL, Sørensen BS, Carus A, Mattheisen M, Alsner J, Overgaard J, Hager H, Hansen LL, Kristensen LS. Hypomethylation and increased expression of the putative oncogene ELMO3 are associated with lung cancer development and metastases formation. *Oncoscience*. 2014;1(5):367–74.
37. Anzick SL, Kononen J, Walker RL, Azorsa DO, Tanner MM, Guan XY, Sauter G, Kallioniemi OP, Trent JM, Meltzer PS. AIB1, a steroid receptor coactivator amplified in breast and ovarian cancer. *Science*. 1997.
38. Lahusen T, Henke RT, Kagan BL, Wellstein A, Riegel AT. The role and regulation of the nuclear receptor co-activator AIB1 in breast cancer. *Breast Cancer Res Treat*. 2009;116:225–237.
39. Boehm JS, , Zhao JJ, Yao J, Kim SY, Firestein R, Dunn IF, Sjöström SK, Garraway LA, Weremowicz S, Richardson AL, Greulich H, Stewart CJ, Mulvey LA, Shen RR, Ambrogio L, Hirozane-Kishikawa T, Hill DE, Vidal M, Meyerson M, Grenier JK, Hinkle G, Root DE, Roberts TM, Lander ES, Polyak K, and Hahn WC. (2007) Integrative genomic approaches identify IKBKE as a breast cancer oncogene. *Cell* 129(6):1065–1079.
40. Shrestha Y, Schafer EJ, Boehm JS, Thomas SR, He F, Du J, Wang S, Barretina J, Weir BA, Zhao JJ, Polyak K, Golub TR, Beroukhi R, and Hahn WC. (2012) PAK1 is a breast cancer oncogene that coordinately activates MAPK and MET signaling. *Oncogene* 31(29):3397–3408.
41. Dunn GP, Cheung HW, Agarwalla PK, Thomas S, Zektser Y, Karst AM, Boehm JS, Weir BA, Berlin AM, Zou L, Getz G, Liu JF, Hirsch M, Vazquez

- F, Root DE, Beroukhir R, Drapkin R, and Hahn WC. In vivo multiplexed interrogation of amplified genes identifies GAB2 as an ovarian cancer oncogene. *Proc Natl Acad Sci USA*. 2014;111(3):1102-7.
42. Nakamizo A, Marini F, Amano T, Khan A, Studeny M, Gumin J, Chen J, Hentschel S, Vecil G, Dembinski J, Andreeff M, and Lang FF. Human bone marrow-derived mesenchymal stem cells in the treatment of gliomas. *Cancer Res*. 2005;65(8):3307-18.
43. Lal S, Lacroix M, Tofilon P, Fuller GN, Sawaya R, Lang FF. An implantable guide-screw system for brain tumor studies in small animals. *J Neurosurg*. 2000;92(2):326-33.
44. URL: <http://www.cbioportal.org/>
45. GTEx Consortium. Human genomics. The Genotype-Tissue Expression (GTEx) pilot analysis: multitissue gene regulation in humans. *Science* 348, 648-60 (2015).
46. URL: https://tcga-data.nci.nih.gov/docs/publications/lgggbm_2016/
47. Ceccarelli, M. Barthel FP, Malta TM, Sabedot TS, Salama SR, Murray BA5, Morozova O, Newton Y, Radenbaugh A, Pagnotta SM, Anjum S, Wang J, Manyam G, Zoppoli P, Ling S, Rao AA, Grifford M, Cherniack AD, Zhang H5, Poisson L, Carlotti CG Jr, Tirapelli DP, Rao A, Mikkelsen T, Lau CC, Yung WK, Rabadan R, Huse J, Brat DJ, Lehman NL, Barnholtz-Sloan JS, Zheng S, Hess K, Rao G, Meyerson M, Beroukhir R, Cooper L, Akbani R, Wrensch M, Haussler D, Aldape KD, Laird PW, Gutmann DH; TCGA Research Network, Noushmehr H, Iavarone A, and Verhaak RG. Molecular

- Profiling Reveals Biologically Discrete Subsets and Pathways of Progression in Diffuse Glioma. *Cell* 164, 550-63 (2016).
48. Wickham, H. *ggplot2: Elegant Graphics for Data Analysis*. (Springer-Verlag New York, 2009).
49. Nathanson DA, Gini B, Mottahedeh J, Visnyei K, Koga T, Gomez G, Eskin A, Hwang K, Wang J, Masui K, Paucar A, Yang H, Ohashi M, Zhu S, Wykosky J, Reed R, Nelson SF, Cloughesy TF, James CD, Rao PN, Kornblum HI, Heath JR, Cavenee WK, Furnari FB, and Mischel PS. Targeted therapy resistance mediated by dynamic regulation of extrachromosomal mutant EGFR DNA. *Science*. 2014;343(6166):72-6.
50. Pennica D, Swanson TA, Welsh JW, Roy MA, Lawrence DA, Lee J, Brush J, Taneyhill LA, Deuel B, Lew M, Watanabe C, Cohen RL, Melhem MF, Finley GG, Quirke P, Goddard AD, Hillan KJ, Gurney AL, Botstein D, and Levine AJ. WISP genes are members of the connective tissue growth factor family that are up-regulated in wnt-1-transformed cells and aberrantly expressed in human colon tumors. *Proc Natl Acad Sci USA*. 1998;95(25):14717-22.
51. Vigneswaran K, Neill S, Hadjipanayis CG. Beyond the World Health Organization grading of infiltrating gliomas: advances in the molecular genetics of glioma classification. *Annals of Translational Medicine*. 2015;3(7):95. doi:10.3978/j.issn.2305-5839.2015.03.57.
52. Berschneider B, Königshoff M. WNT1 inducible signaling pathway protein 1 (WISP1): a novel mediator linking development and disease. *Int J Biochem Cell Biol*. 2011;43(3):306-9.

53. Reid DW, Nicchitta CV. Diversity and selectivity in mRNA translation on the endoplasmic reticulum. *Nat Rev Mol Cell Biol.* 2015;16(4):221-31.
54. Guerrero PA, Yin W, Camacho L, Marchetti D. Oncogenic role of Merlin/NF2 in glioblastoma. *Oncogene.* 2015;34(20):2621-30.
55. Lau YK, Murray LB, Houshmandi SS, Xu Y, Gutmann DH, Yu Q. Merlin is a potent inhibitor of glioma growth. *Cancer Res.* 2008;68(14):5733-42.
56. Berschneider B, Königshoff M. WNT1 inducible signaling pathway protein 1 (WISP1): a novel mediator linking development and disease. *Int J Biochem Cell Biol.* 2011;43(3):306-9.
57. Stephens S, Palmer J, Konstantinova I, Pearce A, Jarai G, Day E. A functional analysis of Wnt inducible signalling pathway protein -1 (WISP-1/CCN4). *J Cell Commun Signal.* 2015;9(1):63-72.
58. Ono M, Inkson CA, Kilts TM, Young MF. WISP-1/CCN4 regulates osteogenesis by enhancing BMP-2 activity. *J Bone Miner Res.* 2011;26(1):193-208.
59. Hou CH, Tang CH, Hsu CJ, Hou SM, Liu JF. CCN4 induces IL-6 production through $\alpha\text{v}\beta 5$ receptor, PI3K, Akt, and NF- κ B signaling pathway in human synovial fibroblasts. *Arthritis Res Ther.* 2013;15(1):R19.
60. Liu JF, Hou SM, Tsai CH, Huang CY, Hsu CJ, Tang CH. CCN4 induces vascular cell adhesion molecule-1 expression in human synovial fibroblasts and promotes monocyte adhesion. *Biochim Biophys Acta.* 2013;1833(5):966-75.

61. Delcommenne M, Tan C, Gray V, Rue L, Woodgett J, Dedhar S.
Phosphoinositide-3-OH kinase-dependent regulation of glycogen synthase kinase 3 and protein kinase B/AKT by the integrin-linked kinase. *Proc Natl Acad Sci USA*. 1998;95(19):11211-6.
62. Sonoda Y, Watanabe S, Matsumoto Y, Aizu-yokota E, Kasahara T. FAK is the upstream signal protein of the phosphatidylinositol 3-kinase-Akt survival pathway in hydrogen peroxide-induced apoptosis of a human glioblastoma cell line. *J Biol Chem*. 1999;274(15):10566-70.
63. Persad S, Attwell S, Gray V, Mawji N, Deng JT, Leung D, Yan J, Sanghera J, Walsh MP, and Dedhar S. Regulation of protein kinase B/Akt-serine 473 phosphorylation by integrin-linked kinase: critical roles for kinase activity and amino acids arginine 211 and serine 343. *J Biol Chem*. 2001;276(29):27462-9.
64. Su F, Overholtzer M, Besser D, Levine AJ. WISP-1 attenuates p53-mediated apoptosis in response to DNA damage through activation of the Akt kinase. *Genes Dev*. 2002;16(1):46-57.
65. Colston JT, De la rosa SD, Koehler M, Gonzales K, Mestrlil R, Freeman GL, Bailey SR, and Chandrasekar B. Wnt-induced secreted protein-1 is a prohypertrophic and profibrotic growth factor. *Am J Physiol Heart Circ Physiol*. 2007;293(3):H1839-46.
66. Hellewell AL, Adams JC. Insider trading: Extracellular matrix proteins and their non-canonical intracellular roles. *Bioessays*. 2016;38(1):77-88.

67. Bazykin GA, Kochetov AV. Alternative translation start sites are conserved in eukaryotic genomes. *Nucleic Acids Res.* 2011;39(2):567-77.
68. Kochetov AV. Alternative translation start sites and hidden coding potential of eukaryotic mRNAs. *Bioessays.* 2008;30(7):683-91.
69. Shinohara ML, Kim HJ, Kim JH, Garcia VA, Cantor H. Alternative translation of osteopontin generates intracellular and secreted isoforms that mediate distinct biological activities in dendritic cells. *Proc Natl Acad Sci USA.* 2008;105(20):7235-9.
70. Clausen MJ, Melchers LJ, Mastik MF, et al. Identification and validation of WISP1 as an epigenetic regulator of metastasis in oral squamous cell carcinoma. *Genes Chromosomes Cancer.* 2016;55(1):45-59.

Vita

Pushan Richard Dasgupta was born in Wichita, Kansas USA to Partha Sarathi Dasgupta and Manisha Dasgupta. Pushan was raised in Brunswick, OH. There he graduated as Valedictorian from Brunswick High School in 2006. In addition to achieving perfect scores on SAT(s) he also discovered the world's first photomechanical rod-coil polymer at NASA when he was in 11th grade. He got numerous awards and honors at that time from many organizations like USA Today, Siemens Westinghouse, Akron Beacon Journal, NASA, Cleveland Plain Dealer etc. He then went to Harvard University. He studied Molecular and Cellular Biology with a secondary field in Mind, Brain, Behavior. He graduated in 2010 with High Honors and a thesis on radiation biology. Unfortunately, at this time he also witnessed a tragedy with the sudden pre-mature death of his father. In spite of that he continued to progress in his studies. He entered the MD-PhD program at McGovern Medical School and MD Anderson Cancer Center. At that time he also joined one of his mother's companies as a President. He completed 2 years of medical school before entering in the PhD program. Now after completion of the PhD he will go back to medical school for 2 years of clinical rotations.

Permanent Address:

3206 Durango Drive

Pearland, TX 77581